The Importance of Acclimation in Driving Plant Physiological Responses to a Changing Environment

Submitted by

Iftakharul Alam

In fulfilment of the requirements for the degree of

Doctor of Philosophy (Natural and Physical Sciences)

College of Science and Engineering

James Cook University

Acknowledgements

The completion of this thesis would not have been possible without the invaluable assistance of numerous individuals to whom I am immensely grateful. I would like to extend my gratitude to my primary supervisor, Prof Lucas Cernusak, for his invaluable guidance and support throughout this journey. His support during the period of the pandemic and beyond was instrumental in enabling me to complete my doctoral studies. He assisted me in comprehending and investigating interesting facts in the intriguing field of plant ecophysiology.

I would also like to acknowledge the contributions of my co-supervisors, Dr. Alexander Cheesman and Prof Will Edwards, who have provided invaluable assistance during challenging periods. Their critical comments and unwavering encouragement have been pivotal in propelling me towards my ultimate objective along this arduous and demanding trajectory. I am grateful for their patience, constructive feedback, and motivation.

Furthermore, I would like to express my gratitude to Prof Mohan Jacob for monitoring my situation during the period of the global pandemic, when I was unable to return to Australia to continue my research. My gratitude extends to Prof Lin Schwarzkopf and Prof Susan Laurance for their constructive and valuable comments before and during my pre-completion seminar. I am deeply indebted to Daniel Keane for setting up the CO_2 glasshouse experiment and undertaking the gas exchange measurements.

During this extended period, I had the privilege of meeting several esteemed researchers, including Dr. Oliver Binks, Dr. Alice Gauthey, Dr. Habacuc Flores-Moreno, and Sophie Zwartsenberg. I recall with great fondness the invaluable experiences gained from the fieldwork done across Queensland, Australia. These experiences have provided me a great deal of insight on ecology, which I believe will prove invaluable in my future endeavours.

I would also like to express my sincerest gratitude to Dr. Sourav Das, who has been, and continues to be, one of my most valuable supporters here in Australia. From the outset of my doctoral studies, he has provided guidance and assistance as a friend, brother, and academic mentor. I hope this unwavering support will continue in the future.

I would like to express that this thesis would not have been possible without the constant support and sacrifices of my family, in particular my wife Shila and my parents, to whom I am deeply indebted. I would like to express my sincerest gratitude to these individuals, who have provided me with unwavering support throughout this endeavour.

My sincere gratitude to my research colleagues and friends with whom I have had the privilege of sharing this journey which was not restricted to only academic activities. Dr. Yoko Ishida and Andrew Gray-Spence have exceeded the boundaries of mere academic colleagues to become cherished friends. Despite the briefness of our time together, Dr. Kelly Trinh and Tom, I am grateful for the meaningful interactions we had and hope that our friendship will endure. I would like to express my gratitude to my colleagues from the Plant Ecophys Lab, Nahid Farha, Tombo Warra (with whom I converse about fishing more than anything else), Kali Middleby, Dr. Nara Vogado, Dr. Arun Singh Ramesh, and Dr. Ana Palma, for their invaluable support and companionship.

I am grateful to my extensive network of friends at the postgraduate centre and in Cairns, including Sophie, Dr. Ting Li, Dwi Sugiharti, Nero, Sid, Sara, Melinda, Janine, Abdullah, Phuntsho, Benedict, Sher, Jayden, Roosje, Xenia, Sebastian, Dr. Maria, Andrew, and Denise. Their presence has made life more enjoyable. I am also thankful for the support of my housemates, Christine and Sean, who made my daily life comfortable and enjoyable. I express my gratitude to the Bengali community in Cairns (both Bangladeshi and Indian residents) for their hospitality and involvement in various occasions, which helped me avoid feelings of homesickness.

In conclusion, I would like to express my gratitude to the College of Science and Engineering at James Cook University for awarding me a research scholarship, as well as to the academic services staff and individuals from the Graduate Research School for their assistance during my tenure at JCU. Financial support from ARC grants during my candidacy extensions was instrumental and is greatly acknowledged.

Statement of the Contribution of Others

The work contained in this thesis has not been previously submitted to meet requirements for an award at this or any other higher education institution. To the best of my knowledge and belief, the thesis contains no material previously published or written by another person except where due reference is made.

The glasshouse experiment for chapter 4 of this thesis was setup and measurements were carried out by Daniel Keane under the guidance and assistance of Prof Lucas Cernusak and Dr Alex Cheeseman. The other data chapters (Chapter 2 and 3) were planned and designed by the author under the guidance of Prof Lucas Cernusak. Samples were processed by the author. Sample analyses were done at the JCU Advanced Analytical Centre (AAC) in Cairns, Australia. Data analysis and interpretation were made by the author with assistance from Prof Lucas Cernusak and Dr Alex Cheeseman. The chapters were written by the author, supported and reviewed by Prof Lucas Cernusak and Dr Alex Cheeseman.

Signature: _____

Date: 11/07/2024 _____

Abstract

The ability of any plant species to acclimate to resource constraints or environmental stress is determined by its inherent capacity to demonstrate phenotypic plasticity, which is itself shaped by evolutionary adaptation across geological time scales. Australia, having been geographically isolated since it separated from Gondwana, features regions with stable, ancient soils. The continent's diverse climatic conditions and the unique evolutionary pressures resulting from its isolation have allowed plant species to evolve across the island continent, leading to the development of Australia's unique native flora. It offers an ideal testing ground to explore how environmental stressors interact and how pre-adaptation, adoption of new biological function without evolutionary modification, determines the limit of species acclimation potential.

Within my thesis I used continental scale transects to explore how edaphic factors, including soil phosphorus and nitrogen, may not only modulate the observed response of plant water use efficiency across gradients in precipitation, but determine why species from across Australia show different responses when grown under common garden conditions. Subsequently, in short term manipulative experiments, I further investigated how physiological responses to drought and elevated temperatures vary across plant species adapted to different rainfall regimes, and how marked differences in photosynthetic and stomatal activity between Australian angiosperms and gymnosperms dictate their responses to elevated CO_2. Taken as a whole, my findings emphasise the importance of assessing the ability of plants to acclimate their physiological responses to a changing environment – driven by both deep phylogenetic divergences (i.e. gymnosperm vs angiosperm) and more recent evolutionary adaptation (i.e. speciation) to local environments.

Table of Contents

List of Tables

List of Figures

CHAPTER 1: INTRODUCTION

1.1 Background

1.1.1 Acclimation of Plant Eco-Physiological Strategies Under Environmental Stressors and Resource Limitations.

Natural selection is expected to have shaped plant eco-physiological strategies to utilise resources more or less efficiently, dependent on their relative availability, where more efficient utilization of limited resources are strongly selected for and vice versa (Stock, 2014). Such adaptive measures enable plants to optimise their performance and survival under varying environmental conditions (Chesson & Huntly, 1997). This involves adjustments in how resources are allocated, how physiological processes operate, and how plants respond to environmental signals (Chaves *et al.*, 2003). In the shorter term, this is generally accomplished through phenotypic plasticity. Understanding how plant adaptation has shaped their acclimation potential is crucial to predicting how they will perform and how ecosystems may function in a changing environment.

Environmental factors, including temperature, drought, and elevated [CO_2], can greatly impact the physiological processes of plants (Qaderi *et al.*, 2006; Wang *et al.*, 2012; Kadam *et al.*, 2014). When faced with environmental stress, plants demonstrate various physiological responses that affect their photosynthesis (*A*), respiration (*R*), stomatal conductance (g_s), and water use efficiency (*WUE*). These responses play a significant role in the acclimation and survival of plants in challenging conditions.

Predicting changes in plant eco-physiological strategies is complex in the presence of multiple resource constraints and environmental stressors. The complexity of these interactions creates challenges for understanding and predicting plant responses due to our inadequate understanding of the relevant interactions (Reich, 2014). In a changing climate, plant phenotypic plasticity acts as a buffer and is of key importance in determining plant responses to resource limitations (Nicotra *et al.*, 2010; Stotz *et al.*, 2021). The importance of plastic responses in woody plants under climate change is highlighted by their genotypic variation in growth plasticity at elevated temperatures (Huang *et al.*, 2015).

It is necessary to realize the significance of phenotypic plasticity when predicting changes in species distributions, community composition, and plant productivity (Nicotra *et al.*, 2010). Environmental stressors can impact a species by pushing the organism beyond its tolerance limits, altering metabolic processes under the new conditions, or disrupting patterns of development and reproduction (Qaderi *et al.*, 2006; Wang *et al.*, 2012). The capacity to withstand and acclimate to a quickly changing environment is essential for survival, but the

particular mechanisms and responses can be complex and challenging to anticipate (Hofmann & Todgham, 2010). Acclimation is the process by which plants adapt their physiological and biochemical processes in response to alterations in their environment. During acclimation there are changes to several elements of plant physiology, encompassing photosynthesis, respiration, phenology, and anatomical characteristics (Matthews & Boyer, 1984; Murchie *et al.*, 2002; Loveys *et al.*, 2003; Atkin *et al.*, 2006; Nicotra *et al.*, 2010; Vitasse *et al.*, 2010; Wang *et al.*, 2011; Fonti *et al.*, 2012; Gratani, 2014; Sanad *et al.*, 2016; Qurani & Yoshimura, 2021).

Furthermore, interactions between constraints on resources and environmental stressors may have domino effects on ecological dynamics (Hu *et al.*, 2023). It is important to understand forest-environment interactions within the framework of climate change for predicting species suitability, competition for restricted resources, and species distributions (Hu *et al.*, 2023). The ability of plants to adjust to fluctuating environmental conditions impacts their resource use efficiencies. Environmental stressors, such as heatwaves and water limitations, have the potential to interact with plant evolutionary strategies and influence resource allocation strategies utilised by plants.

1.1.1.1 Plant acclimation to change in temperature

Despite Earth System Models typically using static responses to temperature to calculate photosynthesis and respiration, experimental evidence suggests that many plants acclimate to prevailing temperatures (Lombardozzi *et al.*, 2015). Certain species are able to cope with rising temperatures by experiencing a sudden increase in g_s. This mechanism helps to cool leaves and keep the leaf temperatures below their thermal limit, thus enabling them to survive heatwaves (Drake *et al.*, 2018). Furthermore, studies have shown that plant respiration can acclimate to changing temperatures, which weakens the positive feedback of plant respiration to rising global air temperature (Reich *et al.*, 2016). Higher temperatures can have a negative impact on respiration and photosynthesis (Berry & Björkman, 1980; Graham *et al.*, 2003; Leakey *et al.*, 2003; Doughty & Goulden, 2008; Galbraith *et al.*, 2010). This can lead to a decrease in tree growth (Clark *et al.*, 2003; Feeley *et al.*, 2007) and an increase in plant mortality (Van Mantgem *et al.*, 2009; Brodribb *et al.*, 2020), which in turn affects net primary productivity (NPP).

The combined effects of high temperature and drought stress on flora are distinct and cannot be extrapolated from the responses observed in each stressor applied separately (Prasad *et al.*, 2011). For example, depending on the precipitation pattern, the physiological responses of plants to drought and elevated temperatures can vary (Zandalinas *et al.*, 2018). Elevated air temperatures can worsen the effects of drought on plant water loss by increasing the vapor

pressure deficit (VPD) of the atmosphere which leads to a greater demand for transpiration (McDowell *et al.*, 2008).

1.1.1.2 Plant acclimation to drought stress

Drought stress can trigger diverse physiological and biochemical reactions in plants at the cellular and whole-organism levels, making it a multifaceted phenomenon (Farooq *et al.*, 2009; Meena & Kaur, 2019). It can cause mortality of mature tress as well as seedlings. In fact, seedlings are highly susceptible to environmental stresses making this the most vulnerable life stage; hence, the dynamics of a plant community have a strong dependence on the fate of seedlings (Will *et al.*, 2013; Johnson *et al.*, 2017). Plant species distributions, along different precipitation gradients, are mainly controlled by their drought tolerance thresholds, with drought induced hydraulic dysfunction leading to tree mortality (Cochard *et al.*, 2013). Severe prolonged droughts might lead to change in forest productivity, growth and species composition as well as increased mortality of drought-stressed species and dispersion of drought tolerant species (Nepstad *et al.*, 2007; Corlett, 2016; Esquivel-Muelbert *et al.*, 2017), leading to a reduction in ecosystem carbon storage (Choat *et al.*, 2012; Will *et al.*, 2013; Apgaua *et al.*, 2019). Additionally, climatic variation plays an important role in maintaining hydraulic traits within diversified species. Drought tolerant species have cavitation resistance capacity or ability to close their stomata early in case of water deficient conditions (Li *et al.*, 2018; Trueba *et al.*, 2019).

Plants in their natural environments adjust to drought stress through different mechanisms, including temporary responses to low soil moisture and survival mechanisms like early flowering in the absence of seasonal rainfall (Kurten *et al.*, 2018). Isohydric plants have adopted a more conservative water use strategy than anisohydric plant species. They close their stomata early at the beginning of a drought. This way they can maintain relatively persistent leaf water potential as soil water content tends to decline. However, this strategy reduces carbon dioxide (CO_2) uptake, which directly limits photosynthesis. Over prolonged drought, the reduction in carbon assimilation can lead to carbon starvation, where the plant lacks sufficient energy reserves to sustain growth and maintenance functions (McDowell, 2011). In case of anisohydric plants, they maintain open stomata although it causes reduction in leaf water potential as soil becomes drier as the drought progresses increasing the risk of hydraulic failure (Li, Ximeng et al., 2019). This can induce xylem cavitation and embolism, potentially resulting in irreversible damage to the plant's vascular system. Such risks place anisohydric plants at a significant disadvantage in environments characterized by prolonged drought or extreme heat, where the increased likelihood of hydraulic failure and dehydration ultimately outweighs the benefits of sustained carbon assimilation.

At the initiation of drought, plants close stomata reducing water loss through transpiration (Li *et al.*, 2018). Gradual stomatal closure helps plants to minimize water loss. This aids in slowing xylem water potential reduction (Nolf *et al.*, 2015). Drought responses like wilting or xylem conductivity loss occur with further intensification of drought stress (Bartlett *et al.*, 2016). During prolonged drought, acclimation responses like osmotic pressure adjustment occur by accumulating solutes in plant leaves. This is a strategy used to maintain turgor pressure when xylem water potential is low (Hsiao *et al.*, 1976; Chen & Jiang, 2010; Harb *et al.*, 2010; Blum, 2017). Plants follow strategies like releasing water from living cells into the transpiration stream to increase the water potential, mitigate developing xylem embolism and hence delay drought stress effects (Gleason *et al.*, 2014; Pfautsch *et al.*, 2015). As the drought persists, plants continue to dehydrate through leaky stomata, leaf and root cuticles (Brodribb *et al.*, 2017; Schuster *et al.*, 2017; Blackman *et al.*, 2019). Severe loss of hydraulic functioning occurs, due to dehydration, and leads to photosynthetic capacity damage (Trueba *et al.*, 2019; Marchin *et al.*, 2020). Consequently, tension within the plant hydraulic system continues inducing cavitation and expansion of air bubbles. Persistent embolism may cause carbon starvation in addition to whole plant dehydration (Li *et al.*, 2018), and high evaporative demand may cause systemic vascular failure leading to rapid plant mortality through desiccation (Choat *et al.*, 2018).

Drought stress can limit photosynthesis by decreasing g_s, which restricts the flow of carbon dioxide into the leaves to balance carbon assimilation and water loss (Zhao *et al.*, 2013; Feller, 2016). Respiration, another crucial process in plants involving the breakdown of carbohydrates to produce energy, could also be reduced under drought stress (Chen *et al.*, 2021).

Under drought stress, plants may show increased intrinsic *WUE* by reducing g_s to limit water loss (Yin *et al.*, 2006). Plants with higher *WUE* can regulate their stomatal function efficiently to decrease transpiration rates (Brodribb & Holbrook, 2003), ultimately leading to less water loss per unit of carbon gained. This adjustment is especially crucial in locations where water resources are scarce. Species with different *WUE* strategies may show diverse competitive abilities and niche preferences, leading to shifts in community composition along environmental gradients.

1.1.1.3 Plant acclimation to edaphic conditions

Plants exhibit a wide range of responses to different edaphic conditions, highlighting their ability to adjust to the soil they grow in. They can adapt to specific soil conditions by establishing a complex association with soil biota, including mycorrhizal fungi (Máčel *et al.*, 2007;

Rúa *et al.*, 2016). The spatial variation in plant traits is also a major driver of the variation in edaphic conditions. Additionally, hydro-edaphic conditions have been observed to significantly affect the composition and richness of plant species (Tuomisto *et al.*, 2014). Plants receive water and nutrients from soils. To produce one gram of dry biomass a plant typically consumes around 300 g of water (Wong *et al.*, 2022). But when water content is reduced in soil, plants are physiologically and biochemically affected in many ways (Sarker *et al.*, 2005). Changes in precipitation and temperature patterns due to climate change will result in frequent and intense droughts in the near future. Plants with different hydraulic strategies react to precipitation changes as well as soil-water content availability in ecosystems and acclimate their resource use efficiencies along precipitation gradients (Limousin *et al.*, 2015). Hydraulic strategies may develop as a result of long-term generational adaptation or short-term acclimation to various environmental stresses. One such strategy is the hydraulic lift mechanism which enables plants to transport water from moister to drier soil layers through their root systems. Deep rooted plants are found to utilize this strategy contributing significantly into evapotranspiration as well as supporting the neighbouring shallow-rooted species (Caldwell *et al.*, 1998). This process is essential for the survival of many plant species in various environments having important impacts on plant water balance, nutrient mobilisation and competition for space and nutrients between plants (Dawson, 1993). Moreover, it has been found that with changes in soil moisture plants can adjust their g_s to optimize their water use efficiency (*WUE*) (Linares & Camarero, 2012; Boyle *et al.*, 2016). Night-time transpiration is another highly effective strategy that can significantly improve nutrient uptake in plants growing in nutrient-poor soils (Scholz *et al.*, 2007; Snyder *et al.*, 2008).

Nutrient availability in soil determines the properties of vegetation communities in natural ecosystems (Funk & Vitousek, 2007; Zhao *et al.*, 2023). When multiple resource limitations interact, as an example in nitrogen (N) and phosphorus (P) limited soils, plants might adjust their resource use pattern to utilize available limited resources more efficiently (Reich *et al.*, 2009; Ellsworth *et al.*, 2022). Moreover, drought causes reduction of water availability in soil which leads to plant nutrient deficiency, even in fertilised soils, as nutrient mobility and absorption are reduced, making it an important stress factor causing global plant mortality (Da Silva *et al.*, 2013). It is assumed plants can transport growth-limiting nutrients to root surfaces through mass flow of the soil solution. This has been tested for nitrogen (Cramer *et al.*, 2008; Cramer *et al.*, 2009), and phosphorus (Cernusak *et al.*, 2011b; Huang *et al.*, 2017; Aoyagi *et al.*, 2022). According to an optimal growth model, it is suggested that plants may need to adjust resource allocation to different plant functions in order to optimise growth under resource

constraints (Schwinning & Weiner, 1998). This could result in a reduced growth rate, altered leaf area, or reduced photosynthetic capacity (Eskelinen & Harrison, 2015). Furthermore, the constraints of limited resources can also influence the competitive dynamics among various species in the ecosystem (Rees *et al.*, 2001). Such limitations may favour certain species over others based on their responses to the limited resources.

1.1.1.4 Plant acclimation to changing atmospheric CO_2 concentration

Plants acclimate to changing CO_2 concentrations, with studies suggesting that different plant species acclimate to different degrees. Extended periods of elevated CO_2 exposure may not substantially affect plant CO_2 uptake (Sage, 1994), while short-term exposure typically results in an increased rate of photosynthesis (Amthor, 1995). This may represent an acclimation strategy that allows plants to efficiently balance resource limitations with the maintenance of other physiological processes (Tissue *et al.*, 1993).

Plant responses to changing CO_2 concentrations vary significantly, depending on exposure duration, species as well as how they interact with other environmental variables like temperature and droughts. Atmospheric CO_2 levels may influence g_s and *WUE* responses to drought and heat stress (Li, Xiangnan *et al.*, 2019). It has been found that drought and elevated temperature effects on plants can be mitigated by elevated levels of CO_2 which eventually reduce g_s and water loss while maintaining photosynthesis (Duan *et al.*, 2014). Increased atmospheric CO_2 reduces plant mortality risk during drought by modifying plant hydraulics as *WUE* is increased with higher available CO_2 (Liu *et al.*, 2017; Apgaua *et al.*, 2019).

Anticipating alterations in plant eco-physiological responses poses greater difficulties when several resource constraints and environmental burdens interconnect. The complex interplay and subsequent feedbacks between these factors hinder precise forecasting of plant reactions and their impact on ecosystem behaviour.

1.1.2 Inherent Ability and Evolutionary Adaptation for Acclimating Physiological Responses to Environmental Change

Plants have the remarkable ability to acclimate their physiological responses to a changing environment, and this ability depends on their inherent capacity. The ability of plants to acclimate is predetermined by their genetic composition and phenotypic flexibility (Boyko & Kovalchuk, 2011). This acclimatation capacity could empower plants to enhance their resilience to impending climate change, providing them the capability to regulate their physiological processes in tandem with changing climate. Plants have developed diverse mechanisms, in response to environmental conditions and selective pressures, like alterations in g_s (Drake *et al.*,

1997), photosynthetic rates (Matthews & Boyer, 1984; Murchie *et al.*, 2002; Atkin *et al.*, 2006), leaf traits (Edwards, 2006; Xue *et al.*, 2017), and physiological processes (Maherali *et al.*, 2004). Genetic diversity is fundamental in determining a plant's capacity to sense changes in its surroundings and generate an adaptive response (Nicotra *et al.*, 2010). Different plant species demonstrate varying degrees of acclimation capacity, with certain species exhibiting greater plasticity than others (Athanasiou *et al.*, 2009). This genetic diversity enables plants to acclimatize to distinct environmental conditions and bolster their innate capabilities against future change in climate (Vitasse *et al.*, 2010).

Phenotypic plasticity, the capacity of an organism to produce distinct phenotypes in response to environmental stimuli, represents a fundamental mechanism by which plants adjust to shifting environments (Nicotra *et al.*, 2010). Plants can undergo large adjustments in the timing of phenological events, including flowering and leaf senescence, in reaction to temperature alterations, for example (Vitasse *et al.*, 2010). Furthermore, phenotypic plasticity provides plants with the ability to regulate their physiological functions, including photosynthesis and respiration, to enhance their efficiency in varying environmental circumstances (Matthews & Boyer, 1984; Murchie *et al.*, 2002; Atkin *et al.*, 2006).

The acclimation potential of angiosperms and gymnosperms, two major groups of plants, differs due to their evolutionary history and traits. Angiosperms, or flowering plants, have diversified and become dominant in many ecosystems. They have undergone substantial evolutionary changes, including the emergence of flowers and fruits, which have enhanced their ability to acclimate and thrive. These adaptations have enabled angiosperms to adapt to diverse environmental conditions and exploit novel ecological niches (Onstein, 2019). In contrast, gymnosperms, encompassing gymnosperms and cycads, exhibit a reduced capacity for acclimation as opposed to angiosperms. Gymnosperms face functional limitations in their growth rates, which has confined them to regions with reduced growth in angiosperm rivals, such as cold or nutrient-scarce environments (Bond, 1989). Gymnosperms exhibit unique characteristics that differentiate them from angiosperms, specifically their capacity to adapt to harsh conditions (Li *et al.*, 2020). Nonetheless, gymnosperms have a comparatively slower evolutionary pace than angiosperms and underwent significant extinctions in the Cenozoic period (66 million years ago until now), which significantly reduced their diversity and adaptability (Crisp & Cook, 2011).

The variance in acclimation potential between angiosperms and gymnosperms can be linked to the different rates of molecular evolution. Gymnosperms exhibit lower rates of

molecular evolution than angiosperms, which could account for their relatively sluggish adaptation to shifting environments (De La Torre *et al.*, 2017). Furthermore, during the Cretaceous period (145 to 66 million years ago), angiosperms experienced a significant increase in the evolution of leaf veins, leading to an enhancement in their ability to acclimate compared to gymnosperms (Feild *et al.*, 2011). It is evident that the rate of climate change may hinder plants' genetic adaptation, leading them to become more reliant on their acclimation capacity (Fonti *et al.*, 2012). Moreover, plant acclimation can be influenced by factors like water and nutrient availability, as well as the severity and duration of environmental stressors (Franks *et al.*, 2013). It is important to understand these factors to investigate how plants adapt and respond to altering environments.

Research has established noteworthy connections between leaf-specific xylem hydraulic conductivity, stomatal pore index, leaf venation density, and leaf size (Edwards, 2006). These characteristics are believed to co-evolve. Additionally, it is widely acknowledged that the development of cuticular wax is crucial in enabling plants to retain water in arid environments, thus constituting a significant adaptive characteristic for terrestrial plants (Xue *et al.*, 2017). Furthermore, the efficacy of a plant's water use can also be attributed to its ability to withstand xylem cavitation. The susceptibility of plants to xylem cavitation can vary across species and is impacted by evolutionary factors (Maherali *et al.*, 2004). Comprehending the evolutionary origin and environmental relevance of xylem transportation and cavitation endurance can improve forecasts of plant water utilisation in response to environmental changes.

The acclimation capacity of vegetation is not boundless and is limited by various factors. Their ability to adapt can be affected by factors such as population size, resource availability and the pace of climate change. It has been demonstrated that a greater ability to develop local adaptation and adjust to changing environments is possessed by larger plant populations (Leimu & Fischer, 2008). Savannah species have the ability to recover from short-term moderate to severe drought and thus can tolerate higher intensity of drought compared to forest species (Fensham *et al.*, 2009). This drought tolerance ability of savannah species results from several factors including higher and faster re-sprouting ability, enhanced flowering and seeding, and ability to withstand fires (Sankaran, 2019). On the other hand, species in the forest-savannah ecotone play a crucial role in ecosystem dynamics and are likely to face rapid changes. These changes might be fast enough to override the adaptation speed of ecological processes, leading to significant changes in forest dynamics (Donoghue & Edwards, 2014; Oliveras & Malhi, 2016). This understanding can provide valuable insights into the ability of plants to survive and thrive in the future changing environment in different habitats.

1.1.3 Australian Native Flora and Climate Change

The geological stability of Australia has facilitated the development of diverse soil compositions throughout the continent (Viscarra Rossel & Bui, 2016). Additionally, Australia consists of diverse climatic conditions characterised by a wide range of rainfall regimes, which greatly influence the diversity of flora across the continent. This variation in climate yields distinct ecological niches for different plant species, enabling the evolution of a wide array of unique native flora (Hellmuth, 1971; Crisp & Cook, 2013).

Plant nutrient-acquisition strategies alter with soil age. Older soils often suffer from weathering and nutrient depletion, while younger soils are usually more fertile (Lambers *et al.*, 2008). This divergence in soil composition has impacted the distribution and adjustment of plant species in Australia.

The correlation between rainfall and plant diversity is complex and can be impacted by multiple elements, such as soil type, vegetation structure, and disturbance regimes. As an example, in the south-eastern Australian woodlands, rainfall gradients, vegetation, and soil furnish a basis for fire occurrence due to continuous accumulation of surface-litter on a regular basis (Gibson *et al.*, 2015). Additionally, annual rainfall, soil texture, and forestry practices influence the cover and diversity of biological soil crusts in arid and semi-arid woodlands (Thompson *et al.*, 2006). These crusts play a crucial role in soil stability and nutrient cycling, and their presence or absence can have significant effects on plant diversity.

Australia's rich flora has its origins in the ancient southern supercontinent of Gondwana. During the Cretaceous period, when Australia was covered in subtropical rainforest, the modern Australian flora began to take shape (Dettmann & Jarzen, 1990). Early Gondwanan angiosperm flora, including Myrtaceae, Proteaceae, and Fabaceae, are present in Australia. During the Oligocene period, from 25 to 10 MYA, there was a rapid succession of species such as Eucalyptus, Casuarina, Allocasuarina, and Banksia, which led to the development of open forests (Crisp *et al.*, 2004).

In recent time, most of the Australian landscape is dominated by eucalypts making them iconic Australian forest trees. Almost 77% of Australia’s total native forest land is covered by different types of eucalypts. About 800 species from three genera- *Eucalyptus*, *Corymbia* and *Angophora*- comprise the eucalypts. Eucalypts have evolved from their rainforest ancestors, becoming especially well adapted to drought, nutrient-poor soils, and frequent fire (Crisp & Cook, 2013). Despite their wide distribution, research has shown that many eucalypts are found within a narrow bio-climatic zone (Hughes *et al.*, 1996); more than 20% of all eucalypt species

have a distribution range that extends across <1°C and experience less than a 20% variation in rainfall. The evolution of range size in eucalypts was significantly influenced by traits related to physiological tolerance and life history (Mathews & Bonser, 2005). Several different diversified mechanisms to cope with drought stress by eucalypt trees have been reported by researchers (White *et al.*, 2000; Callister *et al.*, 2008). In response to drought the primary structural adaptation of some eucalypt species is to shed leaves to reduce leaf area and increase root length to go deeper under-ground in search of water (Dye, 1996; Silva *et al.*, 2004).

Southern gymnosperms as well as Australian endemic gymnosperms have proven their ability to compete effectively with angiosperms in a wide range of habitats (Hill & Brodribb, 1999). They have evolved in geographically isolated regions and have successfully competed with angiosperms. Again, the harsh environmental conditions in Australia may favour stress tolerance over performance, such that gymnosperms successfully tolerate areas with poor soil, drought conditions, or extreme climates (Folk *et al.*, 2020). This is because gymnosperms are more resilient in nutrient-poor and low-water conditions, a trait that is enabled by slower growth rates and lower nutrient requirements. They have evolved under different pressures compared to their northern counterparts (Shindo *et al.*, 1999; Brown *et al.*, 2021). Their fire adaptability, unique evolutionary traits and symbiotic relationships with mycorrhizal fungi as well as lower competitive pressure from angiosperms enabled southern gymnosperms to retain a prominent ecological role. In contrast, Northern Hemisphere gymnosperms faced greater competition from rapidly evolving angiosperms, which diversified faster and occupied a broad range of ecological niches, limiting gymnosperms primarily to harsher or colder climates where angiosperms struggled to compete (Brodribb *et al.*, 2012).

Since 1910, Australia's climate has become warmer by over 1.47 ± 0.24°C (std. deviation) (CSIRO and Bureau of Meteorology, 2022) and is anticipated to increase by 2.8-5.1°C by 2090 (CSIRO and Bureau of Meteorology, 2015). It is expected that regional heatwaves will be longer, more frequent, and warmer because of climate change (Perkins-Kirkpatrick & Lewis, 2020). This magnitude of change in climate will place most of the plants at the edge of their thermal tolerance. According to Brodribb *et al.* (2020), a temperature increase of 5°C by the end of this century could result in a decline of almost 60% in the global tree population unless they acclimate to the changing environmental conditions.

The response of plants to changes in temperature is a complex matter as different species may exhibit varying immediate responses to leaf temperature, while also potentially undergoing a less well-established acclimatory response to the average growing temperature

(Duursma *et al.*, 2019). Moreover, it is evident that plants have the ability to adapt to seasonal or spatial changes in growth temperature by modifying their short-term temperature response of respiration (Sturchio *et al.*, 2021). It is crucial to consider these behaviours when studying the effects of temperature on plant growth and development. For better understanding of the resilience of the unique plants in Australia, it is essential to understand their physiological responses under different environmental stressors. Hence, Australia offers a unique opportunity to investigate the interplay between environmental stressors and the extent to which their evolutionary adaptation defines the limits of species' acclimation potential.

1.2 Objectives

The Australian continent has not faced any major geological disturbances for millions of years, resulting in significant differences in soil and climatic patterns as well as unique native plants across the continent. It provides a perfect place for investigating how plants respond to environmental challenges and to explore their ability to acclimate to new environmental conditions, such as those being ushered in by climate change. Keeping that in mind, my thesis aims to better understand how Australian native plants, such as eucalypts and endemic angiosperms and gymnosperms, with different inherent adaptations adjusted to environmental changes by acclimating their physiological responses. I aimed to answer the following questions:

i) How does the water-use efficiency of trees across Australia respond to precipitation and soil nutrients? And how is this response modulated by their adaptive histories?

ii) How do saplings of eucalypt species from different rainfall regimes physiologically respond to drought and elevated temperatures?

iii) Do angiosperms and gymnosperms acclimate differently to elevated CO_2, potentially reflecting their different evolutionary histories?

1.3 Thesis Structure

This thesis is structured into 5 chapters; in this first chapter I reviewed plant eco-physiological adaptation and acclimatation under different environmental stresses. I aimed to establish the context for how several multiple stressors might interact and how plants acclimate through their physiological responses.

In Chapter 2, I analyse several transects along different rainfall gradients across Australia, exploring how plant water-use efficiency differs and what the modulating factors are behind this variation. Here carbon isotope discrimination ($\Delta^{13}C$) was used as a proxy for plant water-use efficiency. I considered climatic parameters as well as soil nutrients to find potential explanatory variables. These results were then compared with those of two common garden experiments. Finally, an Australia-wide leaf gas-exchange dataset was used to show how soil nutrients influence water-use efficiency of plants. Thus, I aimed to address objective (i) in Chapter 2.

In Chapter 3, I further investigate the short-term physiological responses to drought and elevated temperatures in several eucalypt species adapted to different rainfall regimes. I collected seedlings of four different eucalypts covering a wide precipitation range across Australia and setup a glasshouse experiment where plants were grown under controlled temperature and water stress, thus aiming to address objective (ii). This experiment provided insights into dark respiration, minimum leaf conductance and cuticular conductance.

In Chapter 4, I present another glasshouse experiment with Australian angiosperms and gymnosperms grown under different CO_2 concentrations. Here, I explored how pre-adaptation and evolutionary constraints determine acclimation potential in response to elevated CO_2. Objective (iii) was addressed in this chapter.

In Chapter 5, I provide a general overview of the research results, highlighting their significance, relevance and potential implications. The chapter aims to highlight the contribution of this thesis to the field of plant eco-physiology and to stimulate further exploration of the additional questions raised by the research presented in this thesis.

CHAPTER 2: SOIL PHOSPHORUS DRIVES DIVERGENT PATTERNS IN INTRINSIC WATER-USE EFFICIENCY OF TREES ACROSS AUSTRALIA

Abstract (Chapter 2)

Several transects have been established to study the sensitivity of intrinsic water-use efficiency, as inferred from carbon isotope discrimination ($\Delta^{13}C$), to mean annual precipitation (MAP) in Australia. These have shown a surprising divergence in sensitivity of $\Delta^{13}C$ to MAP among regions. Here, I combine these previous observations with measurements along a new transect in northeast Queensland to show that such sensitivity depends on regional-scale soil phosphorus (P) concentrations. In P-poor regions, $\Delta^{13}C$ decreases less with decreasing MAP, and correspondingly water-use efficiency increases less, than in P-rich regions.

To identify the potential mechanisms underlying this observed divergence I first examined two contrasting transects in northern Australia in more detail. Here I show that leaf $\Delta^{13}C$ correlates with leaf [P] in the P-poor Northern Territory, but not in P-rich northeast Queensland, where it rather correlates with leaf [N]. This demonstrates the influence of both [N] and [P] availability on $\Delta^{13}C$ and thereby inferred water-use efficiency across Australian ecosystems. Furthermore, using an Australia-wide leaf gas-exchange dataset, I show that soil [P] influences the ratio of intercellular to ambient CO_2 concentrations (c_i/c_a), which in turn controls $\Delta^{13}C$, and I find this trend to be driven by changes in stomatal conductance (g_s), rather than by photosynthetic capacity. I hypothesize that some Australian woody plant species have evolved to use high transpiration rates in P-impoverished, ancient soils to facilitate [P] foraging. To further demonstrate this evolutionary strategy, I highlight results from two common-garden experiments, one established in the P-limited Northern Territory and one in P-rich New South Wales which showcase divergent behaviour of species adapted to differences in regional-scale soil [P] status when grown under common conditions of water availability.

2.1 Introduction

Along a gradient of resource availability, plant ecophysiological strategies can be expected to be favoured that use the resource more efficiently as its availability declines. Plants can be expected to conserve and recycle resources, such as water and nutrients, to maximize their growth and productivity when there is a scarcity of any of those resources. Water availability provides one such example, in which water-use efficiency (*WUE*) typically increases in response to increasing environmental aridity. At the leaf-level intrinsic water-use efficiency (WUE_i), defined as the ratio of photosynthesis (A) to stomatal conductance (g_s), provides an index of the amount of CO_2 fixed for a given amount of water lost to the atmosphere at a standardised leaf-to-air vapour pressure difference.

Measurements of carbon isotope discrimination ($\Delta^{13}C$) of plant dry matter can be used to infer WUE_i over the time period the plant tissues were formed (Farquhar & Richards, 1984). This technique has been used to assess intrinsic water-use efficiency of plants grown in common environments (Richards *et al.*, 2002; Cernusak *et al.*, 2007; Rebetzke *et al.*, 2008), as well as along resource gradients (Brooks *et al.*, 1997; Guehl *et al.*, 2004; Cernusak *et al.*, 2009). The term $\Delta^{13}C$ is the discrimination against the ^{13}C isotope which occurs during the conversion of atmospheric CO_2 to plant biomass via photosynthesis and can be related to leaf gas exchange as in equation 2.1 (Farquhar *et al.*, 1982; Farquhar *et al.*, 1989):

$$\Delta^{13}C \approx a_s + (\bar{b} - a_s)\frac{c_i}{c_a} \qquad \text{(Equation 2.1)}$$

where a_s is the $^{13}C/^{12}C$ fractionation during diffusion through stomata (4.4‰), $\bar{b}$ is discrimination against $^{13}CO_2$ by carboxylating enzymes (~27‰) and c_i/c_a is the ratio of the intercellular to ambient CO_2 concentrations.

Additionally, the ratio of $^{13}C/^{12}C$ in plant tissues is typically represented as $\delta^{13}C$. This is derived from measuring the relative deviation of sample's isotope ratio compared to the internationally known standard, Vienna Pee Dee Belemnite (VPDB). To relate the $\delta^{13}C$ of plant tissue to c_i/c_a, equation (2.1) can be written as:

$$\delta^{13}C \approx \delta^{13}C_a - a_s - (\bar{b} - a_s)\frac{c_i}{c_a} \qquad \text{(Equation 2.2)}$$

Here $\delta^{13}C_a$ is the $\delta^{13}C$ of CO_2 in the atmosphere surrounding the plant. The intrinsic water-use efficiency (WUE_i) or A/g_s can be related to the term c_i/c_a by equation 2.3,

$$WUE_i = \frac{A}{g_s} \approx \frac{c_a(1-\frac{c_i}{c_a})}{1.6} \qquad \text{(Equation 2.3)}$$

Substituting equation 2.2. into 2.3 provides the capacity to link $\delta^{13}C$ and water use efficiency, with measurements of plant tissue $\delta^{13}C$ providing a time-integrated proxy for A/g_s, and with the advantage over instantaneous gas exchange measurements of improving the signal to noise ratio (Cernusak & Marshall, 2001). This can be written as equation 2.4,

$$\frac{A}{g_s} = \frac{c_a}{1.6}\left[1 - \frac{\left(\delta^{13}C_a - \delta^{13}C - a_s\right)}{\left(\overline{b} - a_s\right)}\right] \quad \text{(Equation 2.4)}$$

The $\delta^{13}C$ can be measured in previously sampled and preserved plant organic material, making it an attractive option for exploring trends in A/g_s across spatial gradients.

Recent global compilations of WUE_i, as inferred from $\delta^{13}C$, support the idea that intrinsic water-use efficiency increases in response to declining water availability (Harrington *et al.*, 1995; Cornwell *et al.*, 2018; Bai *et al.*, 2020; Adams *et al.*, 2021; Towers *et al.*, 2024). This trend has also been found along aridity gradients in Australia (Stewart *et al.*, 1995; Schulze *et al.*, 1998; Miller *et al.*, 2001; Schulze *et al.*, 2006; Givnish *et al.*, 2014; Cernusak, 2020; Driscoll *et al.*, 2020). However, these Australian transects have also shown a surprisingly large variation in terms of the change in WUE_i for a given change in mean annual precipitation (MAP) (Westerband *et al.*, 2023). A similar divergence in the inferred response of water use efficiency occurs if hydroclimate is instead expressed as aridity index (*AI*), the ratio of precipitation to potential evapotranspiration, considered a macro-scale measure of ecosystem water balance (Towers *et al.*, 2024). One potential explanation that has been suggested for regionally variable $\Delta^{13}C$-MAP relationships is that the sensitivity of $\Delta^{13}C$ to precipitation could be influenced by the seasonality of precipitation (Towers *et al.*, 2024). For example, the rainfall distribution in northern Australia shows a large seasonal variation compared to that in south-eastern Australia, with studies having found contrasting responses of $\Delta^{13}C$ to MAP which might be a result of precipitation seasonality (Schulze *et al.*, 1998; Miller *et al.*, 2001; Cernusak *et al.*, 2011a).

Alternatively, the sensitivity of $\Delta^{13}C$ to precipitation could be influenced by interactions with variable soil nutrient availability. Higher nitrogen (N) availability is known to result in lower $\Delta^{13}C$ (i.e. tissue $\delta^{13}C$ that is less negative, or closer to the atmospheric value of approximately -8‰), through its influence on photosynthetic capacity (Garrish *et al.*, 2010; Cernusak, 2020; Ellsworth *et al.*, 2022). While less is known for phosphorus (P), it could also be expected to similarly influence $\Delta^{13}C$ through modification of photosynthetic capacity. Recent evidence has shown the previously assumed strong relationship between *A* and leaf [N] is reduced by a low level of leaf [P] (Reich *et al.*, 2009; Ellsworth *et al.*, 2022). Both [N] and [P] limitation in soils may lead to plants adjusting their resource use patterns to utilize available limited resources more

efficiently. At the same time, it has been hypothesized that plants can use high transpiration rates, resulting in low water use efficiency, to transport growth-limiting nutrients to root surfaces through mass flow of the soil solution. This argument has been made with respect to [N] (Cramer *et al.*, 2008; Cramer *et al.*, 2009), and [P], including organic P-containing compounds from which phosphate could be cleaved by extracellular enzymes released into the rhizosphere (Cernusak *et al.*, 2011b; Huang *et al.*, 2017; Aoyagi *et al.*, 2022). I suggest that this latter mechanism may be particularly relevant in Australian regions where the soils are severely impoverished with respect to soil [P].

The Australian landscape has been unaffected by major geological disturbances for millions of years. Combined with continuous erosion, leaching, and fire, this has left Australian soils deprived of rock-derived nutrients (Viscarra Rossel & Bui, 2016), resulting in some of the most P impoverished soils on Earth (Orians & Milewski, 2007; Kooyman *et al.*, 2017). In the early stages of soil development weathering of exposed minerals increases the amount of plant available soil P. As the soil matures, the amount of available P decreases due to the formation of insoluble minerals and organic compounds (Lambers *et al.*, 2011).

In attempting to determine why differences in *WUE* may be observed across the Australian continent I collated six existing datasets for $\Delta^{13}C$ of trees growing across precipitation gradients and combined them with data for a new transect in northeast Queensland. After accounting for the trend in $\delta^{13}C$ of atmospheric CO_2 in the year of sample collection, I extracted gridded climate and soil data for sampling sites and accounted for differences in the tissue type collected. With the standardized dataset, I then tested for detectable variation in the sensitivity of $\Delta^{13}C$ to MAP among regions. Upon showing that this indeed exists, I then tested for correlations between the regional slope and regional edaphic and climatic characteristics, including precipitation seasonality, soil [N], and soil [P]. Upon finding that soil [P] was the most promising potential driver, I then examined common garden datasets and an Australia-wide dataset of leaf gas exchange to better understand the role of soil [P] in modulating WUE_i responses to precipitation.

2.2 Materials and methods

2.2.1 Transects and sampling details

Data including site location and leaf carbon isotope composition ($\delta^{13}C$) from six previously published sampling transects were collated from the literature (Figure 2.1, Table 2.1) and combined with novel data from a transect in northeast Queensland. All transects started near the coastal regions, where MAP is generally high, and extended into the arid interior of the Australian continent. For the new transect presented here, leaf samples were collected from trees at 11 sites in northeast Queensland, starting near Cairns at the edge of Australian Wet Tropics, and extending to near Boulia, at the edge of the Simpson desert. This transect is approximately 900 km in length, covering a rainfall gradient from about 1700 to 300 mm MAP. Sampling took place during the dry season in 2015 with samples collected from three trees of one eucalypt species at each site. More details of the sampling procedure and site locations are provided in Cheesman and Cernusak (2017). Data on $\delta^{13}C$ of these samples is presented here for the first time.

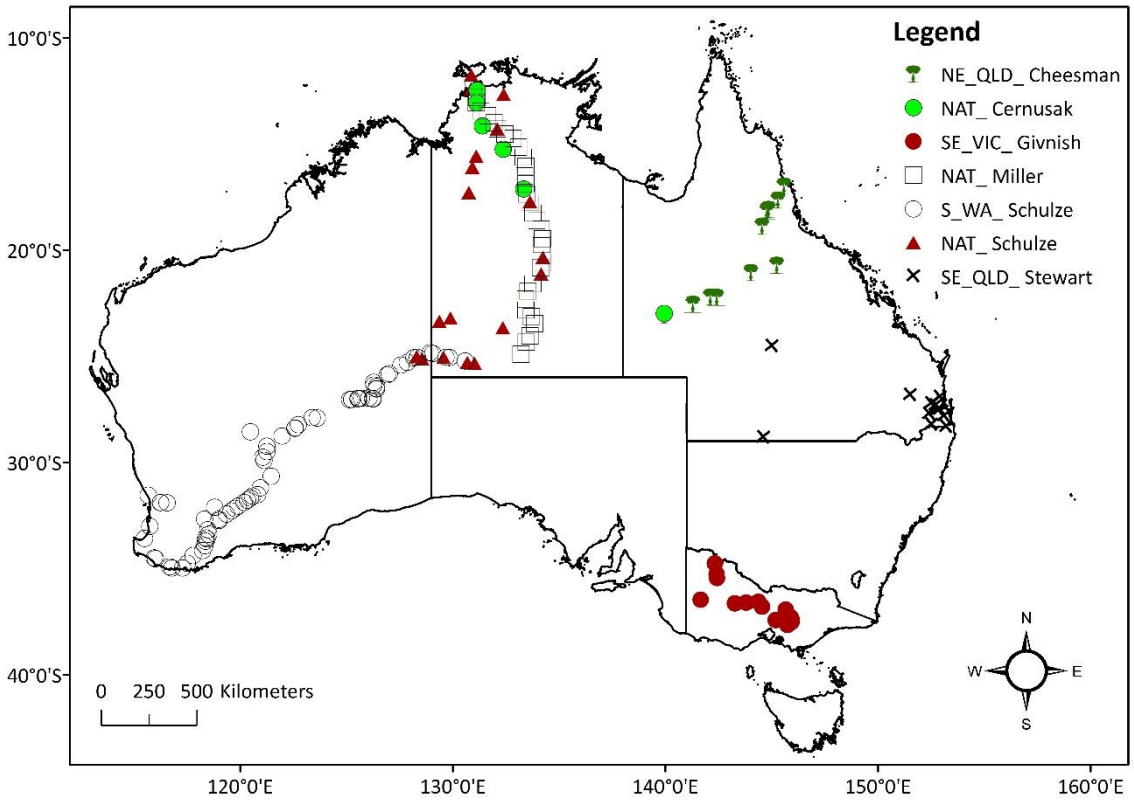

Figure 2.1: Sampling site locations and transects across Australia included in this chapter. Note that there are three sets of samples along a similar transect in the Northern Territory (i.e. NAT-Cernusak, NAT-Miller, NAT-Schulze), which are retained as separate transects given sites, investigators, and methodologies employed differed.

2.2.2 Sample analysis

Leaf samples collected from the northeast Queensland transect (NE-QLD-Cheesman) were oven dried at 60°C and ground to a fine powder (Bench Top Ring Mill, ROCKLABS, New Zealand). The carbon isotope ratios ($\delta^{13}C$, ‰) and leaf [N] (mg g^{-1}) were measured using a ThermoScientific Elemental Analyser coupled via a ConFloIV to a ThermoScientific Delta V PLUS IRMS at James Cook University, Nguma-bada campus (Cairns, Australia). Leaf [P] (mg g^{-1}) was analysed by microwave-assisted acid digestion, followed by detection by inductively-coupled plasma-atomic emission spectrometry (ICP-AES) at the Advanced Analytical Centre, JCU, Bebegu Yumba campus (Townsville, Australia).

Sample analysis procedures for the other transects can be found in the corresponding references shown in Table 2.1. For the transect in Victoria (SE-VIC-Givnish, Table 2.1), stem wood samples were collected instead of leaf samples. Therefore, in order to standardise analyses across the dataset, an offset of −1.5‰ to the wood $\delta^{13}C$ values was applied to make them comparable to leaf $\delta^{13}C$ values (Cernusak & Ubierna, 2022).

For calculating observed isotopic discrimination ($\Delta^{13}C$) of leaf samples, the decreasing trend of $\delta^{13}C$ of atmospheric CO_2 ($\delta^{13}C_a$) has also been considered over the approximately 30-year period of data collection. Estimates of $\delta^{13}C_a$ specific to the period of sampling were used from Cernusak and Ubierna (2022) to calculate $\Delta^{13}C$ as per equation 2.5 where $\delta^{13}C_p$ is the $\delta^{13}C$ of measured plant tissue (Farquhar *et al.*, 1989):

$$\Delta^{13}C = \frac{\delta^{13}C_a - \delta^{13}C_p}{1+\delta^{13}C_a} \quad \text{(Equation 2.5)}$$

2.2.3 Gridded data layers

For each sampling site in the combined dataset, I extracted MAP and annual precipitation seasonality from the TERN Ecosystem Modelling and Scaling Infrastructure (eMAST) data products (Evans *et al.*, 2015) representing a 30-year average (from 1976 to 2005) centred on 1990. Data for each 100 mm MAP band was averaged along each transect to balance the weighting of samples among the transects. The figures illustrating MAP (Figure 2.2a) and precipitation seasonality (quantified using the coefficient of variation; or the ratio of the standard deviation of monthly precipitation to the average monthly precipitation, expressed as a percentage) (Figure 2.2b) were also prepared from eMAST data products. In addition to MAP, I also considered the aridity index (AI), calculated as the ratio of annual potential evapotranspiration to precipitation. The aridity index map (Figure S1) was prepared using the latest global aridity index dataset (Zomer *et al.*, 2022), and values were extracted for each of the sampling sites. In my initial analysis, aridity index was not found to be a stronger predictor in relation to the leaf $\Delta^{13}C$, hence MAP was retained as the favoured explanatory variable and aridity index is not discussed further in this chapter.

The total soil [N] (Figure 2.2c) and total soil [P] (Figure 2.2d) was calculated from the total soil [N] and total soil [P] concentration datasets from the TERN Soil and Landscape Grid of Australia available at CSIRO data access portal (Viscarra Rossel *et al.*, 2018a; Viscarra Rossel *et al.*, 2018b; Viscarra Rossel *et al.*, 2018c). These datasets offer Australia-wide gridded data at a resolution of 3 arc seconds, approximately 90m $\times$ 90 m spatial resolution. I used the total [N] and total [P] concentration (% soil mass) across depth increments (i.e. 0 to 5 cm, 5 to 15 cm and 15 to 30 cm), and soil bulk density (g cm^{-3}) datasets, to develop a depth-weighted average of topsoil (0 to 30 cm) total soil [N] (t ha^{-1}) and total soil [P] (t ha^{-1}).

2.2.4 Continental-scale leaf gas exchange data

A new Australia-wide continental scale trait dataset of instantaneous measurements of leaf gas exchange in Australian plants, spanning 528 species from 67 sites, was compiled by

Westerband *et al.* (2023). This dataset was used and analysed in this research to investigate the relationship between c_i/c_a, g_s and photosynthetic capacity (V_{cmax}) with mean annual precipitation (MAP) and total soil [P] concentration.

2.2.5 Common garden experiment data

Data from two common-garden studies were compared from the literature to provide additional insight into the interaction between soil [P] and MAP in modulating $\Delta^{13}C$ (Anderson *et al.*, 1996; Cernusak, 2020). Common garden experiments are such where different plant species or populations are collected from disparate geographic regions and then grown in a shared environment, with the aim of studying the influence of environmental factors in their home range on their growth and development. The two common garden studies compared here happened to be ideally aligned with the context of this chapter, with one utilizing 34 southeast Australian Eucalyptus tree species (Anderson *et al.*, 1996), and the other utilizing 9 Northern Australian tree species (Cernusak, 2020). The two sets of species had contrasting relationships between $\Delta^{13}C$ and the MAP either at their point of seed collection, in the case of the southeast Australian species, or for the species ranges, in the case of the Northern Territory species. In the latter case, the geographic locations of seed collection were not known, and for this reason the species range MAPs were used. For the species from southeast Australia MAP ranged from approximately 200 mm to 1700 mm whereas for the Northern Territory plants the range was from approximately 500 mm to 1750 mm. Plants were well watered in both experiments in the common gardens.

2.2.6 Statistical methods

Data from the northeast Queensland transect were compared with datasets collated from the literature to test whether $\Delta^{13}C$ responses to MAP differed across transects. To standardize descriptions of sampling site climate, mean annual precipitation and annual precipitation seasonality were estimated from the same gridded climatic dataset for all sites. Because the number of sites sampled within a transect varied broadly (Table 2.1), sites within each 100 mm MAP interval were binned along each transect prior to further analysis, so that the representation of the transects in the combined dataset was better balanced. Within each 100 mm MAP interval on each transect, the site climate data as well as the $\Delta^{13}C$ values were averaged.

In the next step of analysis, a linear model was used to test whether slopes of the relationship between $\Delta^{13}C$ and the natural logarithm of MAP, log(MAP), differed among transects. The linear model included as independent variables log(MAP), transect id, and the

interaction between log(MAP) and transect id. If the interaction term between log(MAP) and transect id was statistically significant, this was considered to be evidence of different slopes among transects. Having demonstrated a significant interaction effect, the slope of $\Delta^{13}C$ to log(MAP) from the model for each transect was extracted. I used the "emmeans" package (Lenth, 2023) in R, specifically the "emtrends" function to analyse the estimated marginal means and trends between $\Delta^{13}C$ and log(MAP) among transects. Following this, transect-wide averages of precipitation seasonality, soil [N], and soil [P] were calculated as the average for all sites within a transect. The $\Delta^{13}C$-log(MAP) slopes among the different transects were then tested for correlations with the transect wide averages of precipitation seasonality, soil [N], and soil [P].

Following this, two transects in northern Australia (i.e. NAT-Cernusak and NE-QLD-Cheesman) were examined in greater detail as both leaf [N] and leaf [P] concentrations were available for the leaf dry matter of the sampled trees. Partial regression was used for teasing apart the dominant nutritional driver of $\Delta^{13}C$ on the two transects. Partial plots were prepared to help visualize the unique contribution of each variable to the dependent variable in a multiple regression. The beta values (β) for each predictor, which represent the regression weights for standardized variables, are reported from partial regression analyses. These values indicate the change in the response variable (in standard deviations) associated with a change of one standard deviation in a given predictor, while holding other predictors constant (Pedhazur & Kerlinger, 1982; Courville & Thompson, 2001).

A similar approach was used for examining the Australia-wide leaf gas exchange dataset of Westerband *et al.* (2023), in order to test whether responses of $\Delta^{13}C$ to soil [P] were driven by g_s or photosynthesis. Average values at each sampling site were calculated and used for partial regression analysis with this dataset. Data from the two common garden experiments were compared with linear regression to test the relationships between leaf $\Delta^{13}C$ and MAP of the species' origin.

All statistical and graphical analyses were performed using R 4.3.1 (R Core Team, 2023) for Windows. Graphs and figures were produced using the R package "ggplot2" (Wickham, 2016). Maps were created in ArcMap version 10.8.

Table 2.1: Transect details and sampling procedures of the datasets analyzed in this study.

Transect	**Location**	**Length (km)**	**Precipitation range**	**Sampling method**	**Number of sites**	**Sampling year**	**Reference**
NE-QLD-Cheesman	Near Cairns to the edge of Simpson desert	~ 900	~300 mm to ~1700 mm	Canopy leaves from three trees at each site	11	2015	(Cheesman & Cernusak, 2017)
SE-VIC-Givnish	South-eastern Australia in a narrow 3° band of latitude	~ 450	~300 mm to ~1600 mm	Wood samples near tree base from three trees at each site	19	2011	(Givnish *et al.*, 2014)
NAT-Schulze	From Melville Island (11°S) to Giles and the Olgas (about 26°S)	~ 900	~200 mm to ~1800 mm	Sun exposed leaves from 3 to 5 individual trees per species from 1 to 14 species per sites	20	1993	(Schulze *et al.*, 1998)
NAT-Miller	From Darwin region about 12.5°S to the southern border of NT about 25°S	~ 1750	~200 mm to ~1600 mm	Sun exposed leaves from the canopy from five individuals of each species per zone	33	1996	(Miller *et al.*, 2001)
NAT-Cernusak	12°S to 23°S in northern Australia	~ 1500	~300 mm to ~1700 mm	Two species at each site and a total of six leaves from each species	6	2008	(Cernusak *et al.*, 2011a)
S-WA-Schulze	From Perth in the north to Walpole in the south and from there along a southwest to northwest transect to near Mount Olga	~ 2500	~300 mm to ~1200 mm	Leaves were sampled from 65 species in total	73	2003	(Schulze *et al.*, 2006)
SE-QLD-Stewart	At the latitude of 27°S	~ 900	~350 mm to ~1700 mm	Recently produced 3 to 12 leaf samples per species from 348 species	12	1992	(Stewart *et al.*, 1995)

2.3 Results

2.3.1 Australian transects

Sampling transects combined here ranged in length from 400 to 2500km with estimated MAP across sampling sites typically ranging from 300 to 1700mm (Table 2.1, Figure 2.2a). As seen in Figure 2.2b, precipitation is highly seasonal across northern Australia, moderately seasonal in south-western Australia, and nearly aseasonal in south-eastern Australia. The geographic distribution of the transects covers nearly this full range of variation. It should be noted that some regions in Figure 2.2b have precipitation seasonality values over 100% because the standard deviation of monthly precipitation throughout the year is larger than the average monthly precipitation for some regions.

The sampling sites from the southeast Victoria transect (SE-VIC-Givnish) contain the highest amounts of total soil [N] in the topsoil (0-30 cm), ranging from 2.2 to 9.5 t ha^{-1} (Figure 2.2c). On the other hand, sampling sites on the three Northern Territory transects are the most soil [N] depleted sites with a range from 2.1 to 3.8 t ha^{-1}. The northeast Queensland transect (NE-QLD-Cheesman) starting from the edge of wet biotropic region has soil [N] of 5.5 t ha^{-1} and the sampling site from the same transect near the simpson desert has 1.48 t ha^{-1} of soil [N]. Meanwhile the total soil [N] for the other two transects ranges from 2.1 to 8.4 t ha^{-1} for southeast Queensland (SE-QLD-Stewart) and the south Western Australia transect (S-WA-Schulze) has a range of 1.1 to 7.5 t ha^{-1}.

The eastern side of Australia has higher soil [P] compared to the western side (Figure. 2.2d). The highest amounts of soil [P] in the topsoil layer (0 to 30 cm) are found in the northeast Queensland transect's sampling sites, ranging from 0.7 to 3.9 t ha^{-1}. The southeast Queensland transect has a range of 0.9 to 1.7 t ha^{-1} whereas the sampling sites in the southeast Victoria transect range from 0.5 to 2.7 t ha^{-1} of total soil [P]. The south Westren Australia transect has 0.4 to 1.3 t ha^{-1}, however the most [P] depleted sampling sites are from the Northern Territory transects ranging from 0.4 to 1.0 t ha^{-1}.

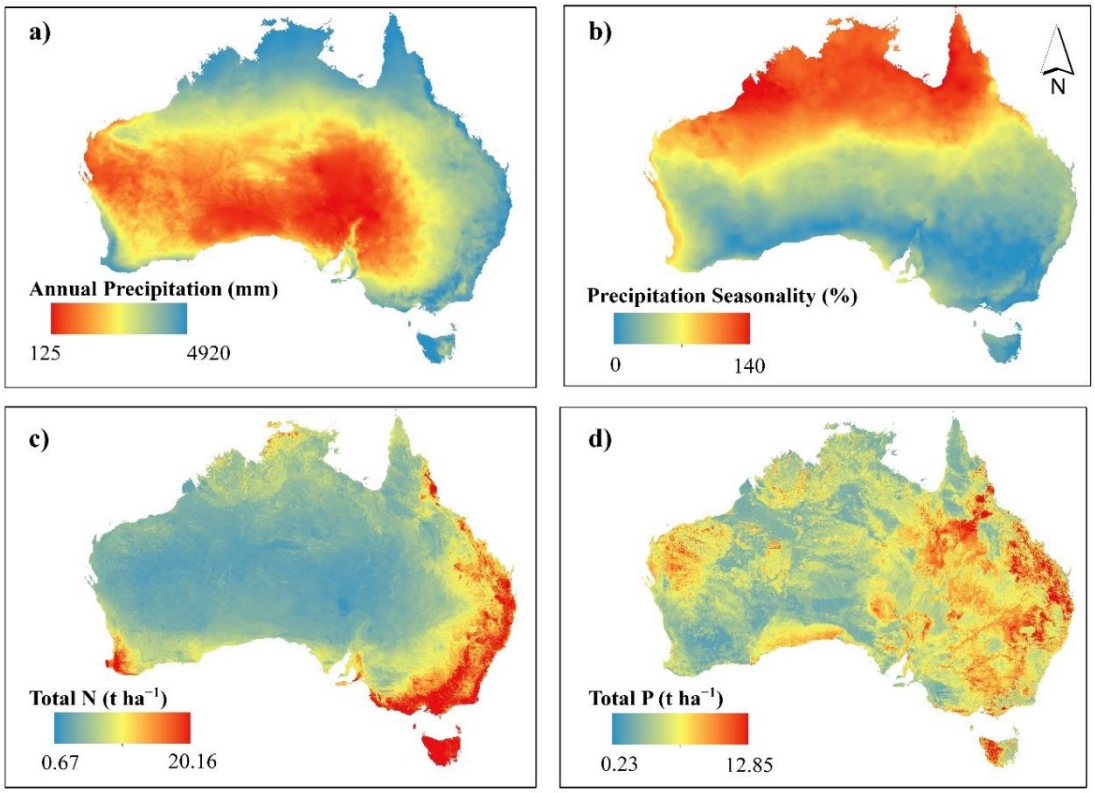

Figure 2.2: Maps showing different hydroclimatic distributions and soil attributes across Australia: a) mean annual precipitation (mm) across Australia where precipitation values represent a 30-year average (from 1976 to 2005) centred on 1990; b) precipitation seasonality (coefficient of variation of monthly precipitation) across Australia. Areas with higher values have more seasonal precipitation, whereas lower values represent areas with less seasonality, having precipitation spread more evenly throughout the year; c) map of total soil nitrogen (t ha^{-1}) in the 0-30 cm topsoil across Australia; and d) map of total soil phosphorus (t ha^{-1}) in the 0-30 cm topsoil across Australia. eMAST data products (Evans *et al.*, 2015) have been used in preparing a) and b); whereas the total soil [N] and total soil [P] datasets have been used for c) and d) from the TERN Soil and Landscape Grid of Australia available at CSIRO data access portal (Viscarra Rossel *et al.*, 2018a; Viscarra Rossel *et al.*, 2018b; Viscarra Rossel *et al.*, 2018c).

2.3.2 Relationship between MAP and leaf $\Delta^{13}C$

In the newly described transect (NE-QLD-Cheesman) MAP varies from 235 mm to 1388 mm across 11 sampling locations stretched across a 900 km gradient (Table 2.1). The values of $\Delta^{13}C$ increased with the increase of MAP, ranging from 16.3‰ to 23.4‰ (Figure 2.3). In examining the correlation between leaf $\Delta^{13}C$ and MAP across transects (Figure 2.3, Table 2.2) it is apparent that all three east Australian transects (i.e. NE-QLD-Cheesman, SE-QLD-Stewart, SE-VIC-Givnish) have steeper slopes compared to north and west Australian transects (Figure 2.3 and Table 2.2). A linear model of leaf $\Delta^{13}C$ values with log(MAP), transect id, and their interaction as independent variables showed that both log(MAP) ($F_{1, n=64}$ =98.81, $p<0.001$) and transect id ($F_{7, n=64}$ =6.50, $p<0.001$) have significant effects on leaf $\Delta^{13}C$ values (Table 2.3 and supplementary table S2.2). Importantly, the interaction between log(MAP) and transect id was also significant ($F_{7, n=64}$ =4.56, $p<0.001$), indicating different slopes with log(MAP) for different transects. The slope of the regression line for southeast Queensland transect was found to be significantly steeper (β = 3.33, SE = 0.56) than rest of the transects described in this chapter. The lowest slope was found for one of the Northern Territory transects (NAT-Cernusak; β = 0.47, SE = 0.51).

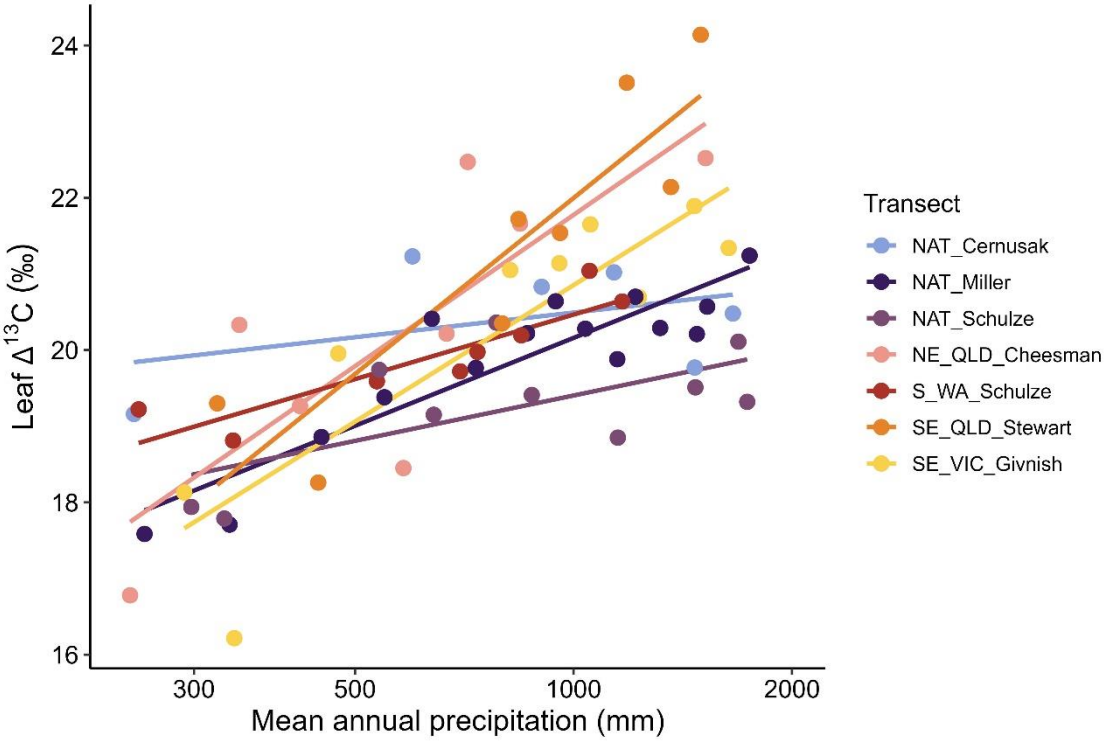

Figure 2.3: Relationship between mean annual precipitation (MAP) of the sampling sites and leaf $\Delta^{13}C$ values for the samples from studied transects. The solid lines show linear regression fits for each transect. Note that the scale on the x-axis is logarithmic (natural logarithm).

Table 2.2: Slope estimates from the linear regression model describing carbon isotope discrimination $\Delta^{13}C$ as a function of log(MAP), transect, and their interaction.

Transects	Slope	SE	Lower CI	Upper CI
NAT- Cernusak	0.47	0.51	−0.56	1.49
NAT- Miller	1.66	0.37	0.91	2.41
NAT- Schulze	0.86	0.42	0.01	1.71
NE-QLD- Cheesman	2.87	0.54	1.79	3.94
SE-VIC- Givnish	2.59	0.45	1.68	3.49
S-WA- Schulze	1.22	0.57	0.09	2.36
SE-QLD- Stewart	3.33	0.56	2.20	4.47

Table 2.3: Analysis of variance results of the linear regression model explaining leaf $\Delta^{13}C$ as a function of log(MAP), transect id, and their interaction.

	Sum Sq	Df	F value	Pr (>F)
log (MAP)	63.68	1.00	98.81	0.00
Transect	25.13	6.00	6.50	0.00
log (MAP) × Transect	17.63	6.00	4.56	0.00
Residuals	32.23	50.00		

2.3.3 *Regional variation in slopes of the leaf $\Delta^{13}C$ response to mean annual precipitation*

Mean transect characteristics of total soil [P], total soil [N] and precipitation seasonality were used to test for correlations with the $\Delta^{13}C$-log(MAP) slopes of the transects (Figure 2.4). Mean transect soil [P] had a significant positive correlation (r = 0.84 and *p* = 0.017) with transect leaf $\Delta^{13}C$ (‰) response to MAP. Mean regional soil [N] had a non-significant positive correlation (r = 0.67) and mean precipitation seasonality had a non-significant negative correlation (r = −0.63).

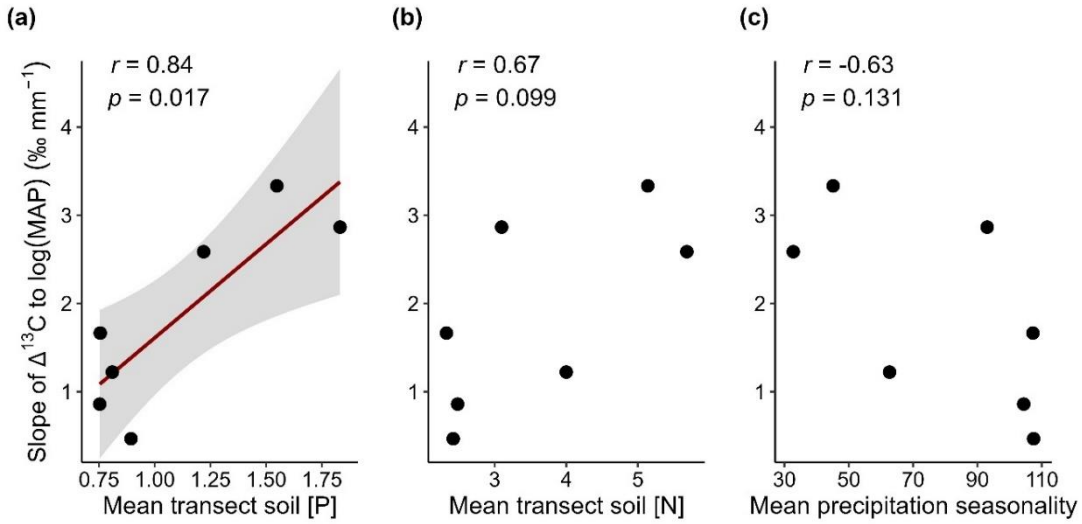

Figure 2.4: Regional relationships between the slope of leaf $\Delta^{13}C$ (‰) to MAP (mm) along each transect and the transect wide mean of a) soil [P], b) soil [N], and c) precipitation seasonality. Each point represents a single transect. The solid red line shows a linear regression fit and the grey shaded area is the 95% CI around the regression line. A regression line is only shown for the case with a p-value <0.05. Units for soil [P] and soil [N] are t ha^{-1} in the top 30 cm of soil, and precipitation seasonality is in %.

2.3.4 Comparison of soil and leaf nutrients on two contrasting transects

The average soil and leaf-level nutrient composition of two sampled transects in northern Australia, one in the Northern Territory and one in northeast Queensland are shown in Figure 2.5. The two transects are compared here because data for leaf [N] and leaf [P] are available for these two transects, and because they provide a contrast of soil nutrients while at the same time experiencing similar precipitation seasonality (Figure 2.2). The two transects show similar distributions of values for total soil [N] (t ha^{-1}) (Figure 2.5a). However, the amount of total soil [P] (t ha^{-1}) is significantly higher for the northeast Queensland transect compared to the Northern Territory transect (Figure 2.5b). This pattern is also reflected in the ratio of soil [N] to soil [P] between the two transects (Figure 2.5c).

The amount of leaf [N] (mg g^{-1}) of the sampled leaves from Northen Territory and northeast Queensland transects do not show any significant statistical differences (Figure 2.5d), reflecting the lack of difference in soil [N]. In the case of leaf [P] however, there is a significant difference between the transects, with the northeast Queensland transect showing higher leaf [P], consistent with the trend for soil [P] (Figure 2.5e). Finally, the ratio of leaf [N] to leaf [P] is significantly higher for the Northen Territory plants compared to the northeast Queensland plants, again consistent with the soil (Figure 2.5f).

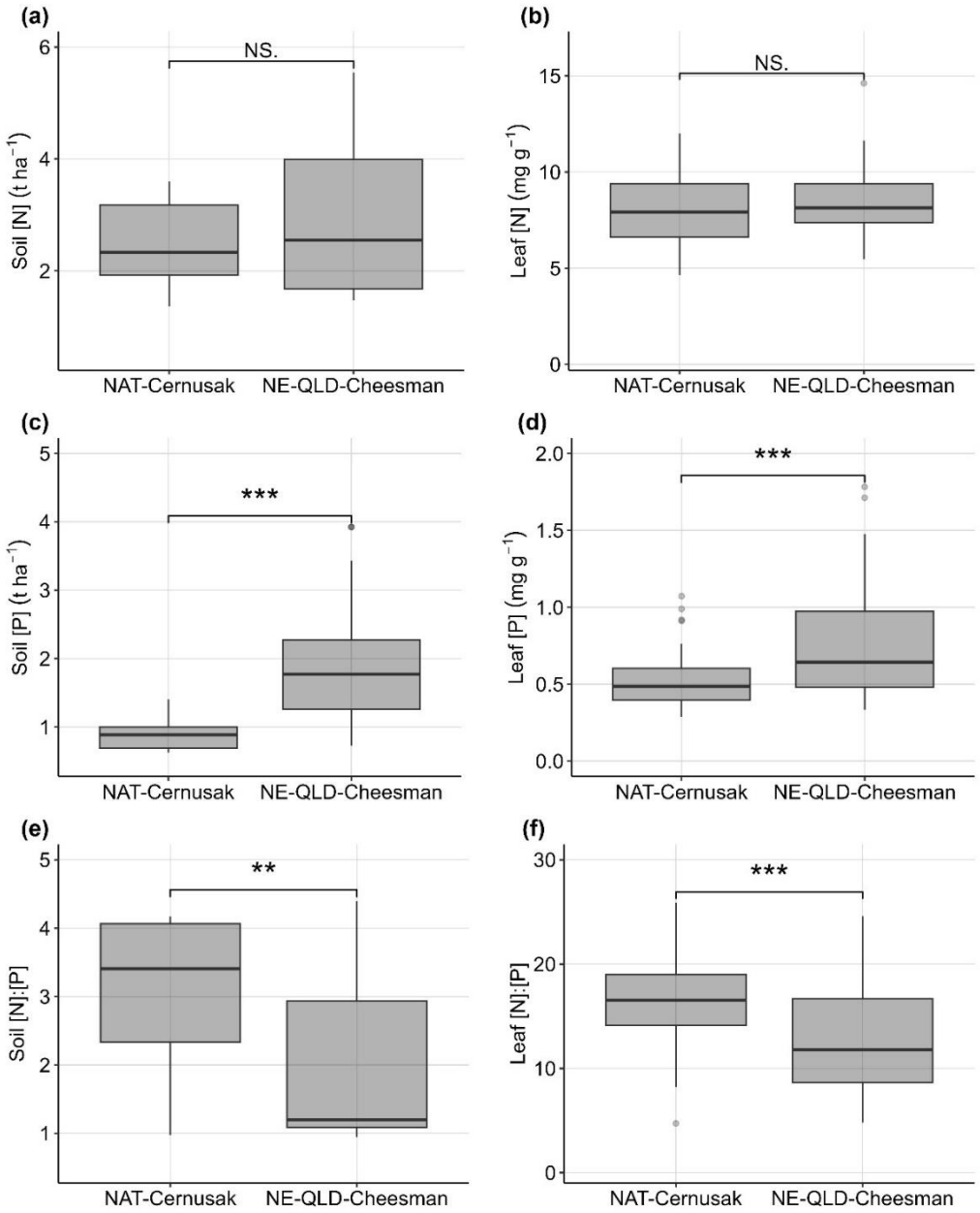

Figure 2.5: Boxplots of soil and leaf nutrients (N and P) in collected soils of the sampling sites (extracted from the gridded soil attribute datasets of Australia) and leaf samples in the Northern Territory (NAT-Cernusak) and northeast Queensland (NE-QLD-Cheesman) transects. Panels a), c) and e) show the amount of soil [N] in t ha^{-1}, soil [P] in t ha^{-1} and the ratio of soil [N] to soil [P] respectively for the sampling sites from the two different transects; b), d) and f) show the amount of leaf [N] in mg g^{-1}, leaf [P] in mg g^{-1} and the ratio of leaf [N] to leaf [P] respectively. Here, the significant terms are described as follows: NS. = not significant; ** p≤0.01; *** p≤0.001.

2.3.5 *Comparison of leaf nutrients and $\Delta^{13}C$ in two contrasting transects*

Multiple regression analysis was used to determine which leaf nutrient, N or P, was more strongly associated with variation in leaf $\Delta^{13}C$ on the two transects studied in detail. On the northeast Queensland transect (NE-QLD-Cheesman), leaf [N] values on a leaf area basis ranged from approximately 1.0 g m^{-2} to 3.0 g m^{-2}, whereas the leaf [P] values ranged from approximately 0.05 g m^{-2} to 0.5 g m^{-2}. The leaf $\Delta^{13}C$ values show a negative partial correlation (p = 0.03), with leaf [N] (g m^{-2}) and no apparent correlation with leaf [P] (g m^{-2}) (Figure 2.6a and 2.6b).

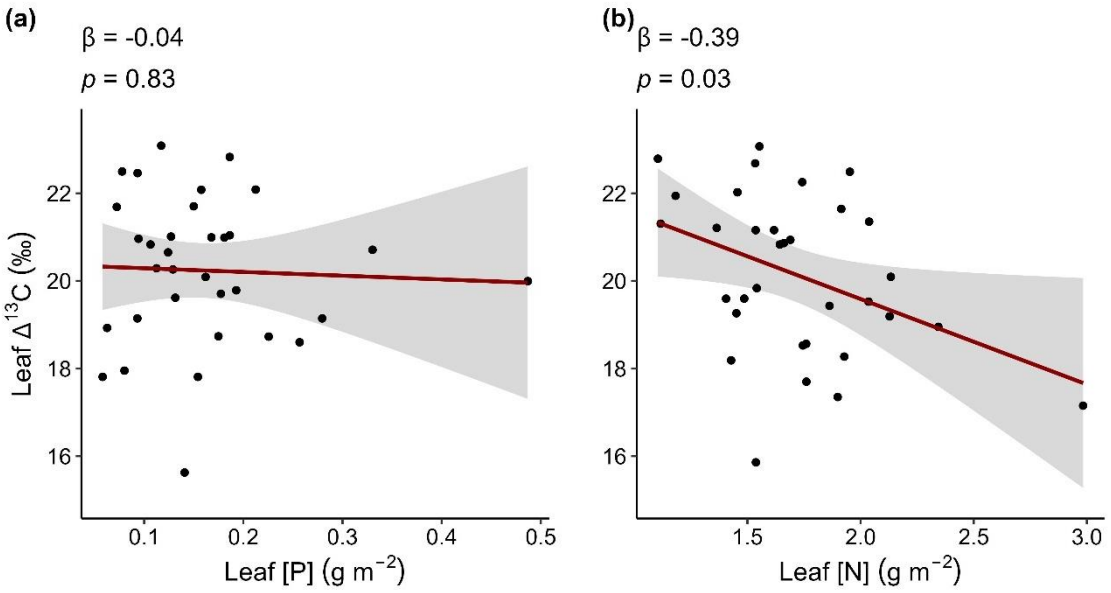

Figure 2.6: Partial regression plots showing the relationship between a) leaf phosphorus (P) and leaf $\Delta^{13}C$ values, and b) leaf nitrogen (N) and leaf $\Delta^{13}C$ values for the samples from northeast Queensland transect. The lines show partial linear regression fits and grey shaded areas are 95% CI around the regression lines.

However, in the [P] impoverished soils of the Northern territory (NAT-Cernusak) there was a highly significant (p<0.001) negative correlation between leaf $\Delta^{13}C$ (‰) and leaf [P] (g m^{-2}), whereas the relationship between leaf $\Delta^{13}C$ and leaf [N] was not significant (Figure 2.7). The contrast between the northeast Queensland and Northern Territory transects shows that the leaf nutrient likely to be in limiting supply, either N or P, is the one most associated with variation in leaf $\Delta^{13}C$, and that this differs between the two transects.

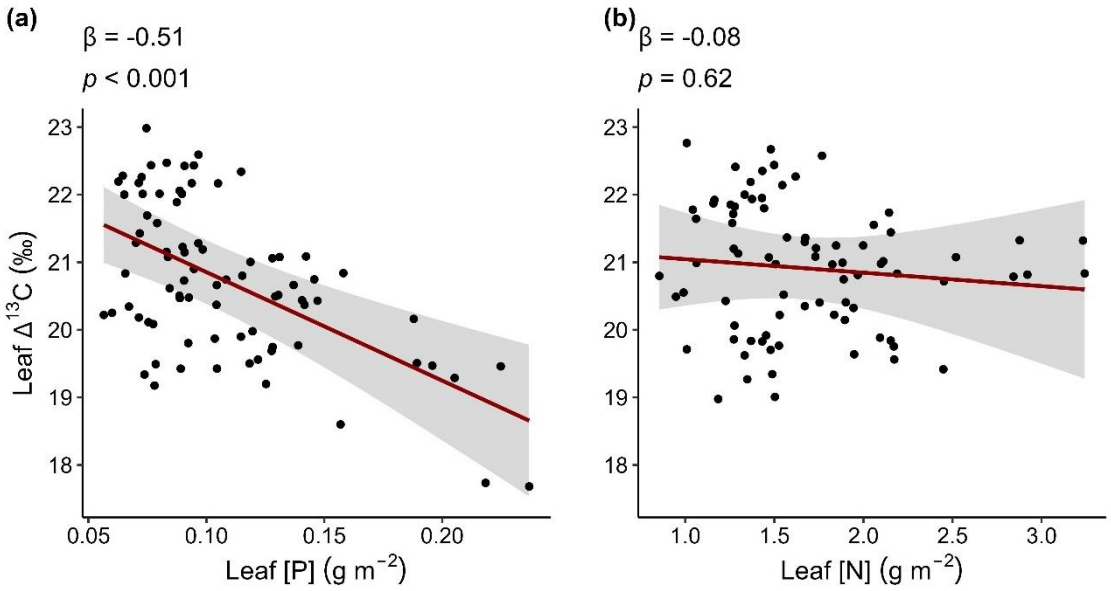

Figure 2.7: Partial regression plots showing the relationships between a) leaf phosphorus (P) and leaf $\Delta^{13}C$ values, and b) leaf nitrogen (N) and leaf $\Delta^{13}C$ values for the samples collected from a transect in the Northern Territory (NAT-Cernusak transect). The lines show partial linear regression fits and grey shaded areas are 95% CI around the regression lines.

2.3.6 Relationships between leaf gas exchange and MAP with soil [P]

A recently compiled dataset of instantaneous measurements of leaf gas exchange in Australian plants (Westerband *et al.*, 2023) was used to investigate how total soil [P] influences the relationships between c_i/c_a, g_s and photosynthetic capacity (V_{cmax}) and mean annual precipitation (MAP) (Figure 2.8). It was found that c_i/c_a varied with both MAP and total soil [P] as expected based on results presented above, increasing at sites with higher MAP ($\beta = 1.25$, $p < 0.001$) and decreasing with an increase in soil [P] ($\beta = -0.69$, $p = 0.009$) (Figure 2.8a and 2.8b).

Leaf-level g_s showed a similar trend to c_i/c_a (Figure 2.8c and 2.8d), having a positive slope with MAP ($\beta = 0.29$, $p = 0.004$) and a negative slope with soil [P] ($\beta = -0.4$, $p < 0.001$). The photosynthetic capacity (V_{cmax}) demonstrated a strongly negative impact of both MAP ($\beta = -0.37$, $p = 0.01$) and soil [P] concentration ($\beta = -0.29$, $p = 0.008$). These results indicate Australian woody plant species at drier sites typically operate with higher V_{cmax} and lower g_s. Meanwhile both g_s and V_{cmax} are lower at sites of high soil [P]. If the trend in c_i/c_a with soil [P] were driven by a relationship between soil [P] and photosynthetic capacity, a positive relationship between V_{cmax} and soil [P] would be expected. However, the fact that the relationship is negative indicates that c_i/c_a is high at sites of low soil [P], not because photosynthetic capacity is low, but because g_s is high. Thus, it is variation in g_s that drives the relationship observed in Figure 2.8b, not variation in V_{cmax}.

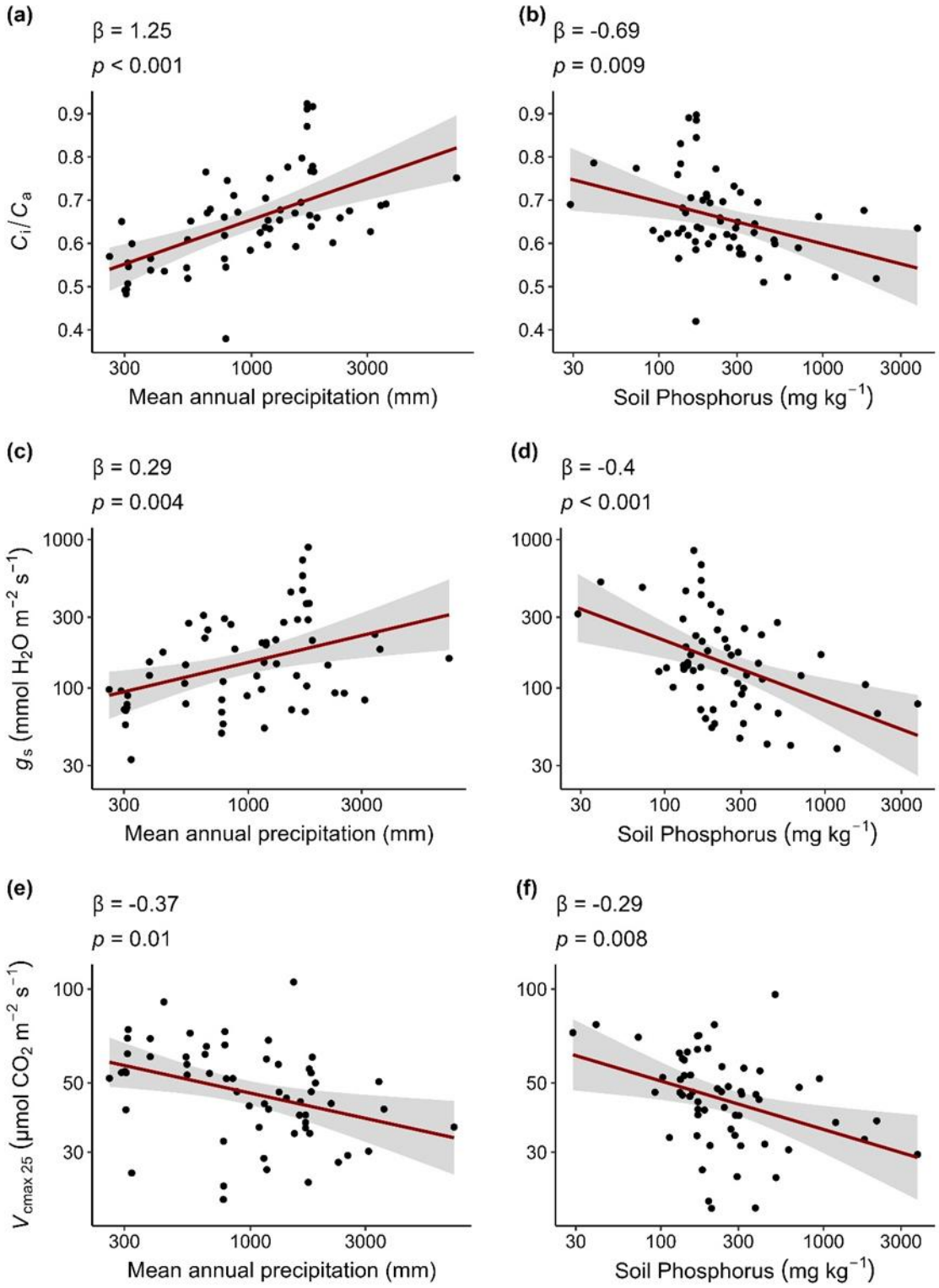

Figure 2.8: Partial regression plots of (a), (c), (e) mean annual precipitation (mm) and (b), (d), (f) soil phosphorus (mg kg^{-1}) effects on (a)-(b) c_i/c_a; (c)-(d) stomatal conductance, g_s (mmol H_2O m^{-2} s^{-1}); and (e)-(f) photosynthetic carboxylation capacity, V_{cmax} (µmol CO_2 m^{-2} s^{-1}). The points are average values at each sampling site; red lines represent partial regression lines with 95% confidence intervals in grey shaded areas.

2.3.7 Results from common garden experiments

Two common garden experiments conducted with tree species collected from different rainfall gradients from southeast Australia (New South Wales or NSW) and northern Australia (Northern Territory or NT) showed opposite responses of $\Delta^{13}C$ to the MAP of the species home range (Figure 2.9). Plants grown from seeds collected from NSW show a positive response of $\Delta^{13}C$ with increasing MAP at the point of origin (r = 0.73 and p = 0.007). In contrast, plants from the experiment in NT show a decrease of $\Delta^{13}C$ with increasing MAP of the species home range (r = −0.80 and p = 0.009).

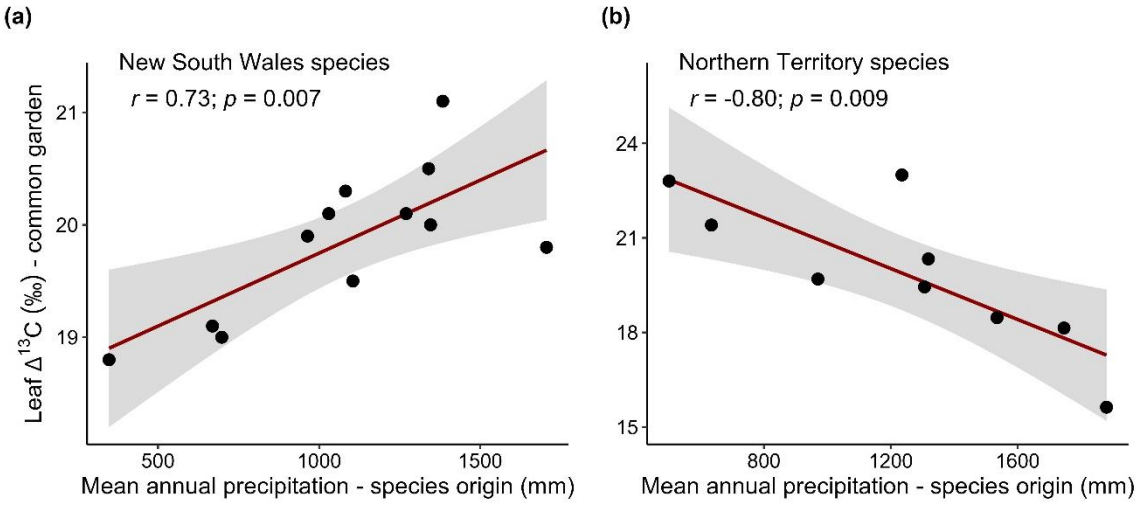

Figure 2.9: Relationships between mean annual precipitation (MAP) of species occurrence sites and leaf $\Delta^{13}C$ values when grown in a common garden from two different common garden experiments conducted with plants grown from seeds collected in a) New South Wales and b) Northern Territory. The red lines show linear regression fits and the grey shaded areas around the regression line are their 95% CI.

2.4 Discussion

Over recent decades, a number of studies have reported trends in $\Delta^{13}C$ with rainfall in Australia that appear to show a variable response of water use efficiency in tree communities to changing precipitation. Here, data from these studies have been assembled, while data from a new transect were added, to test whether the responses do indeed differ when compared in a standardized way. After standardization to account for changing atmospheric $\delta^{13}C$, and tissue type collected, we found that the response of $\Delta^{13}C$ to MAP does indeed vary statistically across subcontinental regions in Australia (Figure 2.3 and Table 2.2-2.3).

Onsite analyses of soil nutrient status were not available for most of the study sites in our combined dataset. Therefore, the Soil and Landscapes Grid of Australia has been used to estimate total soil [P] and total soil [N] at each site. For one of the transects in the Northern Territory (NAT-Cernusak) and the new transect in northeast Queensland, total leaf [P] and total leaf [N] data were collected and could be compared to the predicted trends in total soil [P] and total soil [N]. These leaf data showed that predictions of contrasting [N]: [P] ratios in the soil of the two transects were also reflected in the observed [N]: [P] ratios of the leaves (Figure 2.5), supporting the idea that varying soil nutrients across the subcontinental regions have a role in driving vegetation function. The [N]:[P] ratios of the leaves indicate generally that trees along the Northern Territory transect are more [P] limited in leaf function, whereas those along the northeast Queensland transect are more [N] limited.

With respect to leaf $\Delta^{13}C$, it has been demonstrated that leaf [P] is a more relevant control along the Northern Territory transect (Figure 2.7), whereas leaf [N] is likely more relevant along the northeast Queensland transect (Figure 2.6). For the Northern Territory transect, the number of observations within a site was sufficient that site could have been included as a random factor in the analysis, thus focusing on within site variation to discern the relationship between $\Delta^{13}C$ and leaf [P]. This analysis showed that on this transect, increasing leaf [P] was correlated with decreasing leaf $\Delta^{13}C$ (Figure S2.2).

Leaf [N] and to a lesser extent leaf [P], are known to influence c_i/c_a and $\Delta^{13}C$ through their role in leaf photosynthetic capacity. As photosynthetic capacity increases, the consumption of CO_2 within the chloroplasts increases, drawing down c_i/c_a and decreasing $\Delta^{13}C$. However, as change in c_i/c_a can also result from change in g_s a second possibility exists to account for the observed impact of nutrients on $\Delta^{13}C$ which is that some plants may use enhanced transpiration as a mechanism to aid the acquisition of soil nutrients by inducing mass flow of the soil solution to root surfaces (Dalton *et al.*, 1975; Fiscus, 1975; Cernusak *et al.*, 2011b). In doing so such

species would see a maintenance of a high c_i/c_a by an increase in g_s. Although it was previously assumed that transpiration-induced mass flow might not play a significant role in supplying P to root surfaces (Bieleski, 1973), recent studies have found plant transpiration rates to be higher in plants growing at low soil [P] compared to plants growing in a higher soil [P] (Huang *et al.*, 2017). This supports the idea of transpiration-induced mass flow of soil [P] to plant roots as a mechanism of [P] foraging (Cernusak *et al.*, 2010; Garrish *et al.*, 2010). As much of the Australian landscape is impoverished in soil [P], associated adaptions can be expected to drive species distribution patterns (Viscarra Rossel & Bui, 2016).

To examine whether a change in A or g_s in response to nutrient availability drives the observed regional differences in water-use efficiencies I took advantage of a continent-wide dataset of leaf photosynthetic characteristics recently compiled across Australia (Westerband *et al.*, 2023). Here I tested whether the mechanism of soil [P] influencing $\Delta^{13}C$ more likely results from increased photosynthetic capacity drawing down c_i/c_a, or whether it might alternatively relate to water-use strategies that would favour high g_s and thus high c_i/c_a in low [P] soils. That is, assuming c_i/c_a responds to soil [P] in the Australia-wide dataset, is the response of c_i/c_a driven by g_s or photosynthetic capacity (V_{cmax})? Using multiple regression models to investigate the interactive relationship between MAP and soil [P] concentration with c_i/c_a, g_s and V_{cmax} respectively, I found all these three plant physiological traits were higher in P-impoverished Australian soils (Figure 2.8b, 2.8d and 2.8f). This finding is consistent with previous research by Maire *et al.* (2015) also reporting a negative association between soil [P] and g_s. According to the least-cost theory, c_i/c_a and V_{cmax} are expected to be inversely related, all else being equal (Wright *et al.*, 2003). However, in this case, both c_i/c_a and V_{cmax} were found to be higher at low soil [P] sites. There may be exceptions, and it is worth noting that the Proteaceae, another dominant Australian plant family, has been reported to have a low V_{cmax} when growing on low [P] soils (Sulpice *et al.*, 2014).

Transpiration is suggested to be an important mechanism which aids P acquisition in P-poor soils (Cernusak *et al.*, 2011b; Huang *et al.*, 2017). Westerband *et al.* (2023) has observed higher phosphorus-use efficiency in plants at low soil [P] meaning higher photosynthesis rates (high rates of carboxylation) as well as higher g_s. This supports our assumption that high transpiration may be favoured to aid plants to acquire P in P-poor Australian soils.

Two common-garden studies were available in the literature that could potentially provide further insight into the interaction between soil [P] and MAP in modulating $\Delta^{13}C$ (Anderson *et al.*, 1996; Cernusak, 2020). These two common garden studies happened to be

ideally situated for this question, with one utilizing southeast Australian (New South Wales) tree species, and the other utilizing Northern Territory tree species. These two studies showed that when grown in common conditions, the two sets of species had contrasting relationships between $\Delta^{13}C$ and the MAP either at their point of seed collection, in the case of the southeast Australian species, or for the species ranges, in the case of the Northern Territory species.

The contrasting relationships between $\Delta^{13}C$ and the MAP at the site of origin or for the species range provide two important insights. The first is that the different $\Delta^{13}C$-MAP slopes in the Northern Territory compared to southeast Australia are likely associated with species replacements that tend to reinforce this divergence. In the Northern Territory, as species are replaced along the transect from high rainfall to low rainfall, this likely tends to mute the change in $\Delta^{13}C$, because the drier zone species replacing the wetter zone species show a higher $\Delta^{13}C$, at least in well-watered conditions. On the other hand, in southeast Australia, in common conditions, the drier zone species replacing the wetter zone species along the transect will tend to have lower $\Delta^{13}C$, all else being equal. The second important insight is that the environmental conditions in these two regions appear to have selected for different tree behaviours in relation to variation in MAP. I suggest that through evolutionary time, one of these selecting forces could have been the severe P impoverishment of the soils in the Northern Territory (Figure 2.2d, Figure 2.5b and table S2.1). From the total soil [P] concentration gridded dataset it has been found that the amount of soil [P] is the lowest for sampling sites from Northern Territory (range: 0.53 – 1.40 t ha^{-1}, std. deviation: 0.19).

With this study I aimed to explain how multiple environmental drivers interact to drive variation in plant carbon isotope discrimination across the Australian continent. While carbon isotope discrimination shows a divergent sensitivity towards regional precipitation, this sensitivity depends on the regional extent of soil P impoverishment. It has also been found that soil [P] controls carbon isotope discrimination in plants by influencing the intercellular to ambient CO_2 concentrations (c_i/c_a) and this influence is driven by g_s. Here I hypothesize that Australian woody plant species have evolved to survive in P-poor, ancient soils by adapting to use high transpiration rates to facilitate P foraging.

Supplementary material

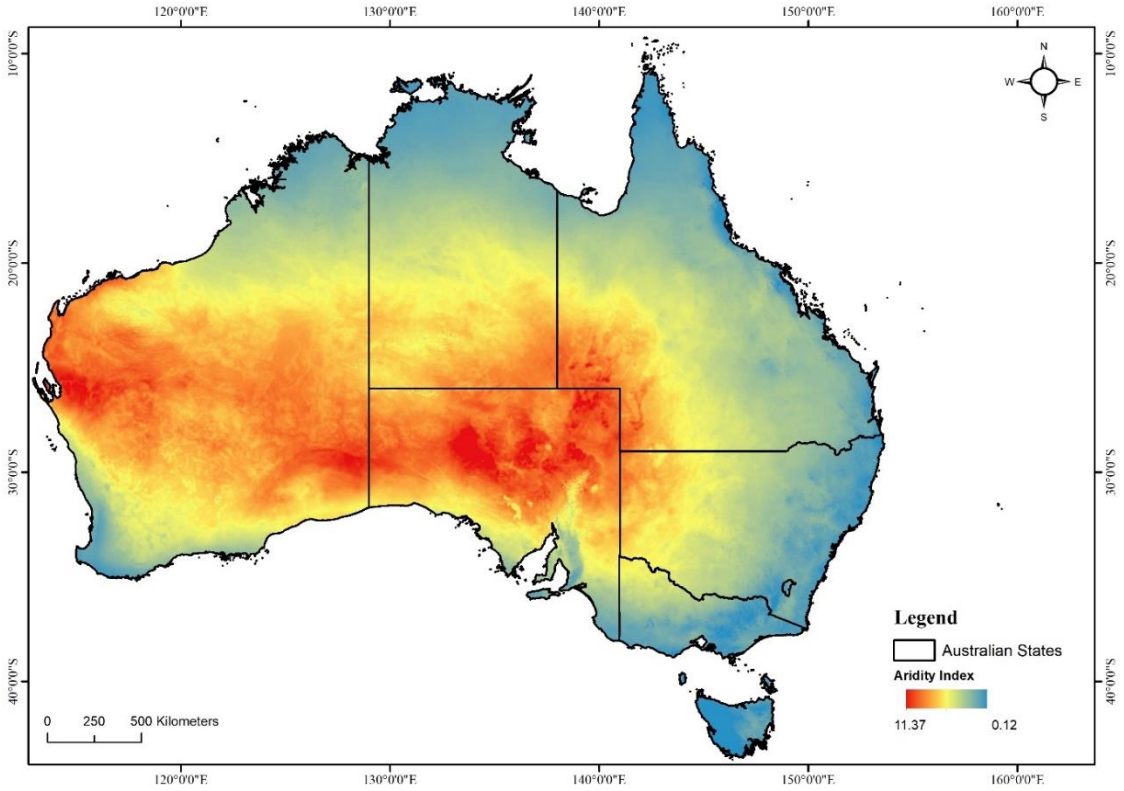

Figure S2.1: Aridity index map of Australia. The aridity index was calculated as the ratio of mean annual potential evapotranspiration to mean annual precipitation (Harwood, 2019).

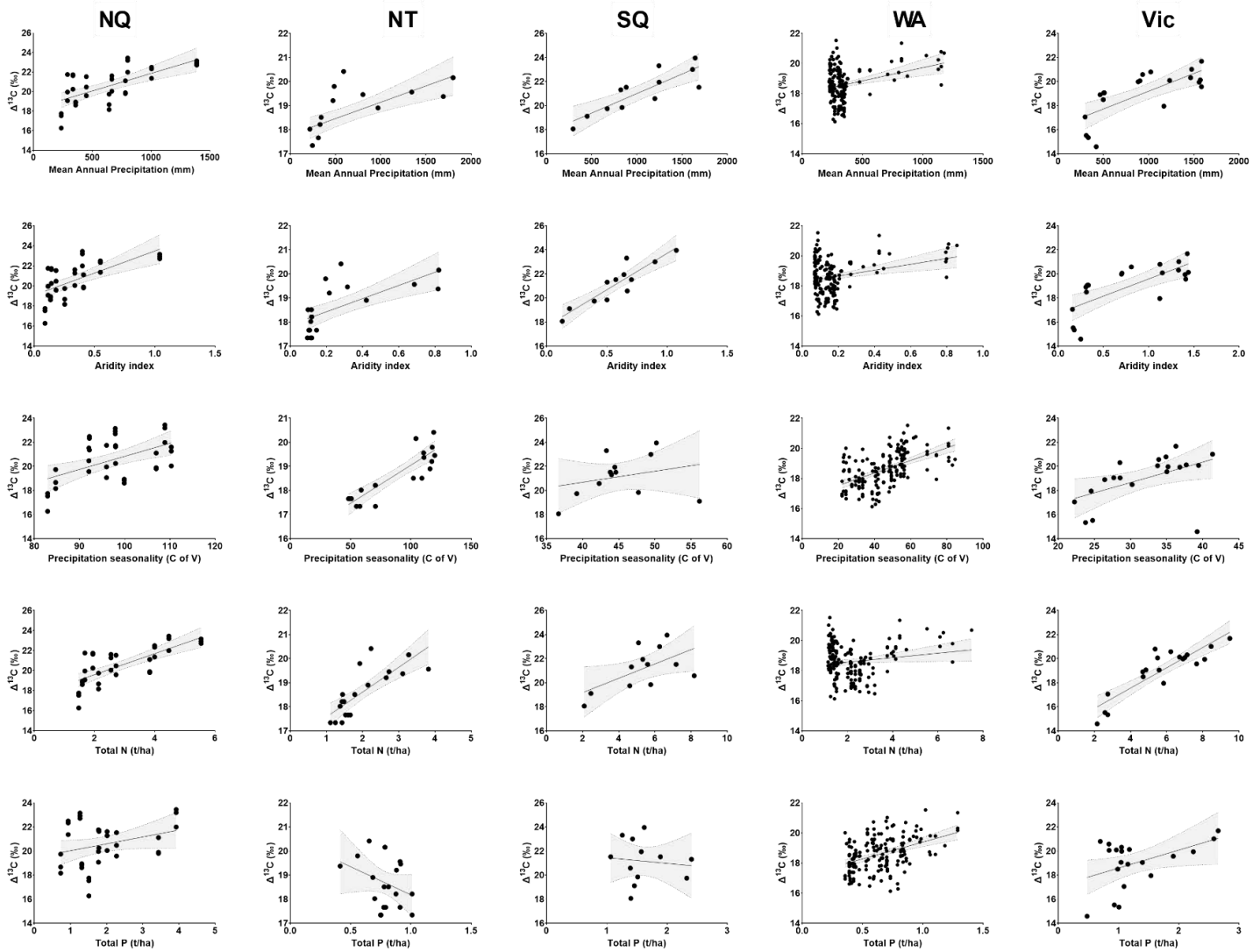

Figure S2.2: Relationship between climatic and soil attributes with leaf $\Delta^{13}C$ (‰) for the transects.

Table S2.1: Summary statistics of Mean annual precipitation (mm), Aridity index, Precipitation seasonality (%), Total soil [N] (t ha^{-1}) and Total soil [P] (tha^{-1}) for transects.

	NAT-Cernusak	NAT- Miller	NAT- Schulze	NE-QLD-Cheesman	S-WA-Schulze	SE-QLD-Stewart	SE-VIC-Givnish
Mean annual precipitation (mm)							
Min	248.00	240.00	297.00	245.00	225.00	323.00	291.00
Mean	1002.67	695.79	673.56	616.09	393.92	923.25	960.55
Max	1658.00	1748.00	1735.00	1520.00	1182.00	1497.00	1661.00
Std.dev	530.35	434.23	504.15	353.24	251.81	333.61	520.24
Aridity Index							
Min	1.15	1.11	1.06	1.28	1.06	1.00	0.74
Mean	2.61	3.68	4.04	3.54	5.24	1.99	1.95
Max	6.20	6.60	6.10	6.35	7.90	5.12	4.65
Std.dev	1.92	1.80	1.95	1.63	2.01	1.26	1.34
Precipitation Seasonality (%)							
Min	82.78	53.93	48.28	82.93	22.01	36.66	22.24
Mean	108.27	102.47	88.19	97.25	49.42	45.15	32.01
Max	119.94	123.29	119.84	110.31	84.56	56.16	41.35
Std.dev	13.80	22.51	29.11	9.08	14.43	5.18	5.85
Total Soil [N] (t ha^{-1})							
Min	1.36	1.16	1.11	1.48	1.14	2.09	2.15
Mean	2.42	2.01	2.03	2.90	2.33	5.33	5.72
Max	3.60	3.89	3.82	5.54	7.49	8.17	9.49
Std.dev	0.83	0.67	0.78	1.36	1.46	1.76	2.06
Total Soil [P] (t ha^{-1})							
Min	0.63	0.53	0.41	0.73	0.36	1.07	0.48
Mean	0.89	0.78	0.78	1.90	0.70	1.61	1.28
Max	1.40	1.12	1.01	3.92	1.29	2.41	2.65
Std.dev	0.28	0.14	0.14	0.99	0.21	0.41	0.61

Table S2.2: Multiple linear regression model summary of leaf $\Delta^{13}C$ relationship with log(MAP), transects and their interaction.

	leaf $\Delta^{13}C$		
Predictors	*Estimates*	*CI*	*p*
(Intercept)	17.268 ***	10.322 – 24.214	<0.001
[log] MAP	0.467	−0.559 – 1.492	0.365
Transect [Cheesman]	−15.287 **	−25.057 – −5.517	0.003
Transect [Givnish]	−14.284 **	−23.488 – −5.080	0.003
Transect [Miller]	−8.610 *	−17.202 – −0.017	0.050
Transect [Schulze06]	−5.248	−15.355 – 4.858	0.302
Transect [Schulze98]	−3.800	−12.777 – 5.176	0.399
Transect [Stewart]	−18.298 ***	−28.626 – −7.969	0.001
[log] MAP × Transect [Cheesman]	2.399 **	0.912 – 3.885	0.002
[log] MAP × Transect [Givnish]	2.120 **	0.754 – 3.486	0.003
[log] MAP × Transect [Miller]	1.198	−0.072 – 2.469	0.064
[log] MAP × Transect [Schulze06]	0.756	−0.774 – 2.286	0.326
[log] MAP × Transect [Schulze98]	0.393	−0.937 – 1.722	0.556
[log] MAP × Transect [Stewart]	2.867 ***	1.337 – 4.396	<0.001
Observations	64		
R^2 / R^2 adjusted	0.764 / 0.702		

** p<0.05 ** p<0.01 *** p<0.001*

CHAPTER 3: ACCLIMATION OF DARK RESPIRATION AND MINIMUM CONDUCTANCE TO DROUGHT AND HEAT STRESS

Abstract (Chapter 3)

Drought and heat stress are critical factors driving plant mortality globally, impacting plant physiological processes, growth, and geographic distributions. The physiological responses of plants to drought may be determined by their adaptation and acclimation potential to water stress experienced as a result of their distributions across a range in water availability. In this study, I investigated species-level responses to drought and heat of four eucalypt species selected from across a rainfall gradient. Seedlings were raised under two temperature regimes and were subjected to periods of water stress to examine both adaptation and acclimation potential in leaf-level traits associated with drought-persistence, minimum leaf-level conductance (g_{min}) and dark respiration (R_d). While measuring R_d at a reference temperature, I found both species-level differences and a reduction in R_d of plants grown under elevated temperatures. However, I found no difference in the temperature sensitivity of R_d nor an impact of drought on R_d despite water stress often leading to potential increases in respiratory energy demand. Minimum conductance (g_{min}) was found to vary among species and decreased in plants grown under elevated temperatures. Indeed, plants grown at elevated temperatures decreased g_{min} to levels comparable to solely cuticular conductance (g_{cw}), indicating minimal stomatal leakage under stressed conditions. While it is apparent that eucalypt species can show acclimation of leaf-functional traits critical to determining drought-persistence, in the four species studied here, I saw little evidence for how the distribution of species across a rainfall gradient may determine this. Further work examining a larger range of species may therefore be needed to examine how adaptation and acclimation of leaf-functional traits play a role in determining continent-wide species distributions.

3.1 Introduction

Across the world tree species are facing the threat of extinction due to recent rapid anthropogenic climate change (Ter Steege *et al.*, 2015). Given the rapid rate of change in global climate it is unlikely that many tree species will be able to migrate or adapt fast enough to survive (Feeley *et al.*, 2012), therefore individual-level trait plasticity and acclimation may be the only way to prevent declines in performance and species extinction. Severe droughts have resulted in widespread tree mortality across biomes, significantly impacting ecosystem function and the global carbon balance (Choat *et al.*, 2018). It is expected that the effects of climate change will exacerbate regional-scale droughts. Indeed, a mechanistic hydraulic model of future drought-induced tree-mortality has estimated that with the average 5°C increase in global temperatures expected by the end of this century almost 60% of global forests will be lost, unless they are able to acclimate (Brodribb *et al.*, 2020). However, predicting tree mortality during drought is complex as multiple, potentially plastic, plant functional traits interact with each other and the environment to determine rates of plant desiccation and ultimately plant drought tolerance (Skelton *et al.*, 2015; Anderegg *et al.*, 2016). To understand the true effects of future droughts, a comprehensive understanding of the interaction between the capacity for acclimation of plant functional traits, especially in the context of often co-occurring stressors, such as elevated temperatures, is needed (Allen *et al.*, 2015; Greenwood *et al.*, 2017) .

During periods of atmospheric or soil water deficit, stomatal closure restricts transpiration, thereby maintaining soil and tree water content (Buckley, 2019); however, water loss continues through stomatal leakage and water loss through the leaf cuticle. This rate can be measured as the minimum leaf conductance (g_{min}). Minimum conductance is increasingly being recognised as an important factor in assessing plant canopy water flux (Barnard & Bauerle, 2013), particularly during heatwaves (Kala *et al.*, 2016), severe droughts (Duursma *et al.*, 2019; Brodribb *et al.*, 2020), and for modelling plant drought responses (Blackman *et al.*, 2016; Martin-StPaul *et al.*, 2017; Cernusak & De Kauwe, 2022). Maintaining lower g_{min} is crucial for plants to prevent residual transpiration after stomatal closure during drought to delay further desiccation and protect themselves from hydraulic failure and damage to the photosynthetic machinery (Haverroth *et al.*, 2023). By lowering g_{min} plants can optimize their water use efficiency and enhance their resilience to drought stress. However, g_{min} itself may be impacted by the elevated temperatures often associated with drought, with g_{min} shown to generally increase with rising temperatures (Schuster *et al.*, 2016; Brodribb *et al.*, 2020), potentially compromising a plant's ability to limit water loss when droughted under warmer conditions.

The g_{min} of plants comprises of two pathways, across the cuticle (cuticular conductance, g_{cw}) and through incompletely closed stomata (g_s). Although the partitioning of g_{min} into cuticular and

stomatal components has proven technically challenging (Duursma *et al.*, 2019), a limited number of studies have sought to examine how either component or the composite g_{min} may vary across species in response to their climate of origin. However, while Brodribb *et al.* (2014) found a positive correlation between g_{min} and rainfall across species, a subsequent metanalysis by Duursma *et al.* (2019) found no such correlation. In an extensive review, Schuster *et al.* (2017) also reported an absence of any significant differences in either g_{min} or g_{cw} when considering the growth forms of plants, or cuticle thickness (Schuster *et al.*, 2016). While recognized as being of fundamental importance to determining drought responses, it is unclear how g_{min} relates to other leaf-functional traits, nor how plasticity and acclimation of g_{min} to environmental conditions may drive observed responses in species across the landscape.

Plants generally tend to decrease g_{min} in response to chronic and prolonged drought stress (James *et al.*, 2008). On the other hand, g_{min} response to temperature is complex as it often shows both an immediate species-specific response to leaf temperature, as well as a less well established acclimatory response to average growing temperature (Duursma *et al.*, 2019). There is also evidence from certain species that a sudden increase of g_{min} with increasing temperature could represent a life-saving mechanism to survive heatwaves by cooling leaves and maintaining the leaf temperature below their thermal limit (Drake *et al.*, 2018). It is certainly clear that g_{min} impacts leaf thermal regime with a generally negative correlation between thermal tolerance and g_{min} found, such that species with enhanced tolerance to high air temperatures often have a lower g_{min} (Schuster *et al.*, 2016).

During episodic drought there is not only a risk of direct hydraulic failure through continued water loss but also a risk of carbon starvation (McDowell *et al.*, 2022) due to stomatal limitation of photosynthesis at the same time as elevated respiration to maintain hydraulic tissue function (Flexas *et al.*, 2006; Meir *et al.*, 2008; Metcalfe *et al.*, 2010). Dark respiration (R_d) plays a pivotal role in providing the energy (ATP) necessary for the maintenance of cellular structures and the repair of damaged cellular components. This includes the synthesis of heat shock proteins and antioxidants, which serve to protect cells from the detrimental effects of drought and heat (Flexas *et al.*, 2007). However, elevated dark respiration rates can result in the depletion of carbon reserves during periods of stress, particularly when photosynthesis is constrained by elevated temperatures or stomatal closure (Atkin & Macherel, 2008). Consequently, a reduction in respiration rate can be advantageous in maintaining metabolic activity over extended periods of stress.

The potential for acclimation, and therefore reduction of respiration in reaction to moisture stress has been recognised as a significant element in determining species drought tolerances (Flexas *et al.*, 2009). It is well established that plants can acclimate multiple facets of their biochemical

functioning in response to temperature (Atkin *et al.*, 2005). Increasing air temperatures in already warm systems have been found to increase respiration (Slot & Kitajima, 2015) and stomatal conductance (g_s) (Urban *et al.*, 2017a; Urban *et al.*, 2017b; Marchin *et al.*, 2022), while reducing photosynthesis (Graham *et al.*, 2003; Leakey *et al.*, 2003; Doughty & Goulden, 2008; Galbraith *et al.*, 2010) leading to a reduction in tree growth (Clark *et al.*, 2003; Feeley *et al.*, 2007) and increasing plant mortality (Van Mantgem *et al.*, 2009; Brodribb *et al.*, 2020). Biochemical acclimation to elevated temperatures can result in both a decline in the absolute respiration rate and the temperature sensitivity (i.e. Q_{10}) of the process (Tjoelker *et al.*, 1999; Medlyn *et al.*, 2002; Hikosaka *et al.*, 2006; Kattge & Knorr, 2007) potentially reducing the likelihood of negative impacts of elevated temperatures.

The geographical range of a tree species represents a climatic envelope in which both temperature and water availability are amenable to plant growth and survival, with the observed distribution of species across a gradient in water availability generally illustrative of a species innate ability to withstand drought (Trueba *et al.*, 2017; Li *et al.*, 2018). However, trait variation observed across a species' home range will represent both a species' innate adaptation and the potential for trait acclimation of that species. By conducting experiments on plants grown in controlled environments under gradual changes in environmental conditions, it may be possible to separate the influences of long-term adaptation and short-term acclimation on trait variation among species (Pfennigwerth *et al.*, 2017; Henn *et al.*, 2018).

In this chapter, I examined the short-term physiological responses to drought, and short and long-term responses to elevated temperatures in four eucalypt species drawn from across a range in rainfall regimes. My objective was to investigate how plants from different rainfall regimes may differ in their capacity to acclimate to drought and elevated temperatures. My hypothesis was that plants from different bioclimatic regions would show different acclimation potential toward drought and elevated temperature stress by modulating their g_{min} and dark respiration, which might play an important role in determining overall environmental tolerances of a species.

3.2 Materials and methods

The study was carried out in a climate-controlled glasshouse located in James Cook University's Environmental Research Complex on the Nguma-bada campus in Cairns, Queensland (https://www.jcu.edu.au/environmental-research-complex). The glasshouse has three parallel chambers, each measuring 3 × 5m, and equipped with autonomous temperature and [CO_2] regulation systems (see Forbes *et al.*, 2020 for detailed information), although only two chambers were used for this experiment.

3.2.1 Species selection

A total of four eucalypt species from the Myrtaceae family were selected for this experiment. These four species (*Eucalyptus camaldulensis*, *Eucalyptus exserta, Eucalyptus pellita and Corymbia clarksoniana*) cover a broad range of the rainfall gradient seen across Australia.

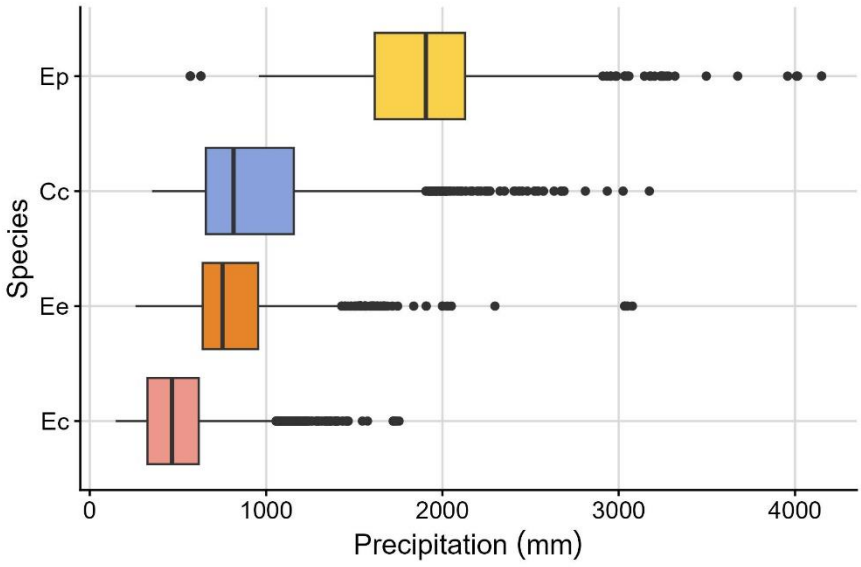

Figure 3.1: Species distribution ranges based on their median annual precipitation (mm) (data derived using Bio 12 layer from ANUCLIM v6 beta) at their recorded occurrence sites (n= 60721) in Australia (ALA, 2024). The species are *Eucalyptus camaldulensis* (Ec)*, Eucalyptus exserta* (Ee)*, Corymbia clarksoniana* (Cc) and *Eucalyptus pellita* (Ep). Species are in an ascending order starting from lower median annual precipitation values at the bottom of the y-axis.

Among the four selected species, it is worth noting that *E. pellita* has both the highest median (1906 mm) and widest range of precipitation, from a minimum of 570 mm to a maximum of 4151 mm with an IQR of 315 mm (Figure 3.1). This medium to tall sized species, typically growing to a height of 40 m, is endemic to north-eastern Queensland in Australia and grows in open forests, particularly wet, near-coastal forests (ALA, 2024). In contrast *E. camaldulensis*, has the lowest median annual precipitation among the studied species with a median annual precipitation of 466 mm, and a mean

annual precipitation range of 146 to 1754 mm (interquartile range, IQR= 291 mm). It is worth noting that *E. camaldulensis* is commonly found along most of the watercourses across Australia and has the widest natural distribution of any eucalypt species. *Eucalyptus exserta* (median MAP of the occurrence sites is 752 mm and IQR = 315 mm) is known to grow in infertile sandy soils as part of the dry sclerophyll woodland community and is commonly found on stony rises and hills throughout Queensland (ALA, 2024). *Corymbia clarksoniana* (median MAP of occurrence sites 815 mm, IQR = 499 mm) is a medium-sized tree, growing up to 20 m, occurring in Queensland and northern New South Wales, Australia. The tree is also able to grow in a variety of soil types, including sand, sandy loam, and skeletal soils on ridges and hilltops. Hence it can be found in inland plains, and grassy woodland and forests as well.

3.2.2 Experimental Design

Thirty seedlings from each of the target species were collected from Yuruga nursery, Walkamin, Queensland and transplanted into 6L pots filled with a commercially available potting mix (Scotts Osmocote Seed & Cutting Premium Potting Mix, ScottsMiracle-Gro, Marysville, OH, USA) with a base of gravel to ensure good drainage. This potting mix contained coir peat, micronutrients, water crystals for better water holding capacity and controlled release fertilisers. Fifteen individual seedlings from each species were randomly assigned to each of the two treatment chambers. At this initial stage, the temperature within the chambers was set to track ambient external air temperature. Plants were watered by hand daily.

After seedling establishment experimental treatments were implemented (Day-0) with one chamber maintained as tracking external air temperatures (Ambient) and with the second set to follow the same diel variation but with an increase of 5°C (Elevated). Plants were grown for 125 days in the two temperature-controlled glasshouse experimental chambers with a daytime average temperature of 30.1 ± 3.2 °C (± std. deviation) and nighttime average of 25.5 ± 2.1 °C in the ambient temperature chamber. In the elevated temperature chamber the daytime average temperature was 34.9 ± 3.3 °C and nighttime average was 30.4 ± 2.2 °C. Relative humidity (*Rh*) was higher in the ambient chamber (with a daytime average of 87.3 ± 6.0 % and a nighttime *Rh* of 87.3 ± 6.5 %) compared to the elevated temperature chamber (daytime average of 68.5 ± 9.3% and nighttime average of 68.6 ± 10.1%). Temperature, *Rh* and vapour pressure deficit (*VPD*) experienced by the plants over the whole experimental period are presented in supplementary figures S3.1 to S3.3 and table S3.1. The total experiment proceeded in two phases. During the first phase, all plants in both chambers were watered every day until Day-46 and then once every 3 days until Day-90. At this point, the first round of gas exchange measurement (details below) was taken under well-watered conditions. The second phase of the experiment began on Day-100 where watering was halted until any sign of a drought induced

effect (wilted leaves) was visible. At this point plants were watered again once in every 2 days until fully recovered and showed signs of recovery (fresh leaf flush). Then again, watering was stopped on Day-115 and gas exchange measurements were taken when drought induced effects were visible on the plants between Day-122 to Day-125. The last measurements were taken on the 125th day.

After each round of leaf-level gas exchange measurements, the measured leaves were harvested and scanned using a CanoScan LiDE 400 scanner (Canon, Tokyo, Japan) and analysed using ImageJ (Schneider *et al.*, 2012) to determine leaf area. Individual leaves were oven dried at 60°C until constant dry mass to determine leaf mass per unit area (LMA, g m^{-2}).

3.2.3 Gas Exchange measurements

At the end of both phases of the experiment gas exchange measurements were taken on one leaf per plant. On any given day, selected seedlings were moved from the glass house experimental chambers to the laboratory and pre-adapted to laboratory conditions within darkened plastic bags for a minimum 15 hours prior to leaf-level gas exchange measurements in darkness. Measurements were conducted using a portable photosynthesis measurement system (Li-6400, Li-Cor Inc., Lincoln, NE, USA) utilizing a transparent leaf cuvette. Gas exchange measurements for dark respiration (R_d) at 25°C leaf temperature (achieved through adjustment of cuvette temperature) were taken in the dark (irradiance of 0 µmol photons m^{-2} s^{-1}). Thereafter leaves were exposed to 100 µmol photons m^{-2} s^{-1} irradiance of red light supplied by an artificial light source (LED-Panel RGBW-L084, Heinz Walz GmbH, Germany) to allow for measuring the minimum leaf surface conductance, g_{min} and the partitioning of g_{min} into g_{cw} and g_s following Márquez *et al.* (2022) red-light method. This method utilizes red light exposure during photosynthetic induction, taking advantage of the fact that red light influences stomatal response differently from other wavelengths. By applying red light and measuring water vapor and gas exchange, the method isolates conductance values that reflect minimum water loss when stomata are nearly closed. This method is based on the development of a stable gas exchange environment in which the diffusion of CO_2 into the leaf is significantly constrained by the stomata, while simultaneously ensuring the optimal functioning of the photosynthetic biochemical processes.

Subsequently, leaf temperatures were raised to 35°C and leaves were returned to darkness at 0 µmol photons m^{-2} s^{-1} for 30 minutes so that R_d could be recorded and the temperature sensitivity of respiration (i.e. Q_{10}) calculated.

3.2.4 Statistical Analysis

All data manipulation and statistical analyses were performed in R version 4.3.1 (R Core Team, 2023). Linear models were used to examine the impact of elevated temperature and water stress on dark respiration (R_d), minimum conductance (g_{min}), cuticular conductance to water (g_{cw}), and leaf mass

per area (LMA). In these models, chamber (i.e. ambient or elevated temperature), water stress (i.e. well-watered and droughted), and species were considered as independent variables. The "lm" function in R was used to fit the linear models. Later, models were compared and best fitted models were selected based on their performances analysed with "DHARMA", "MuMIn", "performance" and "see" packages for R (Lüdecke *et al.*, 2021a; Lüdecke *et al.*, 2021b; Hartig, 2022; Bartoń, 2023). Graphs and figures were produced using the R package "ggplot2" (Wickham, 2016).

3.3 Results

In this study I examined the potential for leaf-level acclimation of g_{min} and R_d to temperature and drought in four eucalypt species found across a rainfall gradient in Australia. Plants were grown for 125 days under ambient or elevated (+5°C) temperature regimes with leaf-level gas exchange determined in leaves exposed to both well-watered and droughted conditions.

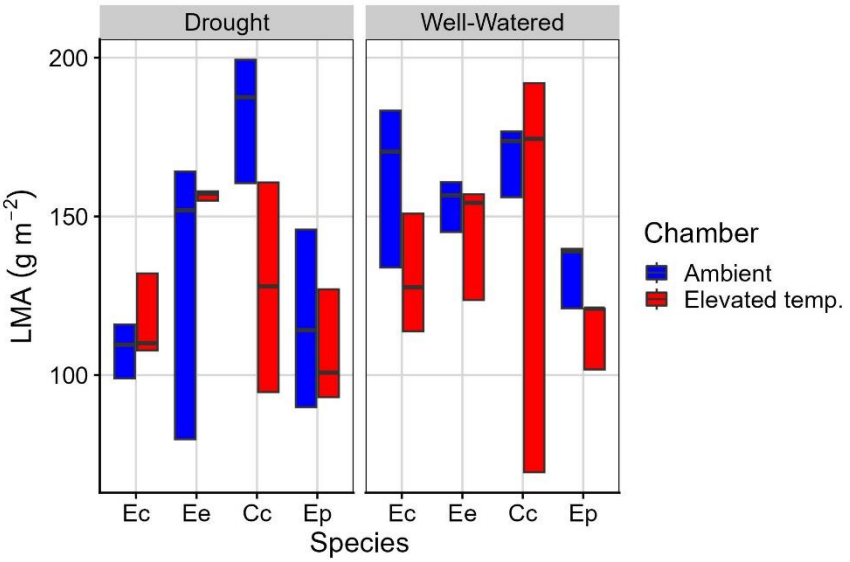

Figure 3.2: Leaf mass per area, LMA (g m^{-2}) of plants grown in two different temperature-controlled chambers, i.e. ambient and elevated temperature, under two different water-controlled conditions, i.e. Well-watered and Drought. The species are *Eucalyptus camaldulensis* (Ec)*, Eucalyptus exserta* (Ee)*, Corymbia clarksoniana* (Cc) and *Eucalyptus pellita* (Ep). Species are in an ascending order starting from lower median annual precipitation values at the left of the x-axis.

Species were found to have significantly different LMA ($F_{3,\ n=90}$ =10.11, *p<0.001;* Figure 3.2) with *Corymbia clarksoniana* having the highest LMA for both temperature treatments and *Eucalyptus pellita* the lowest (Figure 3.2). Furthermore, I found a significant impact of temperature treatment ($F_{1,\ n=90}$ =7.22, *p<0.01*) upon LMA, where leaves developed under elevated temperatures had on average a lower LMA compared to leaves developed under ambient temperatures. During the well-watered period, leaves showed higher LMA compared to those during droughted periods ($F_{1,\ n=90}$ =6.18, *p<0.05*),

except for *C. clarksoniana*. The lowest LMA of 106.99 g m^{-2} was found for *E. pellita* under drought stress at elevated temperature, whereas *C. clarksoniana* showed the highest LMA, 182.45 g m^{-2}, for the leaves developed under drought stress in ambient conditions.

The temperature sensitivity, or Q_{10} of dark respiration was estimated using leaf-level gas exchange measurements conducted at 25 °C and 35 °C. Results showed an average Q_{10} of 3.35 (SD = 0.74) across all species with no significant differences as a result of species ($F_{3, n=42}$ = 0.34, *P=0.80*), temperature treatment ($F_{1, n=42}$ = 0.11, *P=0.74*) or water stress condition ($F_{1, n=42}$ = 0.52, *P=0.47*).

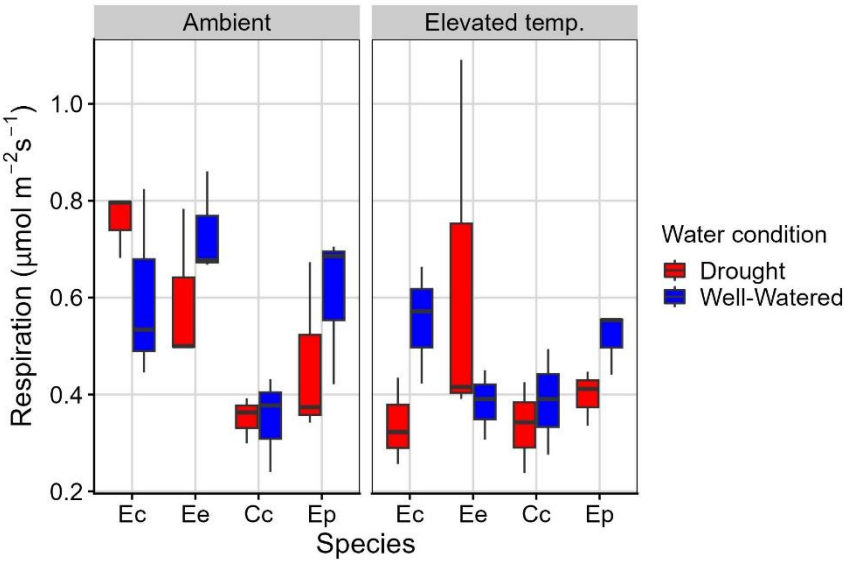

Figure 3.3: Dark respiration of plants from two different temperature-controlled chambers, i.e. ambient and elevated temperature chambers, at two different water-control conditions, i.e. Well-watered and Drought. The species are *Eucalyptus camaldulensis* (Ec)*, Eucalyptus exserta* (Ee)*, Corymbia clarksoniana* (Cc) and *Eucalyptus pellita* (Ep). Species are in an ascending order starting from lower median annual precipitation values at the left of the x-axis.

Leaf minimum conductance, g_{min} was measured during the second phase of this experiment in water stressed plants under both dark condition and redlight illuminated condition (Figure 3.4A). Later, using the equation from Márquez *et al.* (2022), cuticular conductance, g_{cw}, for the same plants was estimated. For estimating g_{cw}, only the measurements taken under redlight illumination at 100 µmol photons m^{-2} s^{-1} was used. Measured g_{min} was statistically significantly different between species ($F_{3, n=20}$ =3.41, *p<0.05*), while also showing to be impacted by temperature treatment ($F_{1, n=20}$ =8.01, *p<0.05*), with plants grown under elevated temperature having a lower g_{min}, on average 2.22 ± 1.71 mmol m^{-2} s^{-1}, as compared to plants from the ambient chamber (4.71 ± 3.08 mmol m^{-2} s^{-1}). *Eucalyptus exserta* showed the highest g_{min} under both ambient (8.56 ± 1.76 mmol m^{-2} s^{-1}) and elevated temperature (3.22 ± 1.22 mmol m^{-2} s^{-1}) treatments (Figure 3.4A). There were no significant differences

found between species for g_{cw} (Figure 3.4B). As there was no statistical difference between temperature treatments for g_{cw} ($F_{3,\ n=19}$ =0.63, *P=0.61*), it is presented here for all the seedlings measured from both ambient and elevated temperature chambers (Figure 3.4B).

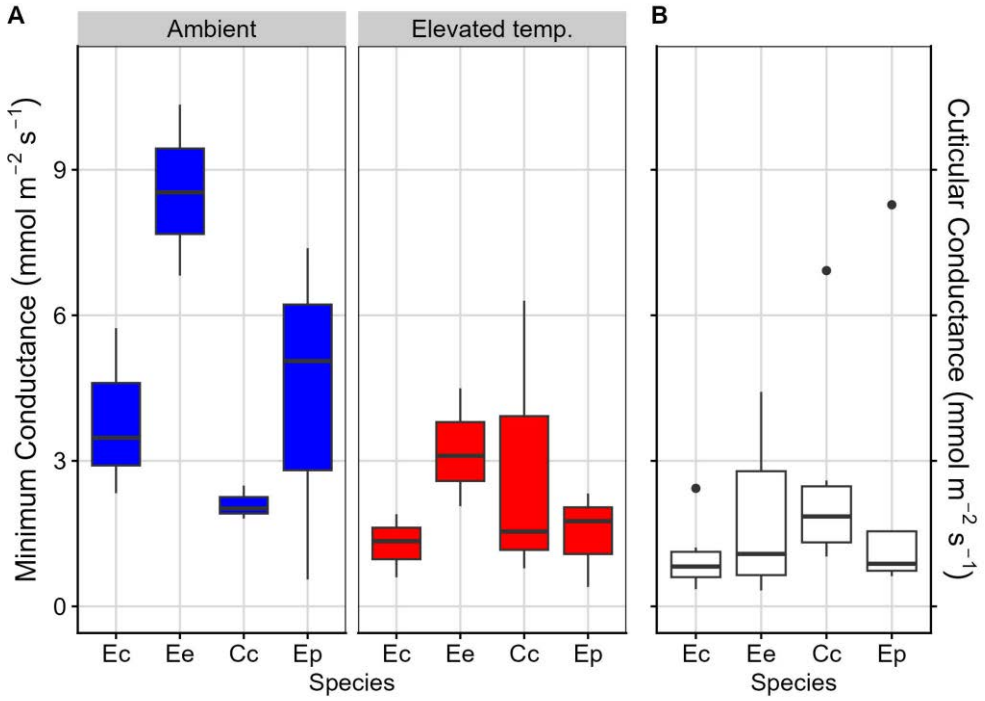

Figure 3.4: A) Minimum leaf conductance to water vapour (mmol m^{-2} s^{-1}) of water stressed plants grown under two temperature regimes, i.e. ambient and elevated by ~5°C. B) Cuticular conductance to water vapour (mmol m^{-2} s^{-1}) of all the measured plants. The species are *Eucalyptus camaldulensis* (Ec)*, Eucalyptus exserta* (Ee)*, Corymbia clarksoniana* (Cc) and *Eucalyptus pellita* (Ep). Species are in an ascending order starting from lower median annual precipitation values at the left of the x-axis in each panel.

3.4 Discussion

Together drought and heat stress are the most common drivers of plant mortality worldwide as they significantly impact plant physiological responses, growth and geographic distributions (Allen *et al.*, 2015; Greenwood *et al.*, 2017). In the previous chapter (Chapter 2) of this thesis, I have explored adaptation and acclimation in leaf-level intrinsic water-use efficiency (WUE_i) using $\Delta^{13}C$ (i.e. carbon isotope discrimination). However, given this proxy for WUE_i is only entrained into leaf tissue during active photosynthesis, it can only reveal aspects of acclimation during daylight hours. Leaf level dark processes are also important as they play a significant role in shaping plant responses to physiological and biochemical events (Sobieszczuk-Nowicka *et al.*, 2016; Rowland *et al.*, 2017; Duursma *et al.*, 2019). In testing the capacity of four eucalypt species to modify their intrinsic leaf-level dark processes (specifically R_d, g_{min} and g_{cw}) in this study I sought to examine how inherent acclimation potential can help these plants to cope with extended drought and heat stress.

The seedlings of four eucalypt species typically found at different points across a rainfall gradient (Figure 3.1) were raised in two temperature-controlled glasshouse chambers where one chamber was set to track ambient temperatures whilst another one was set at +5 °C. All the seedlings in both chambers were well-watered at the first stage of the experiment. After the gas exchange measurements were completed for the well-watered plants, a second stage of the experiment started where all the seedlings were repeatedly water stressed before a second round of gas exchange measurements.

3.4.1 LMA differs between species, and with growth temperature and water availability

An increase in LMA with an increase of site aridity has been observed by many researchers worldwide (Schulze *et al.*, 1998; Niinemets, 2001; Wright & Westoby, 2002) with findings from this experiment aligning with this as the lowest LMA was found for *E. pellita;* a species typically found in more mesic habitats than the other species studied. I also found a statistical difference in LMA between plants under different water conditions ($F_{1, n=90}$ =6.18, $p<0.05$). Well-watered plants showed higher LMA compared to droughted plants. Although some researchers have reported a contrasting trend where increase in LMA is associated with drought stress (Poorter *et al.*, 2009), modifications to leaf mesophyll density and/or thickness could independently respond to changes in water availability, resulting in species-specific variation in LMA in response to water stress (Niinemets, 2001).

With an increase in growth temperature plants were found to have a lower LMA (average difference 14.38 g m^{-2}) than plants grown under ambient conditions, with a similar trend reported by other researchers (Poorter *et al.*, 2009). Yu *et al.* (2012) reported that increased temperature can often result in a reduction of net photosynthesis and dark respiration. These effects can limit plant

growth and potentially lead to a decrease in LMA. In another experiment, Takahashi and Otsubo (2017) discussed a negative correlation between temperature and LMA. Their findings support the result of this experiment where at elevated temperature plants allocate less biomass to leaves per unit leaf area, eventually leading to lower LMA.

3.4.2 Dark respiration differs between species and with growth temperature

Dark respiration at a common temperature was found to be different between species and in plants grown under different temperature regimes but was unchanged between water stress levels. Leaf level R_d has been reported to be sensitive to change in short-term temperature (Wager, 1941; Atkin & Tjoelker, 2003; Kruse *et al.*, 2011) and the fact that R_d for plants from elevated growth temperatures were lower than those from ambient conditions suggests a degree of acclimation (Tjoelker *et al.*, 2001). The acclimation of R_d to growth temperature seems common among different functional types (Atkin & Tjoelker, 2003), although there are indications that broad-leaved plants are more capable of acclimation than gymnosperms (Tjoelker *et al.*, 1999).

Water stress is an abiotic factor that can affect leaf respiration by inhibiting stomatal opening and photosynthetic CO_2 fixation. This can potentially reduce substrate supply to mitochondria, but might eventually increase respiratory energy demand by increasing reactive oxygen species (ROS) production to support cytosolic and chloroplast metabolism (Hoefnagel *et al.*, 1998; Slot *et al.*, 2008; Atkin & Macherel, 2009). In this study no change in R_d of eucalypts was found as a result of the water stressed condition ($F_{1, n=43}$ =0.47, *P=0.50*). In a review on plant drought tolerance pathways, Atkin and Macherel (2009) found about two-thirds of the articles studied reported a decline in respiration during drought stress whereas the rest of them mentioned no change or (in a few cases) reported an increase. This has been expanded in recent years with some additional studies showing an increase in dark respiration in response to water stress *(Slot et al., 2008; Yu et al., 2012; Barreto et al., 2017)*.

3.4.3 Minimum conductance differs between species and with growth temperature

During drought plants tend to close their stomata to reduce water loss. However, even after stomatal closure a discernible amount of residual water is lost from the plant – at a rate which increases with increasing temperature (Brodribb *et al.*, 2020). Through the modulation of g_{min}, plants have the capacity to optimize water use, thereby augmenting their resilience in the face of temperature and drought-induced stress. However, this potential for acclimation is contingent upon the inherent trait plasticity of individual plants, and in contrast to evolutionary mechanisms such as adaptation, acclimation manifests over significantly shorter temporal scales. Researchers have not found any significant links between g_{min} values of different species and their environments, so it is difficult to explain the variation based on climate of origin or other important traits (Duursma *et al.*,

2019). In this experiment, significant statistical difference in g_{min} was found between the four studied eucalypt species (Figure 3.4A), although no difference was found for cuticular conductance, g_{cw} (Figure 3.4B). The elevated temperature chamber had three to four times higher vapor pressure deficit (VPD) compared to the ambient temperature-controlled chamber (Figure S3.3). Global warming is expected to increase both temperature and VPD, because temperature has an exponential effect on saturation vapour pressure. This increase in VPD is expected to surpass any increases in regional precipitation leading to atmospheric water stress (Novick *et al.*, 2024). Plants grown at elevated temperature acclimated to temperature increase and increased VPD and showed a decline in g_{min} to a level that was comparable with g_{cw} suggesting little to no stomatal leakage.

I assume the four species under investigation could potentially reduce their water loss under heat stress as VPD also increased by decreasing their g_{min}, and that this would be most pronounced under water stress conditions. Given this assumption, I measured g_{min} in droughted plants. It is worth noting that, with the exception of *C. clarksoniana*, the g_{cw} of all studied species in this chapter indicates that the minimum conductance is mostly contributed from their stomatal residual conductance rather than cuticular conductance. For *C. clarksoniana*, most of its g_{min} derives from g_{cw}. This implies that this species might be well-adapted to regulate their stomata at full closure compared to the other three species examined in this research.

The four eucalypt species studied in this chapter demonstrated acclimation of LMA, dark respiration and minimum conductance under ambient and elevated (5°C above ambient) temperature. I observed acclimation to low water availability only for the LMA response, whereas dark respiration, and minimum conductance were different for different species and showed an effect of temperature treatment. Here I hypothesized that eucalypts may reduce their minimum conductance as temperature rises, to prolong their survival during periods of heat stress. Furthermore, stomatal remnants, rather than cuticular conductance, accounted for most of the minimum conductance in these eucalypt species. By revealing the dynamics of LMA, dark respiration, minimum conductance and cuticular conductance, this experiment provides valuable insights into how plants respond to drought and elevated temperatures which might help future researchers in modelling global vegetation and carbon cycling.

Supplementary material

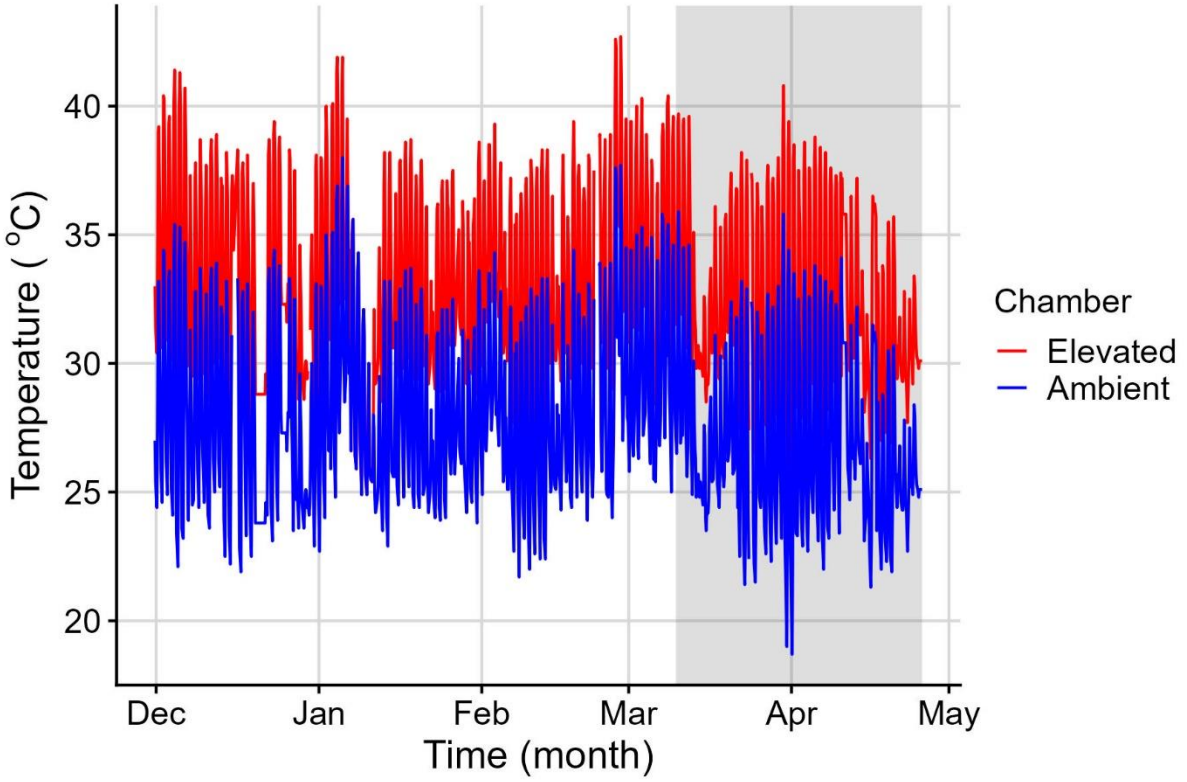

Figure S3.1: Air temperature (°C) of two experimental chambers used to examine the leaf-level acclimation in seedlings of four eucalypt species. Data represent the average conditions over a 10-minute period, with the trace corresponding to the beginning of the experiment. The grey shading represents the period of drought during second phase of the experiment.

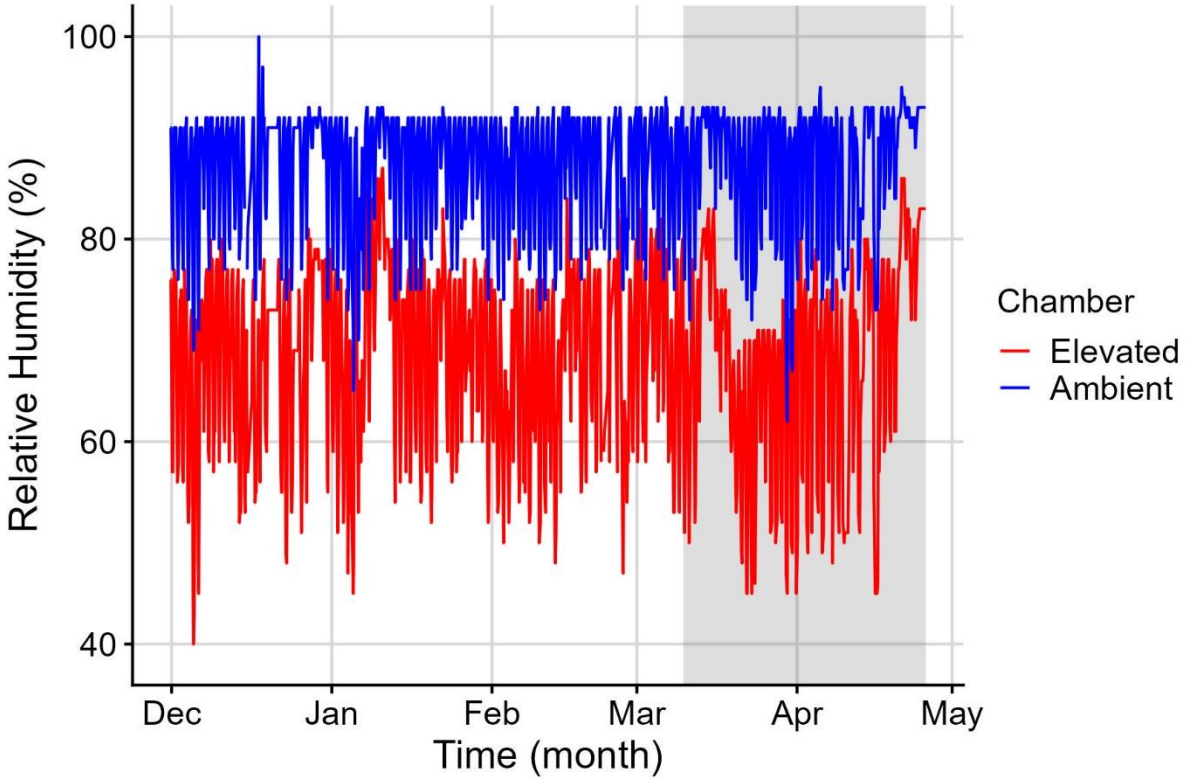

Figure S3.2: Relative humidity (%) of two experimental chambers used to examine the leaf-level acclimation in seedlings of four eucalypt species. Data represent the average conditions over a 10-minute period, with the trace corresponding to the beginning of the experiment. The grey shading represents the period of drought during second phase of the experiment.

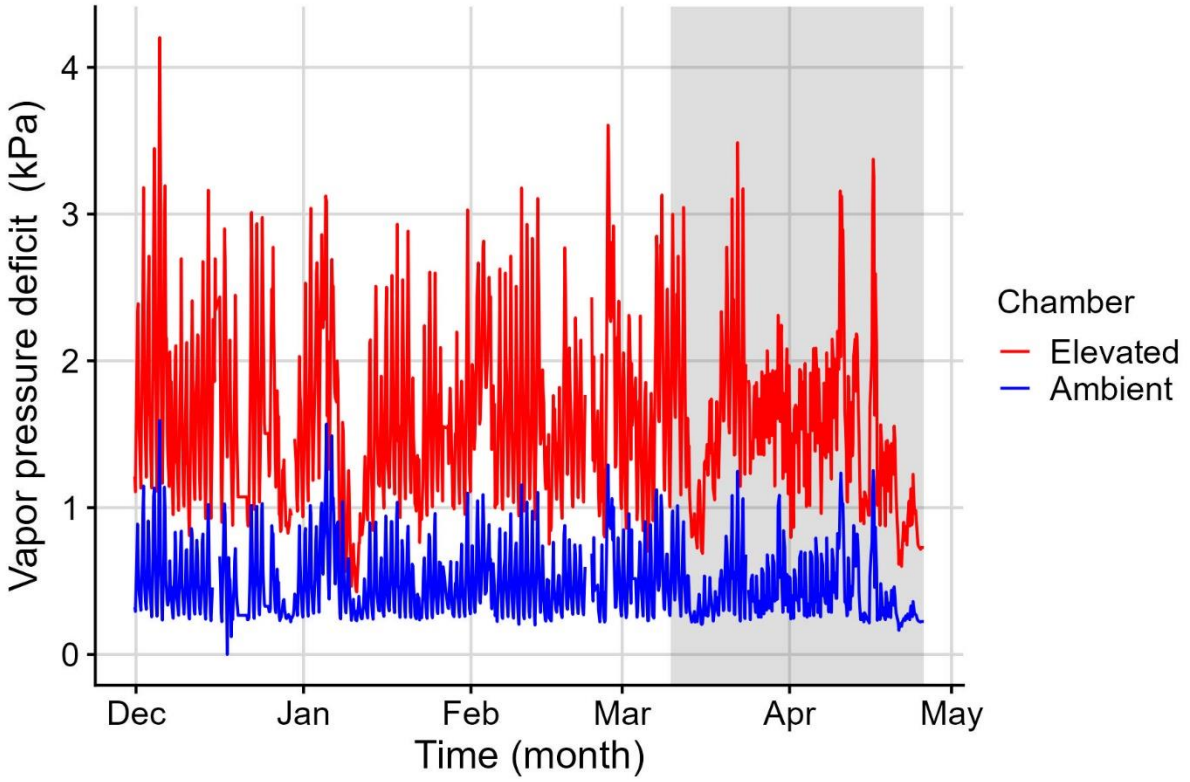

Figure S3.3: Vapor pressure deficit (kPa) of two experimental chambers used to examine the leaf-level acclimation in seedlings of four eucalypt species. Data represent the average conditions over a 10-minute period, with the trace corresponding to the beginning of the experiment. The grey shading represents the period of drought during second phase of the experiment.

Table S3.1: Comparative summary statistics of air temperature, (Temp. °C), relative humidity (Rh %) and vapor pressure deficit (VPD kPa) of the two experimental chambers.

	Ambient			Elevated		
Time	Temp. (°C)	Rh(%)	VPD (kPa)	Temp. (°C)	Rh(%)	VPD (kPa)
Day	30.1 ± 3.2	87.3 ± 6	0.55 ± 0.26	34.9 ± 3.3	68.5 ± 9.3	1.81 ± 0.63
Night	25.5 ± 2.1	87.3 ± 6.5	0.41 ± 0.2	30.4 ± 2.2	68.6 ± 10.1	1.37 ± 0.45

Table S3.2: Outcome of the linear regression models of Leaf mass per area (LMA), minimum conductance (g_{min}) and dark respiration (R_d).

	β		
	LMA	***R_d***	***g_{min}***
Predictors			
(Intercept)	168.99 ***	0.40 ***	2.11
Species [Ec]	-40.30 ***	0.21 **	1.74
Species [Ee]	-32.57 **	0.23 **	6.46 ***
Species [Ep]	-50.32 ***	0.14 *	2.23
Chamber [Elevated_temp]	-39.12 ***	-0.11 *	0.77
Water [Well_watered]	13.30 *	0.03	N/A
Species [Ec] × Chamber [Elevated_temp]	27.47	N/A	-3.34
Species [Ee] × Chamber [Elevated_temp]	46.88 **	N/A	-6.11 *
Species [Ep] × Chamber [Elevated_temp]	24.58	N/A	-3.61
Observations	95	48	24
R^2 / R^2 adjusted	0.404 / 0.349	0.334 / 0.255	0.653 / 0.501

** p<0.05 ** p<0.01 *** p<0.001*

Table S3.3: Comparative summary statistics of leaf water potentials (MPa balance pressure).

Species	Water stress	Chamber	Water potential (mean ± std. deviation)
Corymbia clarksoniana	Drought	Ambient	0.66 ± 0.04
		Elevated	0.66 ± 0.04
	Well-watered	Ambient	1.13 ± 0.4
		Elevated	0.36 ± 0.01
Eucalyptus camaldulensis	Drought	Ambient	3.77 ± 0.32
		Elevated	1.34 ± 0.07
	Well-watered	Ambient	0.52 ± 0.11
		Elevated	1.38 ± 0.01
Eucalyptus exserta	Drought	Ambient	0.83 ± 0.04
		Elevated	1.12 ± 0.26
	Well-watered	Ambient	0.45 ± 0.04
		Elevated	0.41 ± 0.02
Eucalyptus pellita	Drought	Ambient	2.68 ± 0.88
		Elevated	1.14 ± 0.32
	Well-watered	Ambient	1.22 ± 0.38
		Elevated	0.67 ± 0.04

CHAPTER 4: SHORT-TERM AND ACCLIMATED RESPONSES TO CO_2 CONCENTRATION IN ANGIOSPERMS AND BROAD-LEAVED GYMNOSPERMS.

Abstract (Chapter 4)

Angiosperms, now the dominant plant group in most terrestrial biomes, have significantly proliferated since the mid-Cretaceous, coinciding with a decrease in atmospheric CO_2 levels. The rise of angiosperms during a period of declining CO_2 concentrations may have resulted in adaptation of biophysical properties which may result in a differential response of angiosperms and gymnosperms to modern day changes in CO_2 concentrations.

In this study I explored how both adaptation and acclimation potential to changing CO_2 concentrations differ between angiosperms and gymnosperms. This was done by examining plant responses to both short and long-term CO_2 exposure. The experiment involved growing plants from five angiosperm and four broad-leaved gymnosperm species in three different controlled glasshouse chambers with varying CO_2 levels to assess their physiological responses.

Results indicate that angiosperms exhibited a higher relative growth rate (*RGR*) than gymnosperms, independent of growth CO_2 concentration, consistent with previous observations in early growth stages. In addition, angiosperms demonstrated a downregulation of photosynthetic capacity (i.e. maximum rate of carboxylation by RuBisCO, V_{cmax}) resulting in no stimulation of growth in angiosperms to elevated growth [CO_2], unlike gymnosperms which showed a strong positive growth response.

During short-term CO_2 increases, both angiosperms and gymnosperms displayed a rise in photosynthesis, therefore the long-term response of angiosperms could be attributed to an acclimation and high stomatal sensitivity as compared to gymnosperms which showed no acclimation to increased growth CO_2. Indeed gymnosperms, with a lower stomatal sensitivity, maintained consistent photosynthetic rates when evaluated at a constant [CO_2] regardless of growth [CO_2]. Examination of A-C_i curves indicated that this acclimation seen in angiosperms was as a result of decreasing V_{cmax} with unchanged J_{max} (i.e. maximum electron transport rate) where gymnosperms showed no change in either V_{cmax} or J_{max} with increasing growth [CO_2].

This research contributes to understanding the long-term and short-term CO_2 acclimation responses of angiosperms and gymnosperms, addressing gaps in current global vegetation models under changing climate conditions. Future studies utilizing FACE (Free-Air CO_2 Enrichment) facilities, tree rings, and isotopic measurements could expand these findings, providing deeper insights into plant responses to elevated CO_2 levels over extended periods.

4.1 Introduction

Gymnosperms were prevalent and widespread in Mesozoic Earth's flora, particularly during the Triassic and Jurassic periods (250 to 145 Ma). The existing fossil records undeniably show that the diversification and spread of angiosperms expanded rapidly and abruptly since the mid-Cretaceous (Birks, 2020) and the rise to dominance correlates with a decrease in atmospheric carbon dioxide from ~1000 ppm to pre-industrial levels, ~280 ppm (McElwain *et al.*, 2005). This in turn led angiosperms, the flowering plants, to dominate most of the Earth's terrestrial biomes at present (Herendeen *et al.*, 2017; Magallón *et al.*, 2019). Today angiosperms make up at least 90% of the local vascular plant species in almost every terrestrial location including in gymnosperm forests (Kreft & Jetz, 2007).

Recent research indicates the enhanced fall of gymnosperms in number during the Mid- and Late Cretaceous era is best explained as a reaction to angiosperm expansion during the prolonged period of global cooling and long-term biological interactions through clade competition in the presence of a changing climate (Condamine *et al.*, 2020). This result disproved the age-old hypothesis proposing climate change or time are the sole drivers of widespread extinction of gymnosperms during the Cretaceous (Birks, 2020). Researchers suggest that prolonged biotic and, to a certain degree, abiotic alterations might have had a more significant impact on plant evolution than mass extinction incidents (Schneider *et al.*, 2004; Laenen *et al.*, 2014; Lehtonen *et al.*, 2017). The earliest fossil records have shown flowering plants emerged in the early Cretaceous and became predominant by late Cretaceous (Herendeen *et al.*, 2017).

One of the reasons for the decline of gymnosperms was their lower efficiency of photosynthesis. The colder climate and shorter growing seasons reduced their ability to capture energy through photosynthesis, slowing their development and limiting survival (Gamon *et al.*, 2016). Additionally, the evolutionary diversification of flowering plants was vital for their prosperity amid the global cooling. Over half of the existing groups of angiosperms came about during this time, demonstrating their capacity to adjust and thrive in reaction to a changing environment (Zanne *et al.*, 2013). Angiosperms employed various strategies, including the evolution of novel traits and the expansion of their geographic ranges, to prosper in the cooling climate (Qian *et al.*, 2023). This diversification and adaptability enhanced their competitiveness with gymnosperms, resulting in the angiosperms becoming the prevailing plant group.

Flowers are considered the cornerstone of angiosperm hyper-diversity due to their double fertilization resulting in endosperm formation as well as their close coevolution with animal pollinators (Endress, 2011). It is a reasonable assumption that the prosperity of angiosperms is not just from their possession of flowers but also from the extensive divergence of their reproductive structures, which

is unparalleled in any other terrestrial plant clades. Again, it is the development of varied interactions between angiosperms and animal pollinators which was made possible by the evolution of flowers (Xiao *et al.*, 2021).

Angiosperms possess distinctive adaptations that improve their photosynthetic efficiency. These distinctive characteristics have cooperated to increase leaf morphological diversity, allowing for adaptation to a broad spectrum of habitats. Furthermore, they have increased the number of veins and stomata, enabling better regulation of gas exchange. Angiosperms also evolved vessels in their xylem, which are more efficient in transporting soil water to leaves compared to largely tracheid bearing gymnosperms (Sperry *et al.*, 2006). Another innovative adaptation that has evolved in angiosperms is a more condensed leaf venation, up to four times greater vein density than in gymnosperms (Feild *et al.*, 2011). This flexibility of vein density enables angiosperms to sustain the optimum balance of water supply, water consumption, and photosynthetic rate across a diverse range of habitats (De Boer *et al.*, 2012; McElwain *et al.*, 2016). Angiosperms were also successful in undergoing numerous whole genome duplications, leading to multiple stages of evolutionary stimulation (Benton *et al.*, 2022).

Angiosperms exhibit a remarkable ability to adapt and evolve. Their efficient physiology and anatomy have enabled them to capture energy and carbon at a faster rate than other plant groups, contributing to their current high species diversity. Unique forest structures and the coevolution of pollination, herbivory, and dispersal strategies were made possible by the emergence of angiosperms. (Benton *et al.*, 2022).

Global atmospheric CO_2 is on rise since the beginning of the industrial era and the current atmospheric CO_2 concentration is around 420 ppm compared to 278 ppm in 1750 (Friedlingstein *et al.*, 2022). Researchers have been studying the effects of increasing CO_2 on forests as they are one of the main carbon sinks and the results suggest impacts may vary depending on various aspects of the forest ecosystem. Plant responses to elevated CO_2 vary depending on their functional traits as well as species level traits. The impacts of elevated levels of CO_2 on forest ecology are complex and diverse. In general forest shows increased growth and productivity (Norby *et al.*, 2005), although the severity of responses depends on various biotic factors, i.e. species, genotype, and functional group, as well as abiotic factors, i.e. soil type and nutrient status, moisture availability, ambient temperature, and pests (Karnosky, 2003).

Angiosperms and gymnosperms show significantly different responses to increased levels of CO_2 (Norby *et al.*, 1986; Brodribb & Feild, 2008; Brodribb *et al.*, 2009; Brodribb & McAdam, 2013; Dalling *et al.*, 2016; Hasper *et al.*, 2017; Liang *et al.*, 2023). Stomatal sensitivity to CO_2 is higher in

angiosperms compared to gymnosperms (Hasper *et al.*, 2017; Klein & Ramon, 2019). This could possibly be linked to their overall elevated g_s and their thinner leaves, which result in quicker loss of water. Conversely, gymnosperms have lower stomatal sensitivity to CO_2, coinciding with different leaf structure and physiology (Brodribb & McAdam, 2013). Angiosperms have evolutionarily adapted Ca^{2+} dependent stomatal signaling more strongly than other plants enabling their higher *WUE* but in return this higher stomatal sensitivity may penalize their productivity in presently increasing atmospheric CO_2. Another study has found significant variation in the mesophyll conductance of gymnosperms, which was strongly related with pectin to hemicellulose and cellulose ratios (Carriquí *et al.*, 2020). These changes in the cell wall composition might adjust the CO_2 diffusivity effectively, thereby possibly offsetting the adverse effects of thickened walls in gymnosperms. These findings suggest that gymnosperms may have adapted mechanisms better suited to increased levels of atmospheric CO_2.

Interestingly, opposing outcomes have been described by two different studies where angiosperms responded with stomatal reduction and higher *WUE* during short-term exposure to elevated CO_2 (Brodribb *et al.*, 2009), whereas another longer term CO_2 exposure experiment found increased growth and higher *WUE* with increasing growth CO_2 concentration in gymnosperms (Dalling *et al.*, 2016). This suggests that instantaneous and acclimated responses to elevated CO_2 may differ between angiosperms and gymnosperms, potentially with important implications for understanding their overall ecophysiology in the current period of rapid atmospheric CO_2 increase.

We therefore aimed to grow a range of angiosperms and broad-leafed gymnosperms, often found in conjunction within the humid forests of tropical north Queensland, under a range of CO_2 concentrations. In doing so we sought to establish both the short-term instantaneous and long-term acclimation responses in angiosperms and gymnosperms to better understand the mechanisms that might drive divergent responses between the two groups.

4.2 Materials and methods

The experiment was conducted in a climate-controlled glasshouse that is part of James Cook University's Environmental Research Complex on the Nguma-bada campus, Cairns Queensland. This is a walk-in, climate-controlled greenhouse facility measuring 9 × 7 m, comprising three independently regulated chambers of 5(L) × 3(W) × 4(H) m each. The parallel chambers, positioned in a north-south orientation, are enabled with independent regulation of temperature and [CO_2] levels. They were illuminated by natural sunlight, at approximately 50%, via the SOLARO 5220 D O FB climate screen (Ludvig Svensson Inc., Kinna, Sweden). For the duration of the experiment chambers were set to maintain one of three [CO_2] i.e. 450, 650 or 1000ppm while temperatures were set to track external ambient air temperature. The environmental conditions for the duration of this experiment are provided in Table S4.3.

4.2.1 Species selection

A total of nine species, four angiosperm and five gymnosperm tree species, were selected for this experiment (Table 4.1). The four angiosperm species included those locally endemic to the Wet Tropics of Queensland Australia (*Diploglottis bracteata* and *Flindersia brayleyana*) and those with a broad regional distribution (*Elaeocarpus angustifolius* and *Alphitonia petriei*). The five gymnosperm species (*Araucaria bidwillii, Agathis robusta, Podocarpus dispermus, Podocarpus grayae* and *Sundacarpus amarus*) were all broad-leafed gymnosperms drawn from two dominant southern hemisphere families (i.e. Araucariaceae and Podocarpaceae). All seedlings were collected from local single-source populations.

4.2.2 Experimental Design

Individuals of each species were transplanted into 20 L pots filled with a locally sourced, screened, high-organic-matter potting mix with a base of gravel to ensure good drainage on 29th of May, 2016. After 10 days of establishment within a separate shade-house, six individuals of each species were transplanted to each of the three treatment chambers between 4-6 June 2016 to begin a 112-day experimental period. Plants were watered by hand. Each growing chamber was set to a treatment CO_2 concentration (450 ppm, 650 ppm and 1000 ppm). The temperatures for all the chambers were set to track the ambient temperature, whereas relative humidity was not controlled. Once placed in the experimental chambers, the pots were not moved for the duration of the experiment, to prevent plant damage, soil movement and other disturbances.

Table 4.1: Species list for the altered CO_2 experiment and their distribution ranges.

Family	**Species**	**Functional Group**	**Distribution range**
Rhamnaceae	*Alphitonia petriei*	Angiosperm	Eastern and Northern Australia
Sapindaceae	*Diploglottis bracteata*	Angiosperm	Endemic to North-east Queensland
Elaeocarpaceae	*Elaeocarpus angustifolius*	Angiosperm	India to New Caledonia and northern Australia
Rutaceae	*Flindersia brayleyana*	Angiosperm	Endemic to North-east Queensland
Araucariaceae	*Araucaria bidwillii*	Gymnosperm	Queensland
Araucariaceae	*Agathis robusta*	Gymnosperm	Queensland and Papua New Guinea
Podocarpaceae	*Podocarpus dispermus*	Gymnosperm	Endemic to Atherton Tablelands, Queensland
Podocarpaceae	*Podocarpus grayae*	Gymnosperm	Northern territory and Queensland
Podocarpaceae	*Sundacarpus amarus*	Gymnosperm	North-east Queensland and Malesia

4.2.3 Biomass Measurements

For all plants initial measurements of root-collar diameter (along two axes orthogonal to one another), and height (distance between the apical shoot and the root collar) were taken to estimate initial biomass using species specific allometric relationships developed from additional harvested plants (6 individual plants from each species) at the beginning of the experiment (Equation 4.1).

$$initial\ mass\ = height \times root\ collar\ area\ \times\ species \quad \text{(Equation 4.1)}$$

After 112 days all plants were harvested, and separated into leaf, stem and root biomass. Leaves were scanned with a CanoScan LiDE 110 scanner and analysed using ImageJ to determine leaf area. All biomass was dried for at least 72 hours at 70°C and weighed to the nearest 0.01 g.

4.2.4 Gas Exchange measurements

Prior to harvesting the seedlings, leaf-level gas exchange was measured using three portable photosynthesis systems (Li-Cor 6400, Li-Cor Inc., Lincoln, NE, USA). Survey measurements of net photosynthesis were made (irradiance of 1200 µmol photons m^{-2} s^{-1}, supplied by an artificial light source, 6400-02B LED, Li-Cor Inc.) on one leaf per plant at leaf temperatures ranging from 30 to 33 °C and at the treatment [CO_2] (i.e. 450, 650, or 1000 ppm). Over the subsequent two days survey measurements were conducted in each chamber at the other treatment levels of [CO_2] with the entire chamber being set to the target [CO_2] for at least one hour prior to measurements. In addition, A-C_i response curves were measured on a subset of plants grown under the low (450 ppm) and high (1000 ppm) [CO_2] treatments. In this case, chambers remained at the treatment atmospheric [CO_2] before measuring the A-C_i response curve between 50 and 1600 ppm within the leaf cuvette. The A-C_i curves were analysed with the "*fitaci*" function from the R package "plantecophys" (version 1.4.6) (Duursma, 2015) using default parameters to fit the photosynthesis model. The fitted parameters were normalised to 25 °C. We estimated V_{cmax} (maximum carboxylation rate, µmol CO_2 m^{-2} s^{-1}); J_{max} (maximum electron transport rate, µmol e^- m^{-2} s^{-1}); J_{max}/V_{cmax} (ratio of maximum electron transport rate and maximum carboxylation rate, mol e^- mol^{-1} CO_2) and C_i *transition* (intercellular CO_2 concentration for the transition point from V_{cmax} to J_{max} limited photosynthesis, µmol mol^{-1}) from the fitted A-C_i curves.

4.2.5 Statistical Analysis

All data manipulation and statistical analyses were performed in R version 4.3.1 (R Core Team, 2023). We calculated relative growth rates (*RGR*) of individual plants using the predicted initial dry mass, observed final dry mass and total number of days with the methods outlined by Pommerening and Muszta (2016) and shown in equation (4.2). This calculation gave the *RGR* in units of g g^{-1} day^{-1}.

$$RGR = \frac{\log\left(\frac{final\ mass}{inital\ mass}\right)}{Number\ of\ days} \quad \text{(Equation 4.2)}$$

To examine the impact of growth [CO_2] treatment and plant functional group (i.e. angiosperm or gymnosperm) on the *RGR* a linear mixed effect model was used where species was a random effect. For the gas exchange parameters including photosynthesis (A, µmol CO_2 m^{-2} s^{-1}), stomatal conductance to H_2O (g_s, mmol m^{-2} s^{-1}), intrinsic water-use efficiency (WUE_i, mmol CO_2 mol^{-1} H_2O) calculated as A/g_s, and the ratio of the leaf's internal to ambient [CO_2] (c_i/c_a) multiple linear mixed effects models were used to test for differences between growth [CO_2] treatment, functional group and [CO_2] in the LI-6400 leaf cuvette (i.e. c_a). Species and individual plants were used as random effects for these linear mixed effect models, the latter to account for repeated measures of the same plant. I used the R package "glmmTMB" (Magnusson *et al.*, 2017) to fit the models. Models were compared and best fitted models were selected based on their performances analysed with "DHARMA", "MuMIn", "performance" and "see" packages for R (Lüdecke *et al.*, 2021a; Lüdecke *et al.*, 2021b; Hartig, 2022; Bartoń, 2023). Graphs and figures were produced using the R package "ggplot2" (Wickham, 2016).

4.3 Results

We successfully grew nine tropical tree species for 112 days in three different growing chambers under three preset [CO_2] conditions. Environmental conditions between chambers showed no substantive differences, except [CO_2]. Temperature was set to track the outside ambient condition, whereas the relative humidity was not controlled. Average (± standard deviation) day-time temperature within the chambers was 29.4 ± 3.1 °C and average night-time temperature was 23.2 ± 3.1 ^{o}C. More details on environmental conditions inside the chambers can be found in Table S4.5.

I used a general linear mixed effect model (gamma family with log link) to explain and predict *RGR* with treatment (growth CO_2 concentration in the glasshouse chambers), functional group of the plants, and their interaction as fixed effects, and species was included as a random effect. The interaction term allowed me to assess whether the effect of functional group on *RGR* depends on treatment levels. Model outcomes are shown in Table 4.2.

The *RGR* of angiosperms was higher than gymnosperms at all the treatment levels (Figure 4.1A) and the main effect of group was statistically significant ($\chi^2_{1,\ n=149} = 4.79$; *P*= 0.029). I did not observe a statistically significant main effect of treatment ($\chi^2_{2,\ n=149} = 2.40$; *P*= 0.301). However, I found a significant interaction between treatment and group ($\chi^2_{2,\ n=149} = 13.88$; *p*< 0.001) meaning the effect of growth [CO_2] treatment on *RGR* depends on the functional groups. The highest median *RGR* for angiosperms was at 650 ppm CO_2 treatment level (median = 27.7 mg g^{-1} day^{-1}, SD = 14.5), followed by angiosperms at 1000 ppm (median = 27.0 mg g^{-1} day^{-1}, SD = 15.9) and 450 ppm (median = 25.1 mg g^{-1} day^{-1}, SD = 15.1). In the case of gymnosperms, I observed increases in *RGR* with each increase in growth CO_2 concentration. The highest median *RGR* for gymnosperms was at 1000 ppm (median = 16.5 mg g^{-1} day^{-1}, SD = 5.38), followed by 650 ppm (median = 13.9 mg g^{-1} day^{-1}, SD = 5.77) and 450 ppm (median = 10.5 mg g^{-1} day^{-1}, SD = 4.81) treatment level.

Figure 4.1B illustrates the predicted values from the statistical model of *RGR* for angiosperms and gymnosperms at different growth CO_2 concentrations. The model shows that with the increase in growth CO_2 concentration angiosperms will show little change in *RGR* whereas gymnosperms show an increasing trend.

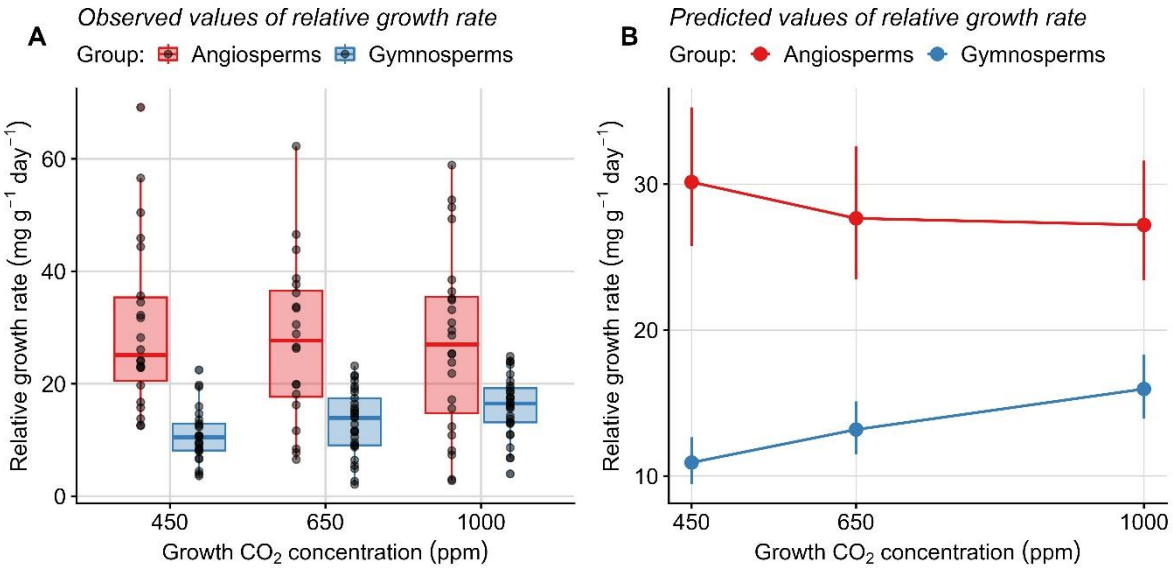

Figure 4.1: Boxplots of **A)** observed relative growth rates (mg g^{-1} day^{-1}) for angiosperms and gymnosperms grown at different CO_2 concentrations, and **B)** predicted relative growth rates from the best fitted linear mixed effect model illustrating estimated marginal mean relative growth rates (mg g^{-1} day^{-1}) of angiosperms and gymnosperms grown at different CO_2 concentrations. Here, angiosperms are represented in red whereas gymnosperms are in blue.

Table 4.2: Summary of mixed effect models describing the effects of functional group, CO_2 treatment, ambient CO_2 concentration, and their interactions on relative growth rate (*RGR*) and gas exchange parameters (Photosynthesis, *A*; cube root of stomatal conductance, $^3\sqrt{g_s}$; intrinsic water use efficiency, A/g_s and the ratio of intercellular airspace CO_2 concentration to atmospheric CO_2 concentration, c_i/c_a) for angiosperms and gymnosperms.

	RGR	*A*	$^3\sqrt{g_s}$	A/g_s	c_i/c_a
Intercept [Angiosperms]	***	***	***	***	***
Treatment [linear]	ns	*** ↓	*** ↓	ns	ns
Group [gymnosperms]	*	*** ↓	*** ↓	* ↑	* ↓
c_a		*** ↑	* ↓	*** ↑	ns
Treatment [linear] × Group [gymnosperms]	***	***	***	ns	ns
Group [gymnosperms] × c_a		***	ns	ns	ns

ns = not significant; * p≤0.05; ** p≤0.01; *** p≤0.001

Gray fields are terms not available for that model and arrows indicate the direction of change in the response variable for the respective main effect.

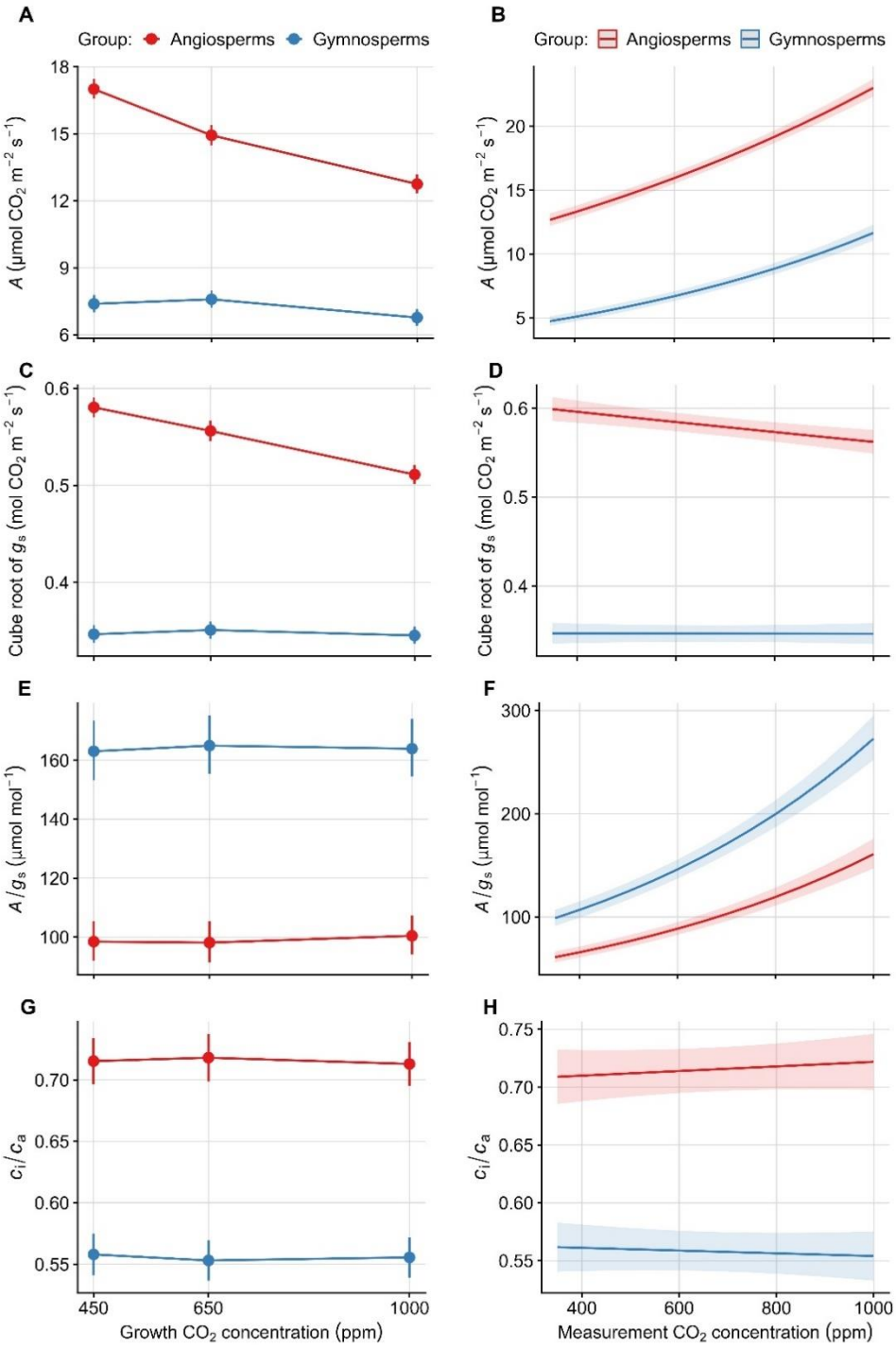

Figure 4.2: Partial plots from the best fitted linear mixed effect models illustrating relationships of estimated marginal mean **A-B**) net photosynthesis, *A* (µmol CO_2 m^{-2} s^{-1}); **C-D**) cube root of stomatal conductance, g_s (mol CO_2 m^{-2} s^{-1}); **E-F**) intrinsic water use efficiency, A/g_s (µmol mol^{-1}) and **G-H**) ratio of intercellular airspace to atmospheric CO_2 concentration, c_i/c_a with (**A, C, E, G**) shown as a function of growth CO_2 concentration (ppm) and (**B, D, F, H**) shown as a function of measurement CO_2 concentration (ppm). Angiosperms are in red and gymnosperms in blue. The shaded areas are the 95% confidence intervals. The left panels represent acclimated responses assessed at a single CO_2 concentration, and the right panels represent instantaneous responses to varying CO_2 concentration.

Next, I fitted models for the gas exchange parameters (e.g. Photosynthesis, *A*; cube root of stomatal conductance, $^{3}\sqrt{g_s}$; intrinsic water use efficiency, A/g_s and intercellular airspace CO_2 concentration to atmospheric CO_2 concentration ratio, c_i/c_a) with generalized linear mixed effect models (gaussian and gamma family with log link, and gaussian family with identity based on distribution) with treatment, functional group, and cuvette CO_2 level during measurements as fixed effects, and species and individual as random effects. The two-way interaction terms between the fixed effects were included in the models. Model outcomes are presented in Table 4.2.

When measured at the growth CO_2 concentration, photosynthesis was significantly higher in angiosperms compared to gymnosperms ($\chi^2_{1,\ n=454} = 20.55$, p < 0.001). The main effect of treatment (growth CO_2 concentration) was statistically significant ($\chi^2_{2,\ n=454} = 20.16$, p < 0.001) when measurement CO_2 concentration was controlled for within the model. We found a decreasing trend in photosynthesis when evaluated at a common cuvette CO_2 concentration with increasing growth CO_2 concentration for angiosperms (Figure 4.2A). In the instantaneous responses, photosynthesis measured at different CO_2 concentrations in angiosperms showed an increasing trend with increasing measurement CO_2 concentration (Figure 4.2B). Gymnosperms from different chambers did not show any statistical differences in photosynthesis rate with increasing growth CO_2 concentration when evaluated at a constant measurement CO_2 concentration (Figure 4.2A). Like for the angiosperms, the effect of cuvette CO_2 concentration during measurements (c_a) on photosynthesis was significant and high, as seen in figure 4.2B ($\chi^2_{1,\ n=454} = 5.26$, p = 0.02). Both the interaction terms (treatment × group, and group × c_a) in the mixed effect model for photosynthesis were significant and high ($\chi^2_{2,\ n=454} = 6.80$, p =0.03 and $\chi^2_{1,\ n=454} = 35.33$, p < 0.001 respectively).

Angiosperms showed significantly higher g_s compared to gymnosperms ($\chi^2_{1,\ n=454} = 21.20$, p < 0.001). The treatment effect was significant and small ($\chi^2_{2,\ n=454} = 10.63$, p = 0.001). I did not find any treatment effect on gymnosperms but for angiosperms conductance was significantly lower between 450 ppm and 1000 ppm treatment levels (P < 0.01) (Figure 4.2C and 4.2D). c_a has a low significance in describing conductance ($\chi^2_{1,\ n=454} = 5.26$, p = 0.02). In this model, the only interaction effect that approached significance was that between treatment and group ($\chi^2_{2,\ n=454} = 5.59$, p = 0.06).

In the case of intrinsic water use efficiency (A/g_s), gymnosperms showed higher values compared to angiosperms and the difference between gymnosperms and angiosperms was significant and large ($\chi^2_{1,\ n=152} = 10.63$, p = 0.008). There were no statistical differences for different treatments when A/g_s was evaluated at the mean measurement CO_2 level (Figure 4.2E), but when measured at different levels of CO_2 concentration both angiosperms and gymnosperms showed an

increasing trend with higher level of CO_2 (Figure 4.2F). The effect of measurement c_a was significant and high ($\chi^2_{1,\ n=454} = 431.38$, $p < 0.001$). Contrarily to g_s, the A/g_s model showed a significant interaction between groups and c_a ($\chi^2_{1,\ n=454} = 4.01$, $p = 0.045$).

A similar trend was found for c_i/c_a (Figure 4.2G) where I did not find any difference between treatment levels at both growth and measured CO_2 concentrations. But in this case, c_i/c_a was significantly higher for angiosperms ($\chi^2_{2,\ n=152} = 6.96$, $p = 0.008$). The other fixed effects and two-way interactions did not show any significant differences.

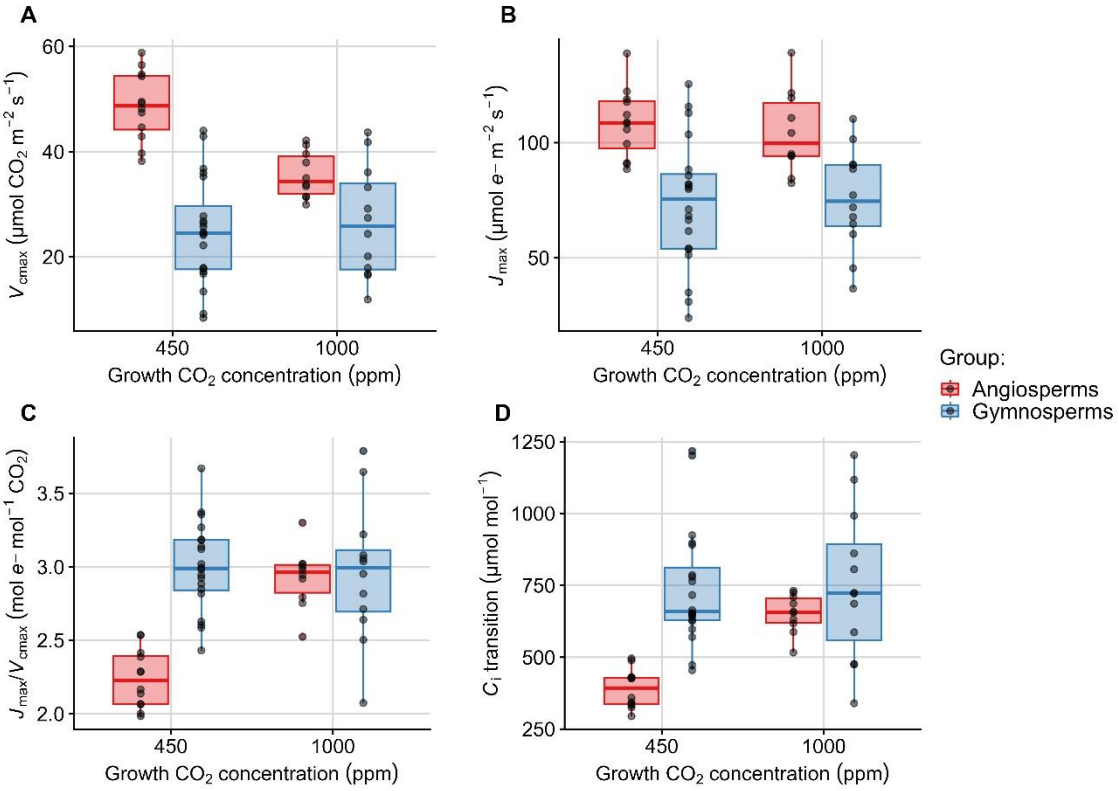

Figure 4.3: Boxplot of A) Maximum carboxylation rate, V_{cmax} (µmol CO_2 m^{-2} s^{-1}); B) Maximum electron transport rate, J_{max} (µmol e^- m^{-2} s^{-1}); C) Ratio of maximum electron transport rate and maximum carboxylation rate, J_{max}/V_{cmax} (mol e^- mol^{-1} CO_2) and D) Intercellular CO_2 concentration for the transition point from V_{cmax} to J_{max} limited photosynthesis, C_i *transition* (µmol mol^{-1}); measurements for plants grown at two different CO_2 concentrations (450 ppm and 1000 ppm). Angiosperms are illustrated in red coloured boxes and gymnosperms in blue boxes.

From the *A*-C_i curves, I calculated maximum carboxylation rate (V_{cmax}), maximum electron transport rate (J_{max}), ratio of J_{max} to V_{cmax}, and the intercellular CO_2 concentration for transition from V_{cmax} to J_{max} limited photosynthesis. Boxplots in figure 4.3 illustrate the comparison of these parameters for angiosperms and gymnosperms grown at 450 ppm and 1000 ppm CO_2 concentrations. This analysis provides insight into how photosynthetic capacity changed in plants grown at the lowest and highest CO_2 concentrations. For that purpose, I fitted linear mixed effect models (gaussian family with log link or with identity link, whichever was needed based on distribution) for V_{cmax}, J_{max}, ratio of V_{cmax} to J_{max}, and C_i transition. The fixed effects were treatment and functional group, and their two-way interaction term. Species was a random effect. Model outcomes are presented in Table 4.3.

V_{cmax} was statistically significant and higher for angiosperms (Figure 4.3A; $\chi^2_{1,\ n=54}$ = 28.03; p < 0.001) in both 450 ppm and 1000 ppm CO_2 concentration compared to gymnosperms (Figure 4.3A). The interaction between treatment and functional group was significant ($\chi^2_{1,\ n=54}$ = 22.99; p < 0.001), showing that the treatment effect on V_{cmax} was different depending on functional group.

Angiosperms showed higher J_{max} (Figure 4.3B; $\chi^2_{1,\ n=54}$ = 4.97; p= 0.03) than gymnosperms but there was no significant effect of growth CO_2 level or interaction between functional group and growth CO_2 level on J_{max}.

The ratio of J_{max} to V_{cmax} was significantly higher for gymnosperms (Figure 4.3C; $\chi^2_{1,\ n=54}$ = 29.02; p<0.001). The treatment effect was significant ($\chi^2_{1,\ n=54}$ = 31.90; p<0.001) and the difference between gymnosperms and angiosperms was significantly larger at 450 ppm growth CO_2 concentration (t= -4.90; p<0.001), and there was no difference at 1000 ppm growth CO_2 concentration (P= 0.64). This was indicated by the significant interaction effect between functional group and treatment on J_{max}/V_{cmax} ($\chi^2_{1,\ n=54}$ = 17.20 and p<0.001).

The C_i transition point (intercellular CO_2 concentration for transition from V_{cmax} to J_{max} limitation) showed a similar trend same as J_{max}/V_{cmax}, where gymnosperms showed significantly higher values (Figure 4.3D; $\chi^2_{1,\ n=54}$ = 13.62; p<0.001). Although gymnosperms did not show any significant difference between treatment levels, angiosperms showed higher J_{max} to V_{cmax} ratio at 1000 ppm (t= -3.95; p<0.001), shown by a significant treatment effect ($\chi^2_{1,\ n=54}$ = 15.61; p<0.001). The different behaviour of the functional groups was evidenced by a significant interaction effect with growth CO_2 concentration ($\chi^2_{1,\ n=54}$ = 7.67; P= 0.0056).

Table 4.3: Outcome of the mixed effect models of maximum carboxylation rate, V_{cmax} (µmol CO_2 m^{-2} s^{-1}); maximum electron transport rate, J_{max} (µmol e^- m^{-2} s^{-1}); ratio of maximum electron transport rate and maximum carboxylation rate, J_{max}/V_{cmax} (mol e^- mol^{-1} CO_2), and intercellular CO_2 concentration for transition from V_{cmax} to J_{max} limited photosynthesis, C_i *transition* (µmol mol^{-1}).

Predictors	V_{cmax}			J_{max}			J_{max}/V_{cmax}			C_i *transition*		
	B	*CI*	*p*	β	*CI*	*p*	β	*CI*	*p*	β	*CI*	*p*
(Intercept)	48.6702	39.8860 – 57.4544	***	108.5741	86.8845 – 130.2637	***	2.2390	1.9987 – 2.4794	***	5.9703	5.6784 – 6.2621	***
Group [gymnosperms]	-23.4900	-34.6044 – -12.3757	***	-34.0358	-61.4814 – -6.5901	*	0.7611	0.4568 – 1.0654	***	0.6257	0.2833 – 0.9680	***
Treatment [1000]	-13.2448	-17.4457 – -9.0439	***	-4.0984	-16.2051 – 8.0084	ns	0.6922	0.4519 – 0.9324	***	0.5146	0.2593 – 0.7698	***
Group [gymnosperms] × Treatment [1000]	13.7770	8.1461 – 19.4079	***	4.5658	-11.6477 – 20.7793	ns	-0.6807	-1.0023 – -0.3590	***	-0.4186	-0.7148 – -0.1224	**
Random Effects												
σ^2	24.9454			207.2097			0.0816			21799.1982		
τ_{00}	54.0234 $_{Species}$			315.5876 $_{Species}$			0.0247 $_{Species}$			0.0311 $_{Species}$		
N	8 $_{Species}$			8 $_{Species}$			8 $_{Species}$			8 $_{Species}$		
Observations	54			54			54			54		
Marginal R^2 / Conditional R^2	0.537 / 0.854			0.327 / 0.733			0.483 / 0.603			0.485 / 0.694		

ns = not significant; * p≤0.05; ** p≤0.01; *** p≤0.001

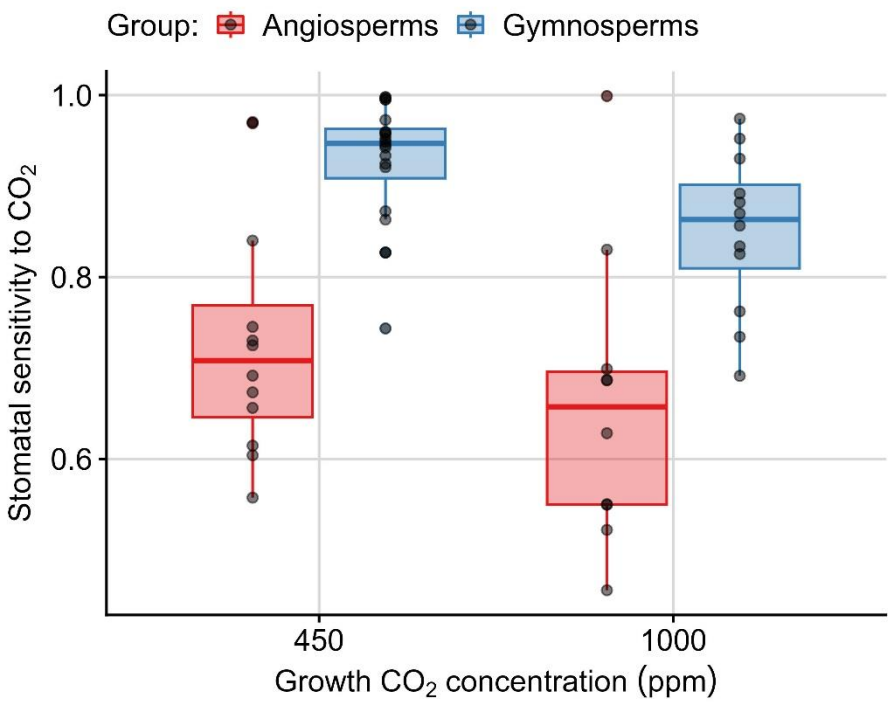

Figure 4.4: Boxplot of stomatal sensitivity to CO_2 for seedlings grown at two different CO_2 concentrations (450 ppm and 1000 ppm). Angiosperms are illustrated in red-coloured boxes whereas gymnosperms are illustrated in blue boxes. Lower values on the y-axis indicate a more pronounced stomatal closure response to increasing CO_2 concentration based on short term exposure.

Table 4.4: Mixed effect model of stomatal sensitivity to growth CO_2 concentration.

Predictors	Stomatal Sensitivity		
	β	*CI*	*p*
(Intercept)	0.7314	0.6682 – 0.7947	<0.001
Group [gymnosperms]	0.1955	0.1154 – 0.2756	<0.001
Treatment [1000]	-0.0706	-0.1619 – 0.0208	0.130
Group [gymnosperms] × Treatment [1000]	-0.0050	-0.1255 – 0.1154	0.935
Random Effects			
σ^2	0.0118		
$\tau_{00\ Species}$	0.0002		
$N_{\ Species}$	8		
Observations	54		
Marginal R^2 / Conditional R^2	0.480 / 0.487		

ns = not significant; * p≤0.05; ** p≤0.01; *** p≤0.001

I plotted stomatal sensitivity to CO_2 derived from the *A*-C_i curves against growth CO_2 concentration for angiosperms and gymnosperms (Figure 4.4). Stomatal sensitivity to CO_2 was calculated as the g_s during the *A*-C_i curve when the cuvette CO_2 concentration was 1200 ppm divided by the g_s when the cuvette CO_2 was 200 ppm. Therefore, a smaller value indicates a stronger stomatal closure response to CO_2 during the *A*-C_i curve. A mixed effect model was fitted (gaussian family with identity function) with plant functional group and growth CO_2 treatment level (450 ppm and 1000 ppm CO_2 concentration), and their two-way interaction as fixed effects. Species was again a random effect. Model outcomes are shown in table 4.4.

Although stomatal sensitivity to CO_2 appeared to decrease with increased growth CO_2 concentration for both angiosperms and gymnosperms, the difference was not significant between treatment levels (Figure 4.4 and Table 4.4). On the other hand, angiosperms showed stronger stomatal sensitivity compared to gymnosperms ($\chi^2_{1,\ n=54}$ = 22.89; p<0.001). The interaction effect between functional group and growth CO_2 level was not significant.

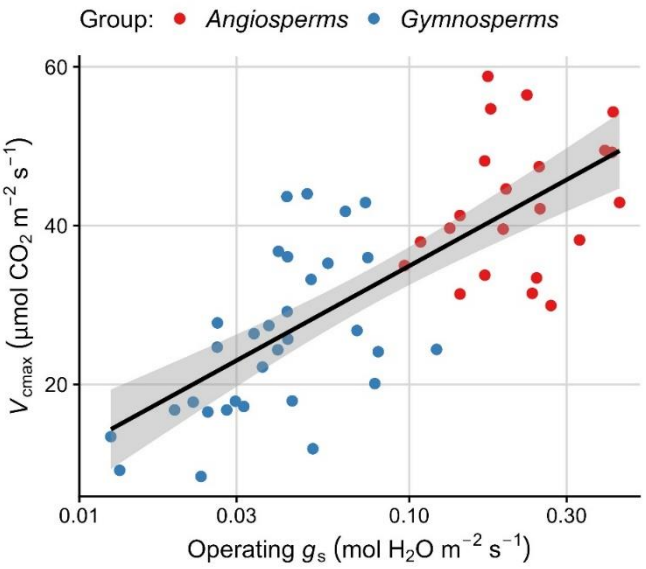

Figure 4.5: Relationship between maximum carboxylation rate, V_{cmax} (µmol CO_2 m^{-2} s^{-1}) and operating stomatal conductance, g_s (mol H_2O m^{-2} s^{-1}). The black line presented here is the regression line and grey shaded area represents the 95% confidence interval. Angiosperms are illustrated with red dots whereas gymnosperms are in blue dots. Note the log scale on the x-axis.

Finally, I plotted V_{cmax} against the operating g_s of both angiosperms and gymnosperms for the plants for which *A*-C_i curves had been measured. The operating g_s was taken from the survey measurements in which plants in each growth CO_2 concentration had their leaf gas exchange measured under those same conditions. Figure 4.5 shows a general coordination between V_{cmax} and the operating g_s across all the plants, with gymnosperms occupying the lower end of the spectrum

and angiosperms the upper end. The implication of this general relationship is that it shows coordinated changes in V_{cmax} and g_s, if one or the other changes in response to growth CO_2 concentration. For example, in angiosperms grown at 1000 ppm CO_2 concentration, in which V_{cmax} was shown to decrease compared to the plants grown at 450 ppm, the relationship in figure 4.5 suggests that this would also be accompanied by a decline in the operating g_s.

4.4 Discussion

We grew five species of gymnosperms and four species of angiosperm trees, all native to the Australian Wet Tropics bioregion, at three CO_2 concentrations in a glasshouse under tropical climate conditions and examined their growth and leaf gas exchange responses. Overall, the angiosperm trees had higher *RGR* than the gymnosperm trees. This aligns with a well-known pattern among these two groups at the seedling and sapling growth stages, whereby angiosperms tend to accumulate biomass more rapidly during early growth (Bond, 1989; Brodribb *et al.*, 2012). However, most intriguingly, the gymnosperm tree species showed a linear increase in *RGR* with increasing growth CO_2 concentration, whereas the angiosperm tree species showed no significant response. This is consistent with observations in the only previous study in which tropical gymnosperms and angiosperm counterparts were compared for their growth responses to CO_2 in a tropical climate (Dalling *et al.*, 2016). My analyses of the leaf-level photosynthetic responses to the growth CO_2 concentrations, which is the acclimated responses, and responses to short-term changes in CO_2 concentration around the leaf, provided insight into the physiological drivers of the difference in growth rates in response to growth CO_2 concentrations between the two groups. The angiosperm species showed downregulation of photosynthetic capacity, through downward adjustment of V_{cmax}, in response to growth at elevated CO_2, whereas the gymnosperms showed no such response. As a result, the proportional increases in photosynthesis with increasing growth CO_2 concentration were larger in the gymnosperm species than in the angiosperm species.

Figure 4.2 shows that this downregulation of photosynthetic capacity, an acclimated response to growth at higher CO_2 concentrations, would not be detected in short-term CO_2 response measurements. The top left panel (Figure 4.2A) shows the linear decline in angiosperm photosynthesis when measurement CO_2 concentration was held constant at the mean value of all measurements within the statistical model. Therefore, evaluated at a single reference CO_2 concentration, the decrease in photosynthetic rate in the angiosperms reflects their downregulation of photosynthetic capacity across the increase in growth CO_2 concentrations. On the other hand, the top right panel (Figure 4.2B) shows that when short term changes in measurement CO_2 concentration were imposed, photosynthetic rates in both groups increased when exposed in the short term to higher CO_2 concentrations. This latter set of measurements do not reflect the acclimation that occurs during growth at the different CO_2 concentrations, because the changes in CO_2 that the plants were exposed to for these measurements were made over the course of a couple of hours.

The acclimated response also shows a decline in g_s in the angiosperms, but not in the gymnosperms (Figure 4.2C). This is consistent with analyses across a range of experiments, which showed more marked decreases in g_s in response to growth at elevated CO_2 in angiosperm tree species

than in gymnosperms (Medlyn *et al.*, 2001; Klein & Ramon, 2019). Interestingly our short-term response measurements of leaf gas exchange responses to changes in the [CO_2] in the glasshouse chambers over a couple of hours did not detect a strong response of stomatal closure in the angiosperms (Figure 4.2D). This lack of a strong statistical trend was probably related to general variability among these survey style measurements. When I examined the A-C_i curve data for stomatal responses to the changes in CO_2 concentration imposed within the gas exchange cuvette, I did indeed observe a stronger response in the angiosperms than in the gymnosperms (Figure 4.4). Figure 4.4 shows that the g_s at a cuvette CO_2 concentration of 1200 ppm was about 0.7 times that at a cuvette concentration of 200 ppm in the angiosperms, whereas in the gymnosperms the ratio of the two conductances was about 0.9, with the difference between the two groups being significant (Table 4.4). This shows a stronger stomatal closure response in the angiosperm leaves than in gymnosperm leaves in response to an increase in CO_2 concentration within a gas exchange cuvette, as has also been observed previously (Brodribb *et al.*, 2009).

When evaluated at the mean measurement CO_2 concentration of the survey style measurements, intrinsic water-use efficiency (A/g_s) was insensitive to growth CO_2 concentration (Figure 4.2E). Thus, for the angiosperms, there were correlated reductions in A and g_s with increasing growth CO_2 concentration, such that the ratio of A to g_s remained constant. In the gymnosperms, neither A nor g_s changed with growth CO_2 concentration, when evaluated at the same mean CO_2 concentrations. Therefore, their ratio of A to g_s also did not change across growth CO_2 concentrations, when assessed at a reference mean measurement CO_2 concentration.

When measurement CO_2 concentration was varied, A/g_s increased with increase in measurement CO_2 in both the angiosperms and the gymnosperms (Figure 4.2F). This response can be further clarified by examining the ratio of intercellular to ambient CO_2 concentrations, c_i/c_a, as illustrated in Figures 4.2G and 4.2H. Within both groups, c_i/c_a remained consistent regardless of the growth CO_2 concentration or the measurement CO_2 concentration. When considering the measurement CO_2 concentration, the variation in A/g_s can be explained by its relationship to c_i/c_a. Specifically, A/g_s can be expressed as $A/g_s = c_a(1-c_i/c_a)$, indicating that, because c_i/c_a remained stable, any change in the CO_2 concentration around the leaf, c_a, would proportionally alter A/g_s. A similar pattern of relatively stable c_i/c_a values across changes in atmospheric CO_2 concentration has been observed in tropical trees in natural environments, inferred from the carbon isotope ratios in their tree rings over decades of rising atmospheric CO_2 levels (van der Sleen *et al.*, 2015; Cernusak *et al.*, 2019).

These results with respect to intrinsic water-use efficiency, particularly those shown in Figure 4.2E, differ rather markedly from what was inferred based on measurements in which the CO_2 concentration within a measurement cuvette was varied over a relatively short time period (Brodribb *et al.*, 2009). In the latter study, the short-term increase in cuvette CO_2 concentration led to a sharper decrease in g_s in angiosperms than in gymnosperms, and correspondingly a larger increase in A/g_s. Such a short-term exposure experiment does not encompass the acclimation that takes place when a plant is grown at different CO_2 concentrations. Such acclimation in our experiment led to a decrease in photosynthetic capacity accompanying the sharper decrease in g_s in the angiosperms compared to the gymnosperms. Therefore, our results contradict the conclusion that angiosperms are better able to optimise water-use efficiency in response to different CO_2 concentrations. This was not the case in our growth CO_2 experiment, rather the two groups benefitted similarly in terms of increasing A/g_s with increasing growth CO_2.

The gymnosperms overall had higher A/g_s and lower c_i/c_a than the angiosperms in our experiment. This may reflect that the gymnosperms were from the families Podocarpaceae and Araucariaceae, which have also been shown to have relatively high water-use efficiency compared to angiosperm counterparts in other studies (Cernusak *et al.*, 2008; Dalling *et al.*, 2016; Palma *et al.*, 2020). However, the generally high water-use efficiency may not be a characteristic of all gymnosperms, for example species of Pinaceae grown in a common garden showed considerably lower intrinsic water-use efficiency than species of Cupressaceae, based on measurements of stable carbon isotope ratios (Zhang & Cregg, 1996), and considerable variation has also been observed within Cupressaceae and Podocarpaceae (Brodribb & Hill, 1998). However, among tropical gymnosperms with broad leaves, there does seem to be a tendency toward high A/g_s, associated with less efficient hydraulic systems than in angiosperms, which results in less ability to deliver water to evaporative sites, and therefore a more constrained g_s (Palma *et al.*, 2020).

The biochemical model of photosynthesis for C_3 plants (Farquhar *et al.*, 1980) provides a basis for better understanding the photosynthetic acclimation that took place in the angiosperm species. The model represents C_3 photosynthesis as being limited by one of two processes under most conditions, either the electron transport rate, controlled by the parameter J_{max}, or the carboxylation rate, controlled by the parameter V_{cmax}. These two rates represent two different sets of reactions within the leaf, the first involved in the capture of light energy, and the second in the carbon reduction cycle catalysed by Rubisco. Acclimation of photosynthetic capacity could take place by adjustment of either V_{cmax} or J_{max}, or both. Because the two sets of reactions have different sensitivities to the CO_2 concentration inside the leaf, acclimation by a change in one versus the other could influence the net photosynthetic rate at the new growth conditions.

Figures 4.3A and 4.3B show that angiosperms acclimated their photosynthetic capacity under growth at elevated CO_2 by reducing V_{cmax}, whereas J_{max} remained unchanged. As a result, the C_i transition point shifted up at the higher growth CO_2 concentration, as would be expected if investment in V_{cmax} and J_{max} was such that the two would co-limit the net photosynthetic rate at the new operating C_i. The fact that the angiosperms made this adjustment to the C_i transition point by reducing V_{cmax} meant that the stimulation of photosynthesis by elevated CO_2 in the acclimated leaves was less than it would have been if the C_i transition point had instead been shifted up by increasing J_{max}. Surprisingly, the gymnosperms showed no downregulation of photosynthetic capacity with growth at elevated [CO_2]. The changes in photosynthetic parameters between the two groups align very well with the observed growth responses. The angiosperms downregulated their photosynthetic capacity by reducing V_{cmax} in response to growth at elevated CO_2, whereas the gymnosperms did not. Thus, the net photosynthetic rates of the gymnosperms increased more in response to elevated CO_2, and they showed a positive growth response, whereas the angiosperms did not show a stimulation of growth rates (Figure 4.1).

There was a relationship between V_{cmax} and the operating g_s across all plants in the dataset, where the x-axis on which g_s was plotted was on a log scale (Figure 4.5). This relationship is consistent with the observation that photosynthetic capacity and g_s are correlated, and that changing one tends to lead to a change in the other (Wong *et al.*, 1979). Movement along this scaling relationship would suggest that the stronger stomatal closure response in the angiosperm species grown at elevated CO_2 would be likely to coincide with a correlated reduction in V_{cmax}. On the other hand, because the gymnosperm species did not reduce their g_s in response to increased growth CO_2 concentration, this scaling relationship would not predict a change in V_{cmax}, which is consistent with our observations. It is an open question as to whether these correlated acclimated responses are led by one process or the other, or whether they are coincidental and not linked mechanistically by signalling pathways. Better understanding the underlying mechanisms could lead to an improved framework for predicting how different kinds of species, such as gymnosperms and angiosperms, will respond to rising atmospheric CO_2 concentration.

In mixed angiosperm-gymnosperm forests, rising atmospheric CO_2 concentrations may shift competitive dynamics between these groups. Angiosperms generally benefit from increased CO_2 through enhanced photosynthesis and water-use efficiency, which might initially give them a competitive edge by enabling faster growth and resource acquisition. Gymnosperms, however, often exhibit conservative water-use strategies and are less responsive to CO_2 in terms of photosynthetic upregulation, which has historically positioned them as more drought-resistant but slower-growing. Considering anthropogenic climate change, if vapor pressure deficit (VPD) also increases significantly

alongside CO_2, it could counteract some of the advantages angiosperms gain from higher CO_2. Higher VPD may intensify water stress, potentially forcing angiosperms to downregulate photosynthesis even more frequently to conserve water. This could reduce their competitive advantage, as gymnosperms, with their inherently lower water requirements and drought-adapted physiology, may be less affected by VPD increases. In such cases, gymnosperms might better withstand prolonged environmental stress, allowing them to maintain or even expand their niche in mixed forests where water stress becomes more limiting due to higher VPD. This could be a valuable direction for expanding the findings of this research, providing deeper insights into plant physiological responses under complex, interactive environmental stress conditions.

Supplementary material

Table S4.1: Mixed effect model values for relative growth rate, *RGR*

	Relative growth rate, *RGR*		
Predictors	β	*CI*	*p*
Fixed Effects			
(Intercept)	24.01	15.65 – 36.84	**<0.001**
Treatment [linear]	0.91	0.78 – 1.06	0.238
Group [Gymnosperms]	0.53	0.30 – 0.94	**0.029**
Treatment [linear] × Group [Gymnosperms]	1.48	1.20 – 1.83	**<0.001**
Random Effects			
σ^2 (residual)	0.14		
$\tau_{00\ Species}$ (intercept variance)	0.18		
ICC	0.56		
$N_{\ Species}$	9		
Observations	149		
Marginal R^2 / Conditional R^2	0.268 / 0.680		

Table S4.2: Outcome of the mixed effect models of net photosynthesis, *A* (µmol CO_2 m^{-2} s^{-1}); cube root of stomatal conductance, g_s (mol CO_2 m^{-2} s^{-1}); intrinsic water use efficiency, A/g_s (µmol mol^{-1}), and Leaf's intercellular airspace CO_2 concentration and atmospheric CO_2 concentration ratio, c_i/c_a.

	A			$\sqrt[3]{g_s}$			WUE_i			c_i/c_a		
Predictors	B	*CI*	*p*	β	*CI*	*p*	β	*CI*	*p*	β	*CI*	*p*
(Intercept)	1.9885	1.6623 – 2.3146	<0.001	-0.5836	-0.7351 – -0.4321	<0.001	37.4645	29.8057 – 47.0913	<0.001	0.6915	0.6211 – 0.7619	<0.001
Treatment [linear]	-0.1947	-0.2799 – -0.1096	<0.001	-0.0816	-0.1306 – -0.0325	0.001	1.0234	0.9324 – 1.1232	0.627	0.0006	-0.0280 – 0.0293	0.965
Group [Gymnosperms]	-1.0407	-1.4907 – -0.5907	<0.001	-0.4874	-0.6949 – -0.2799	<0.001	1.5141	1.1140 – 2.0579	0.008	-0.1271	-0.2216 – -0.0326	0.008
C_a	0.0010	0.0009 – 0.0011	<0.001	-0.0001	-0.0001 – -0.0000	0.022	1.0014	1.0012 – 1.0015	<0.001	0.0000	-0.0000 – 0.0001	0.136
Treatment [linear] × Group [Gymnosperms]	0.1498	0.0243 – 0.2754	0.019	0.0842	0.0137 – 0.1548	0.019	0.9711	0.8565 – 1.1011	0.648	-0.0026	-0.0413 – 0.0361	0.894
Group [Gymnosperms] × C_a	0.0005	0.0003 – 0.0006	<0.001	0.0001	-0.0000 – 0.0002	0.123	1.0002	1.0000 – 1.0004	0.045	-0.0000	-0.0001 – 0.0000	0.106
Random Effects												
σ^2	4.4623			0.0027			0.0487			0.0043		
τ_{00}	$0.1044_{Species}$			$0.0217_{Species}$			$0.0435_{Species}$			$0.0042_{Species}$		
	0.0358_{Pot}			0.0112_{Pot}			0.0353_{Pot}			0.0035_{Pot}		
N	$9_{Species}$			$9_{Species}$			$9_{Species}$			$9_{Species}$		
	152_{Pot}			152_{Pot}			152_{Pot}			152_{Pot}		
Observations	454			454			454			454		
Marginal R^2 / Conditional R^2	0.506/ 0.893			0.577 / 0.968			0.614 / 0.852			0.333 / 0.761		

Table S4.3: Environmental conditions inside the three glasshouse growth chambers during the experiment period.

Location	CO_2 (ppm)		RH (%)		Temp (^oC)		Time
	Mean	SD	Mean	SD	Mean	SD	
Chamber 1	457.49	43.57	80.36	7.31	29.44	3.15	Day
Chamber 2	643.84	57.82	78.47	7.87	29.36	3.02	
Chamber 3	950.94	158.73	79.08	7.73	29.48	3.02	
Ambient	457.35	21.69	68.24	11.29	29.63	3.27	
Chamber 1	529.03	52.45	91.34	4.12	23.18	3.15	Night
Chamber 2	644.51	43.85	91.08	4.11	23.02	2.98	
Chamber 3	959.26	138.88	92.32	3.74	23.3	3.12	
Ambient	475.96	34.37	90.6	8.62	22.45	3.8	

Table S4.4: Summary statistics of gas exchange parameters (Photosynthesis, *A*; cube root of stomatal conductance, $\sqrt[3]{g_s}$; intrinsic water use efficiency, A/g_s and the ratio of intercellular airspace CO_2 concentration to atmospheric CO_2 concentration, c_i/c_a) for angiosperms and gymnosperms.

Group	Treatment	Species	*A*	$\sqrt[3]{g_s}$	A/g_s	c_i/c_a
Angiosperms	450	APE	21.22 ± 6.89	0.69 ± 0.11	68.54 ± 30.69	0.79 ± 0.07
		DBR	11.04 ± 4.48	0.41 ± 0.08	170.88 ± 82.32	0.57 ± 0.07
		EAN	19.43 ± 4.18	0.66 ± 0.09	76.74 ± 41.52	0.78 ± 0.06
		FBR	17.26 ± 6.2	0.55 ± 0.05	102.06 ± 36.55	0.71 ± 0.05
	650	APE	18.77 ± 5.51	0.67 ± 0.1	68.35 ± 28.04	0.8 ± 0.06
		DBR	9.51 ± 3.98	0.37 ± 0.04	200.04 ± 79.48	0.52 ± 0.08
		EAN	16.15 ± 4.61	0.58 ± 0.07	86.96 ± 38.13	0.75 ± 0.07
		FBR	14.77 ± 5.83	0.55 ± 0.05	88.58 ± 34.93	0.74 ± 0.08
	1000	APE	13.82 ± 5.81	0.51 ± 0.08	114.5 ± 55.62	0.69 ± 0.09
		DBR	8.24 ± 2.84	0.41 ± 0.07	141.23 ± 81.63	0.65 ± 0.12
		EAN	14.03 ± 4.38	0.57 ± 0.09	86.34 ± 50.18	0.76 ± 0.09
		FBR	15.59 ± 5.08	0.57 ± 0.04	87.86 ± 35.35	0.75 ± 0.05

Group	Treatment	Species	*A*	$3\sqrt{g_s}$	A/g_s	c_i/c_a
Gymnosperms	450	ABI	7.08 ± 3.2	0.38 ± 0.05	129.93 ± 48.05	0.66 ± 0.06
		ARO	12.24 ± 5.83	0.39 ± 0.05	201.72 ± 76.43	0.48 ± 0.08
		PDI	4.42 ± 2.72	0.29 ± 0.04	174.84 ± 76.93	0.57 ± 0.06
		PGR	8.37 ± 3.77	0.35 ± 0.04	192.93 ± 75.92	0.52 ± 0.06
		SAM	5.69 ± 3.41	0.31 ± 0.05	171.85 ± 59.57	0.56 ± 0.04
	650	ABI	7.35 ± 3.21	0.36 ± 0.04	166.06 ± 71.84	0.58 ± 0.07
		ARO	12.16 ± 5.38	0.4 ± 0.06	196.17 ± 86.45	0.5 ± 0.11
		PDI	4.39 ± 2.9	0.28 ± 0.05	181.2 ± 93.94	0.55 ± 0.11
		PGR	10 ± 3.98	0.39 ± 0.05	171.6 ± 74.99	0.56 ± 0.1
		SAM	6.21 ± 4.22	0.32 ± 0.09	175.25 ± 71.95	0.57 ± 0.08
	1000	ABI	7.2 ± 3.65	0.36 ± 0.06	163.32 ± 79.35	0.6 ± 0.07
		ARO	10.08 ± 4.66	0.36 ± 0.04	228.84 ± 97.55	0.44 ± 0.08
		PDI	5.03 ± 2.04	0.34 ± 0.05	140.91 ± 71.37	0.64 ± 0.1
		PGR	7.34 ± 3.5	0.35 ± 0.07	176.43 ± 79.86	0.55 ± 0.1
		SAM	6.3 ± 3.28	0.33 ± 0.06	179.42 ± 85.43	0.55 ± 0.13

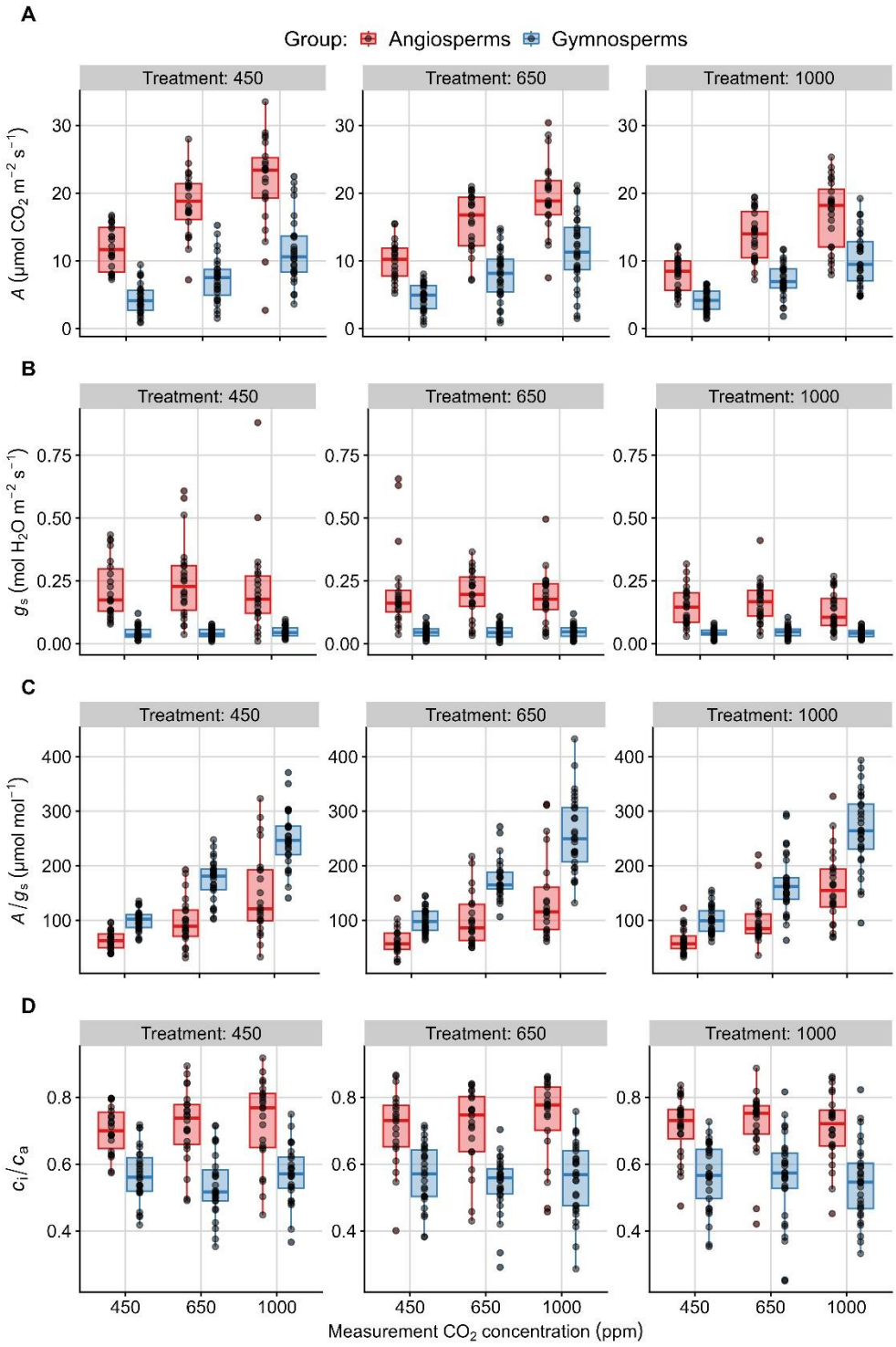

Figure S4.1: Boxplot of observed **A**) net photosynthesis, *A* (µmol CO_2 m^{-2} s^{-1}); **B**) stomatal conductance, g_s (mol H_2O m^{-2} s^{-1}); **C**) intrinsic water use efficiency, A/g_s (µmol mol^{-1}) and **D**) ratio of CO_2 concentration in the intercellular airspace of a leaf to CO_2 concentration in the atmosphere, c_i/c_a for the seedlings grown at three different CO_2 levels (450 ppm, 650 ppm and 1000 ppm of CO_2 concentration). The x-axis represents the measurement CO_2 concentrations.

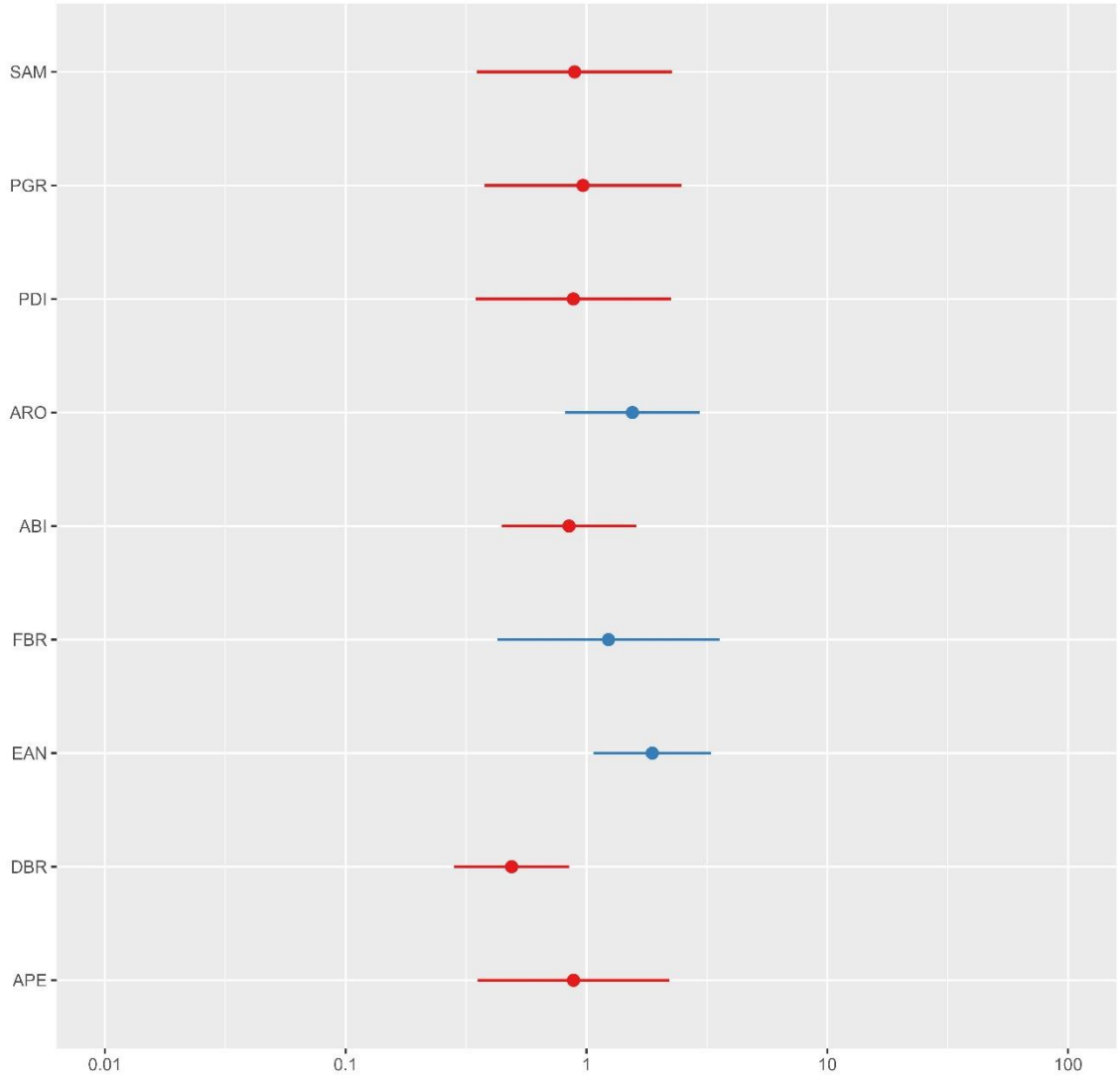

Figure S4.2: Random effect variance for relative growth rate (RGR) where the four species presented at the bottom are angiosperms and top five species are gymnosperms.

CHAPTER 5: GENERAL DISCUSSION AND CONCLUSION

In this thesis, I sought to investigate how the ability of plants to acclimate their physiological responses amidst varying environmental conditions is influenced and possibly constrained by their intrinsic adaptive capacity. I explored the unique physiological acclimation responses of Australian flora to environmental stressors, providing insights that bridge Australia's evolutionary history and the mechanisms plants might use to adapt to future climates. In doing so, I studied a range of plant functional traits and evolutionary scales, from how eucalypts across rainfall gradients in Australia varied in their response to water availability due to differences in phosphorus availability (Chapter 2) to how fundamental biophysical characteristics of gymnosperms and angiosperms shape their response to both long and short-term exposure to elevated CO_2 (Chapter 4). The distinct evolutionary trajectory of Australian flora, particularly due to its geologically stable environment and nutrient-poor soils, appears to have shaped the acclimation responses observed in species today.

The ability of plants to generally improve water use efficiency (*WUE*) in response to water limitation, characterized by reduced precipitation or increased atmospheric aridity is well established (Towers *et al.*, 2024). However, in the geologically diverse yet stable environment of Australia I had an opportunity to examine why the degree of acclimation in *WUE* often varies between studies. In Chapter 2 of this thesis, I explored the modulation of intrinsic *WUE* (WUE_i), using carbon isotope discrimination ($\Delta^{13}C$) as a proxy, considering both climatic variables as well as soil nutrient availability. By analysing $\Delta^{13}C$ data of plant samples from six transect studies across Australia and incorporating findings from a new transect study in northeast Queensland I identified regional variations that correlated significantly with soil P availability (Figure 2.4). Upon further investigation using a continent-wide dataset of leaf-level gas exchange I found that soil [P] controls plants WUE_i by impacting stomatal conductance (g_s) (Figure 2.8), as opposed to photosynthetic capacity (V_{cmax}) with plants in phosphorus depauperate areas having a relative increase in g_s, thereby putatively employing transpiration as an adaptive trait to gather P as a limiting resource via mass flow of the soil solution (Cramer *et al.*, 2009; Cernusak *et al.*, 2011b; Aoyagi *et al.*, 2022). Moreover, comparative analysis of common garden experiments using eucalypt species from regions with different soil P availability suggests that divergent physiological responses are evolutionarily constrained with the degree of variation seen in WUE_i being determined by where a species has evolved (Figure 2.9). This finding is significant because it aligns with broader evidence that soil phosphorus strongly influences WUE across ecosystems globally, as plants adjust stomatal conductance to balance water and nutrient acquisition (Reich *et al.*, 2006; Köhler *et al.*, 2016).

For plants to demonstrate resilience and survival during periods of drought and heat stress, it is essential that they reduce their water loss and lower respiration of stored carbon (McDowell *et al.*, 2008; McDowell *et al.*, 2022). This can be achieved through the reduction in minimum conductance g_{min} as well as the base rate and temperature sensitivity of respiration (R_d). It is reasonable to assume that the ability of species to modify these traits may be related to the nature and severity of drought to which they have evolved to survive. In chapter 3 I investigated the immediate physiological responses of four different eucalypt species, found across a rainfall gradient, to both increased temperature and reduced water availability. I observed that eucalypt species exhibited a tendency to reduce their g_{min} with increasing growth temperature (Figure 3.4A) lowering g_{min} to values comparable with cuticular conductance g_{cw} (Figure 3.4B), suggesting almost no stomatal leakage. I also found significant species-level variations in both R_d and g_{min} under elevated temperature conditions (although not reduced water availability). Species-level differences, and their capacity to acclimate, were not found to be related to the 'typical' water availability of the species. However, as this study was performed with only four eucalypt species further research with a larger range of species covering a broader range in water availability might yield a more robust indication of how these important, yet often overlooked, traits may respond to environmental stressors.

In contrast to chapter 2 and 3 in which I sought to examine how relatively recent evolutionary adaptation to edaphic conditions and water availability may impact acclimation in eucalypts, in chapter 4 I examined a more fundamental evolutionary divergence between angiosperms and broad-leaved southern gymnosperms. Southern gymnosperms are much more morphologically and ecologically diverse compared to their northern counterpart (Fragnière *et al.*, 2015). Specifically, we designed a glasshouse experiment to investigate both the immediate and long-term acclimation responses of Australian angiosperms and broad-leaved gymnosperms to varying [CO_2]. Angiosperms generally displayed higher relative growth rates (*RGR*); however they did not consistently show enhanced growth at elevated [CO_2], unlike gymnosperms which exhibited a strong positive response (Figure 4.1). In seeking to explain this differential response I observed that while angiosperms showed higher stomatal sensitivity (Figure 4.4) and downward acclimated adjustment of photosynthetic capacity in response to increased growth [CO_2] gymnosperms showed little to no acclimation (Figure 4.3) – resulting in a more pronounced acclimated increase in photosynthetic rates under elevated [CO_2]. The ability of angiosperms to successfully acclimate to declining [CO_2] probably helped their rise to dominance during the mid-Cretaceous era, a period of reduced [CO_2]. However, in the rapidly

changing modern era of increasing [CO_2] gymnosperms may yet increase their competitiveness with angiosperms.

In conclusion, this thesis underscores the pivotal role of the inherent capacities of plants in shaping their acclimation responses to environmental change. A clearer picture of the capacity for Australian tree species to acclimate to future climates emerges. Drawing from findings across chapters, it is evident that plants across diverse habitats and phylogenetic backgrounds exhibit nuanced physiological adjustments in response to varying environmental stressors. Insights from these studies highlight the importance of understanding both species-specific adaptations and broader ecological patterns to anticipate how vegetation may respond to future environmental shifts. Future research directions could leverage advanced ecophysiological techniques, such as tree-ring data and isotopic measurements to gain insights into past climate responses of trees. Moreover, to further elucidate acclimation responses in a changing world large scale experiments like Free-air CO_2 Enrichment (*FACE*) facilities will provide opportunities to explore how mature forest ecosystems will respond the continuing increases in atmospheric CO_2 exposure as climate change continues to unfold.

REFERENCE

Adams MA, Buckley TN, Binkley D, Neumann M, Turnbull TL. 2021. CO_2, nitrogen deposition and a discontinuous climate response drive water use efficiency in global forests. *Nature Communications* **12**(1): 5194.

ALA 2024. Occurrence records Atlas of Living Australia.

Allen CD, Breshears DD, McDowell NG. 2015. On underestimation of global vulnerability to tree mortality and forest die-off from hotter drought in the Anthropocene. *Ecosphere* **6**(8): 1-55.

Amthor JS. 1995. Terrestrial Higher-plant Response to Increasing Atmospheric [CO_2] in Relation to the Global Carbon Cycle. *Global Change Biology*(4): 243-274.

Anderegg WR, Klein T, Bartlett M, Sack L, Pellegrini AF, Choat B, Jansen S. 2016. Meta-analysis reveals that hydraulic traits explain cross-species patterns of drought-induced tree mortality across the globe. *Proceedings of the National Academy of Sciences* **113**(18): 5024-5029.

Anderson JE, Williams J, Kriedemann PE, Austin MP, Farquhar GD. 1996. Correlations between carbon isotope discrimination and climate of native habitats for diverse eucalypt taxa growing in a common garden. *Functional Plant Biology* **23**(3): 311-320.

Aoyagi R, Kitayama K, Turner BL. 2022. How do tropical tree species maintain high growth rates on low-phosphorus soils? *Plant and Soil*: 1-26.

Apgaua DM, Tng DY, Forbes SJ, Ishida YF, Vogado NO, Cernusak LA, Laurance SG. 2019. Elevated temperature and CO_2 cause differential growth stimulation and drought survival responses in eucalypt species from contrasting habitats. *Tree physiology* **39**(11): 1806-1820.

Athanasiou K, Dyson BC, Webster RE, Johnson GN. 2009. Dynamic Acclimation of Photosynthesis Increases Plant Fitness in Changing Environments. *Plant physiology* **152**(1): 366-373.

Atkin OK, Bruhn D, Hurry VM, Tjoelker MG. 2005. Evans Review No. 2: The hot and the cold: unravelling the variable response of plant respiration to temperature. *Functional Plant Biology* **32**(2): 87-105.

Atkin OK, Macherel D. 2008. The crucial role of plant mitochondria in orchestrating drought tolerance. *Annals of Botany* **103**(4): 581-597.

Atkin OK, Macherel D. 2009. The crucial role of plant mitochondria in orchestrating drought tolerance. *Annals of Botany* **103**(4): 581-597.

Atkin OK, Scheurwater I, Pons TL. 2006. High Thermal Acclimation Potential of Both Photosynthesis and Respiration in Two Lowland *Plantago* Species in Contrast to an Alpine Congeneric. *Global Change Biology* **12**(3): 500-515.

Atkin OK, Tjoelker MG. 2003. Thermal acclimation and the dynamic response of plant respiration to temperature. *Trends in Plant Science* **8**(7): 343-351.

Bai Y, Zha T, Bourque CPA, Jia X, Ma J, Liu P, Yang R, Li C, Du T, Wu Y. 2020. Variation in ecosystem water use efficiency along a southwest-to-northeast aridity gradient in China. *Ecological Indicators* **110**: 105932.

Barnard D, Bauerle W. 2013. The implications of minimum stomatal conductance on modeling water flux in forest canopies. *Journal of Geophysical Research: Biogeosciences* **118**(3): 1322-1333.

Barreto P, Yassitepe JE, Wilson ZA, Arruda P. 2017. Mitochondrial uncoupling protein 1 overexpression increases yield in Nicotiana tabacum under drought stress by improving source and sink metabolism. *Frontiers in Plant Science* **8**: 282206.

Bartlett MK, Klein T, Jansen S, Choat B, Sack L. 2016. The correlations and sequence of plant stomatal, hydraulic, and wilting responses to drought. *Proceedings of the National Academy of Sciences* **113**(46): 13098-13103.

Bartoń K 2023. MuMIn: Multi-Model Inference.

Benton MJ, Wilf P, Sauquet H. 2022. The Angiosperm Terrestrial Revolution and the origins of modern biodiversity. *New Phytologist* **233**(5): 2017-2035.

Berry JA, Björkman O. 1980. Photosynthetic Response and Adaptation to Temperature in Higher Plants. *Annual review of plant physiology* **31**: 491-543.

Bieleski R. 1973. Phosphate pools, phosphate transport, and phosphate availability. *Annual review of plant physiology* **24**(1): 225-252.

Birks HJB. 2020. Angiosperms versus gymnosperms in the Cretaceous. *Proceedings of the National Academy of Sciences* **117**(49): 30879-30881.

Blackman CJ, Li X, Choat B, Rymer PD, De Kauwe MG, Duursma RA, Tissue DT, Medlyn BE. 2019. Desiccation time during drought is highly predictable across species of Eucalyptus from contrasting climates. *New Phytologist* **224**(2): 632-643.

Blackman CJ, Pfautsch S, Choat B, Delzon S, Gleason SM, Duursma RA. 2016. Toward an index of desiccation time to tree mortality under drought. *Plant, Cell & Environment* **39**(10): 2342-2345.

Blum A. 2017. Osmotic adjustment is a prime drought stress adaptive engine in support of plant production. *Plant, Cell & Environment* **40**(1): 4-10.

Bond WJ. 1989. The Tortoise and the Hare: Ecology of Angiosperm Dominance and Gymnosperm Persistence. *Biological Journal of the Linnean Society* **36**(3): 227-249.

Boyko A, Kovalchuk I. 2011. Genome instability and epigenetic modification—heritable responses to environmental stress? *Current opinion in plant biology* **14**(3): 260-266.

Boyle R, McAinsh MR, Dodd IC. 2016. Daily irrigation attenuates xylem abscisic acid concentration and increases leaf water potential of pelargonium × hortorum compared with infrequent irrigation. *Physiologia Plantarum* **158**(1): 23-33.

Brodribb T, Hill RS. 1998. The photosynthetic drought physiology of a diverse group of southern hemisphere conifer species is correlated with minimum seasonal rainfall. *Functional Ecology* **12**(3): 465-471.

Brodribb TJ, Feild TS. 2008. Evolutionary significance of a flat-leaved Pinus in Vietnamese rainforest. *New Phytologist* **178**(1): 201-209.

Brodribb TJ, Holbrook NM. 2003. Stomatal Closure during Leaf Dehydration, Correlation with Other Leaf Physiological Traits. *Plant physiology* **132**(4): 2166-2173.

Brodribb TJ, McAdam SA, Carins Murphy MR. 2017. Xylem and stomata, coordinated through time and space. *Plant, Cell & Environment* **40**(6): 872-880.

Brodribb TJ, McAdam SA, Jordan GJ, Feild TS. 2009. Evolution of stomatal responsiveness to CO_2 and optimization of water-use efficiency among land plants. *New Phytologist* **183**(3): 839-847.

Brodribb TJ, McAdam SA, Jordan GJ, Martins SC. 2014. Conifer species adapt to low-rainfall climates by following one of two divergent pathways. *Proceedings of the National Academy of Sciences* **111**(40): 14489-14493.

Brodribb TJ, McAdam SAM. 2013. Unique Responsiveness of Angiosperm Stomata to Elevated CO_2 Explained by Calcium Signalling. *PLOS ONE* **8**(11): e82057.

Brodribb TJ, Pittermann J, Coomes DA. 2012. Elegance versus speed: examining the competition between conifer and angiosperm trees. *International Journal of Plant Sciences* **173**(6): 673-694.

Brodribb TJ, Powers J, Cochard H, Choat B. 2020. Hanging by a thread? Forests and drought. *Science* **368**(6488): 261-266.

Brooks JR, Flanagan LB, Buchmann N, Ehleringer JR. 1997. Carbon isotope composition of boreal plants: functional grouping of life forms. *Oecologia* **110**(3): 301-311.

Brown MJM, Brodribb TJ, Jordan GJ. 2021. No-analogue associations in the fossil record of southern conifers reveal conservatism in precipitation, but not temperature axes. *Global Ecology and Biogeography* **30**(12): 2455-2466.

Buckley TN. 2019. How do stomata respond to water status? *New Phytologist* **224**(1): 21-36.

Caldwell MM, Dawson TE, Richards JH. 1998. Hydraulic lift: consequences of water efflux from the roots of plants. *Oecologia* **113**(2): 151-161.

Callister AN, Arndt SK, Ades PK, Merchant A, Rowell D, Adams MA. 2008. Leaf osmotic potential of Eucalyptus hybrids responds differently to freezing and drought, with little clonal variation. *Tree physiology* **28**(8): 1297-1304.

Carriquí M, Nadal M, Clemente-Moreno MJ, Gago J, Miedes E, Flexas J. 2020. Cell Wall Composition Strongly Influences Mesophyll Conductance in Gymnosperms. *The Plant Journal* **103**(4): 1372-1385.

Cernusak LA. 2020. Gas exchange and water-use efficiency in plant canopies. *Plant Biology* **22**(S1): 52-67.

Cernusak LA, Aranda J, Marshall JD, Winter K. 2007. Large variation in whole-plant water-use efficiency among tropical tree species. *New Phytologist* **173**(2): 294-305.

Cernusak LA, De Kauwe MG. 2022. Red light shines a path forward on leaf minimum conductance. *New Phytologist* **233**(1): 5-7.

Cernusak LA, Haverd V, Brendel O, Le Thiec D, Guehl J-M, Cuntz M. 2019. Robust response of terrestrial plants to rising CO_2. *Trends in Plant Science* **24**(7): 578-586.

Cernusak LA, Hutley LB, Beringer J, Holtum JA, Turner BL. 2011a. Photosynthetic physiology of eucalypts along a sub-continental rainfall gradient in northern Australia. *Agricultural and Forest Meteorology* **151**(11): 1462-1470.

Cernusak LA, Marshall JD. 2001. Responses of foliar δ13C, gas exchange and leaf morphology to reduced hydraulic conductivity in Pinus monticola branches. *Tree physiology* **21**(16): 1215-1222.

Cernusak LA, Ubierna N 2022. Carbon isotope effects in relation to CO_2 assimilation by tree canopies. *Stable isotopes in tree rings: Inferring physiological, climatic and environmental responses*: Springer International Publishing Cham, 291-310.

Cernusak LA, Winter K, Aranda J, Turner BL. 2008. Conifers, angiosperm trees, and lianas: growth, whole-plant water and nitrogen use efficiency, and stable isotope composition ($\delta^{13}C$ and $\delta^{18}O$) of seedlings grown in a tropical environment. *Plant physiology* **148**: 642-659.

Cernusak LA, Winter K, Turner BL. 2009. Physiological and isotopic (δ13C and δ18O) responses of three tropical tree species to water and nutrient availability. *Plant, Cell & Environment* **32**(10): 1441-1455.

Cernusak LA, Winter K, Turner BL. 2010. Leaf nitrogen to phosphorus ratios of tropical trees: experimental assessment of physiological and environmental controls. *New Phytologist* **185**(3): 770-779.

Cernusak LA, Winter K, Turner BL. 2011b. Transpiration modulates phosphorus acquisition in tropical tree seedlings. *Tree physiology* **31**(8): 878-885.

Chaves MM, Maroco JP, Pereira JS. 2003. Understanding plant responses to drought—from genes to the whole plant. *Functional Plant Biology* **30**(3): 239-264.

Cheesman AW, Cernusak LA. 2017. Infidelity in the outback: climate signal recorded in $\Delta^{18}O$ of leaf but not branch cellulose of eucalypts across an Australian aridity gradient. *Tree physiology* **37**(5): 554-564.

Chen H, Jiang J-G. 2010. Osmotic adjustment and plant adaptation to environmental changes related to drought and salinity. *Environmental Reviews* **18**(NA): 309-319.

Chen S, Li P, Tan S-L, Pu X, Zhou Y, Hu K, Huang W, Liu L. 2021. Combined Proteomic and Physiological Analysis of Chloroplasts Reveals Drought and Recovery Response Mechanisms in Nicotiana Benthamiana. *Plants* **10**(6): 1127.

Chesson P, Huntly N. 1997. The roles of harsh and fluctuating conditions in the dynamics of ecological communities. *The American Naturalist* **150**(5): 519-553.

Choat B, Brodribb TJ, Brodersen CR, Duursma RA, López R, Medlyn BE. 2018. Triggers of tree mortality under drought. *Nature* **558**(7711): 531-539.

Choat B, Jansen S, Brodribb TJ, Cochard H, Delzon S, Bhaskar R, Bucci SJ, Feild TS, Gleason SM, Hacke UG. 2012. Global convergence in the vulnerability of forests to drought. *Nature* **491**(7426): 752.

Clark DA, Piper S, Keeling CD, Clark DB. 2003. Tropical rain forest tree growth and atmospheric carbon dynamics linked to interannual temperature variation during 1984–2000. *Proceedings of the National Academy of Sciences* **100**(10): 5852-5857.

Cochard H, Badel E, Herbette S, Delzon S, Choat B, Jansen S. 2013. Methods for measuring plant vulnerability to cavitation: a critical review. *Journal of Experimental Botany* **64**(15): 4779-4791.

Condamine FL, Silvestro D, Koppelhus EB, Antonelli A. 2020. The rise of angiosperms pushed conifers to decline during global cooling. *Proceedings of the National Academy of Sciences* **117**(46): 28867-28875.

Corlett RT. 2016. The Impacts of Droughts in Tropical Forests. *Trends in Plant Science* **21**(7): 584-593.

Cornwell WK, Wright IJ, Turner J, Maire V, Barbour MM, Cernusak LA, Dawson T, Ellsworth D, Farquhar GD, Griffiths H. 2018. Climate and soils together regulate photosynthetic carbon isotope discrimination within C3 plants worldwide. *Global Ecology and Biogeography* **27**(9): 1056-1067.

Courville T, Thompson B. 2001. Use of Structure Coefficients in Published Multiple Regression Articles: β is not Enough. *Educational and Psychological Measurement* **61**(2): 229-248.

Cramer MD, Hawkins H-J, Verboom GA. 2009. The importance of nutritional regulation of plant water flux. *Oecologia* **161**(1): 15-24.

Cramer MD, Hoffmann V, Verboom GA. 2008. Nutrient availability moderates transpiration in Ehrharta calycina. *New Phytologist* **179**(4): 1048-1057.

Crisp M, Cook L, Steane D. 2004. Radiation of the Australian flora: what can comparisons of molecular phylogenies across multiple taxa tell us about the evolution of diversity in present–day communities? *Philosophical Transactions of the Royal Society of London. Series B: Biological Sciences* **359**(1450): 1551-1571.

Crisp MD, Cook LG. 2011. Cenozoic Extinctions Account for the Low Diversity of Extant Gymnosperms Compared With Angiosperms. *New Phytologist* **192**(4): 997-1009.

Crisp MD, Cook LG. 2013. How was the Australian flora assembled over the last 65 million years? A molecular phylogenetic perspective. *Annual Review of Ecology, Evolution, and Systematics* **44**(1): 303-324.

Da Silva EC, De Albuquerque MB, De Azevedo Neto AD, Da Silva Junior CD 2013. Drought and its consequences to plants–from individual to ecosystem. In: Akinci S ed. *Responses of organisms to water stress*, 18-47.

Dalling JW, Cernusak LA, Winter K, Aranda J, Garcia M, Virgo A, Cheesman AW, Baresch A, Jaramillo C, Turner BL. 2016. Two tropical conifers show strong growth and water-use efficiency responses to altered CO_2 concentration. *Annals of Botany* **118**(6): 1113-1125.

Dalton F, Raats P, Gardner W. 1975. Simultaneous Uptake of Water and Solutes by Plant Roots 1. *Agronomy journal* **67**(3): 334-339.

Dawson TE. 1993. Hydraulic lift and water use by plants: implications for water balance, performance and plant-plant interactions. *Oecologia* **95**(4): 565-574.

De Boer HJ, Eppinga MB, Wassen MJ, Dekker SC. 2012. A critical transition in leaf evolution facilitated the Cretaceous angiosperm revolution. *Nature Communications* **3**(1): 1221.

De La Torre AR, Li Z, Van de Peer Y, Ingvarsson PK. 2017. Contrasting rates of molecular evolution and patterns of selection among gymnosperms and flowering plants. *Molecular Biology and Evolution* **34**(6): 1363-1377.

Dettmann ME, Jarzen DM. 1990. The Antarctic/Australian rift valley: Late cretaceous cradle of nortteastern Australasian relicts? *Review of Palaeobotany and Palynology* **65**(1): 131-144.

Donoghue MJ, Edwards EJ. 2014. Biome shifts and niche evolution in plants. *Annual Review of Ecology, Evolution, and Systematics* **45**: 547-572.

Doughty CE, Goulden ML. 2008. Are tropical forests near a high temperature threshold? *Journal of Geophysical Research: Biogeosciences* **113**(G1): 1-12.

Drake BG, Gonzàlez-Meler MA, Long SP. 1997. MORE EFFICIENT PLANTS: A Consequence of Rising Atmospheric CO_2. *Annual Review of Plant Physiology and Plant Molecular Biology* **48**: 609-639.

Drake JE, Tjoelker MG, Vårhammar A, Medlyn BE, Reich PB, Leigh A, Pfautsch S, Blackman CJ, López R, Aspinwall MJ. 2018. Trees tolerate an extreme heatwave via sustained transpirational cooling and increased leaf thermal tolerance. *Global Change Biology* **24**(6): 2390-2402.

Driscoll AW, Bitter NQ, Sandquist DR, Ehleringer JR. 2020. Multidecadal records of intrinsic water-use efficiency in the desert shrub Encelia farinosa reveal strong responses to climate change. *Proceedings of the National Academy of Sciences* **117**(31): 18161-18168.

Duan H, Duursma RA, Huang G, Smith R, Choat B, O'Grady AP, Tissue DT. 2014. Elevated [CO_2] does not ameliorate the negative effects of elevated temperature on drought-induced mortality in *Eucalyptus radiata* seedlings. *Plant Cell & Environment* **37**(7): 1598-1613.

Duursma RA. 2015. Plantecophys - An R Package for Analysing and Modelling Leaf Gas Exchange Data. *PLOS ONE* **10**(11): e0143346.

Duursma RA, Blackman CJ, Lopéz R, Martin-StPaul NK, Cochard H, Medlyn BE. 2019. On the minimum leaf conductance: its role in models of plant water use, and ecological and environmental controls. *New Phytologist* **221**(2): 693-705.

Dye P. 1996. Response of Eucalyptus grandis trees to soil water deficits. *Tree physiology* **16**(1-2): 233-238.

Edwards EJ. 2006. Correlated Evolution of Stem and Leaf Hydraulic Traits in *Pereskia* (Cactaceae). *New Phytologist* **172**(3): 479-789.

Ellsworth DS, Crous KY, De Kauwe MG, Verryckt LT, Goll D, Zaehle S, Bloomfield KJ, Ciais P, Cernusak LA, Domingues TF, et al. 2022. Convergence in phosphorus constraints to photosynthesis in forests around the world. *Nature Communications* **13**(1): 5005.

Endress PK. 2011. Evolutionary diversification of the flowers in angiosperms. *American journal of botany* **98**(3): 370-396.

Eskelinen A, Harrison S. 2015. Resource Colimitation Governs Plant Community Responses to Altered Precipitation. *Proceedings of the National Academy of Sciences* **112**(42): 13009-13014.

Esquivel-Muelbert A, Galbraith D, Dexter KG, Baker TR, Lewis SL, Meir P, Rowland L, Da Costa ACL, Nepstad D, Phillips OL. 2017. Biogeographic distributions of neotropical trees reflect their directly measured drought tolerances. *Scientific Reports* **7**(1): 8334-8311.

Evans B, Whitley R, Pauwels J, Hutchinson M, Xu T, Han W 2015. eMAST-R-Package collection.In Australia N.

Farooq M, Wahid A, Kobayashi N, Fujita D, Basra SMA. 2009. Plant drought stress: effects, mechanisms and management. *Agronomy for Sustainable Development* **29**(1): 185-212.

Farquhar G, Richards R. 1984. Isotopic composition of plant carbon correlates with water-use efficiency of wheat genotypes. *Functional Plant Biology* **11**(6): 539-552.

Farquhar GD, Ehleringer JR, Hubick KT. 1989. Carbon isotope discrimination and photosynthesis. *Annual review of plant biology* **40**(1): 503-537.

Farquhar GD, O'Leary MH, Berry JA. 1982. On the relationship between carbon isotope discrimination and the intercellular carbon dioxide concentration in leaves. *Functional Plant Biology* **9**(2): 121-137.

Farquhar GD, von Caemmerer S, Berry JA. 1980. A biochemical model of photosynthetic CO_2 assimilation in leaves of C_3 species. *Planta* **149**: 78-90.

Feeley KJ, Joseph Wright S, Nur Supardi M, Kassim AR, Davies SJ. 2007. Decelerating growth in tropical forest trees. *Ecology Letters* **10**(6): 461-469.

Feeley KJ, Rehm EM, Machovina B. 2012. Perspective: the responses of tropical forest species to global climate change: acclimate, adapt, migrate, or go extinct? *Frontiers of biogeography* **4**(2): 69-84.

Feild TS, Brodribb TJ, Iglesias A, Chatelet DS, Baresch A, Upchurch GR, Gomez B, Mohr BAR, Coiffard C, Kvacek J, et al. 2011. Fossil evidence for cretaceous escalation in angiosperm leaf vein evolution. *Proceedings of the National Academy of Sciences* **108**(20): 8363-8366.

Feller U. 2016. Drought stress and carbon assimilation in a warming climate: Reversible and irreversible impacts. *Journal of Plant Physiology* **203**: 84-94.

Fensham R, Fairfax R, Ward D. 2009. Drought-induced tree death in savanna. *Global Change Biology* **15**(2): 380-387.

Fernández-Pascual E, Jiménez-Alfaro B. 2014. Phenotypic Plasticity in Seed Germination Relates Differentially to Overwintering and Flowering Temperatures. *Seed Science Research* **24**(4): 273-280.

Fiscus EL. 1975. The interaction between osmotic-and pressure-induced water flow in plant roots. *Plant physiology* **55**(5): 917-922.

Flexas J, Baron M, Bota J, Ducruet JM, Galle A, Galmes J, Jimenez M, Pou A, Ribas-Carbo M, Sajnani C, et al. 2009. Photosynthesis limitations during water stress acclimation and recovery in the drought-adapted Vitis hybrid Richter-110 (V. berlandierixV. rupestris). *J Exp Bot* **60**(8): 2361-2377.

Flexas J, Bota J, Galmés J, Medrano H, Ribas-Carbó M. 2006. Keeping a positive carbon balance under adverse conditions: responses of photosynthesis and respiration to water stress. *Physiologia Plantarum* **127**(3): 343-352.

Flexas J, Diaz-espejo A, Galmés J, Kaldenhoff R, Medrano H, Ribas-carbo M. 2007. Rapid variations of mesophyll conductance in response to changes in CO_2 concentration around leaves. *Plant, Cell & Environment* **30**(10): 1284-1298.

Folk RA, Siniscalchi CM, Soltis DE. 2020. Angiosperms at the edge: Extremity, diversity, and phylogeny. *Plant, Cell & Environment* **43**(12): 2871-2893.

Fonti P, Heller O, Cherubini P, Rigling A, Arend M. 2012. Wood Anatomical Responses of Oak Saplings Exposed to Air Warming and Soil Drought. *Plant Biology* **15 Suppl 1**: 210-219.

Forbes SJ, Cernusak LA, Northfield TD, Gleadow RM, Lambert S, Cheesman AW. 2020. Elevated temperature and carbon dioxide alter resource allocation to growth, storage and defence in cassava (Manihot esculenta). *Environmental and Experimental Botany* **173**: 103997.

Fragnière Y, Bétrisey S, Cardinaux L, Stoffel M, Kozlowski G. 2015. Fighting their last stand? A global analysis of the distribution and conservation status of gymnosperms. *Journal of Biogeography* **42**(5): 809-820.

Franks SJ, Weber JT, Aitken SN. 2013. Evolutionary and Plastic Responses to Climate Change in Terrestrial Plant Populations. *Evolutionary Applications* **7**(1): 123-139.

Friedlingstein P, O'sullivan M, Jones MW, Andrew RM, Gregor L, Hauck J, Le Quéré C, Luijkx IT, Olsen A, Peters GP. 2022. Global carbon budget 2022. *Earth System Science Data Discussions* **2022**(11): 1-159.

Funk JL, Vitousek PM. 2007. Resource-use efficiency and plant invasion in low-resource systems. *Nature* **446**(7139): 1079-1081.

Galbraith D, Levy PE, Sitch S, Huntingford C, Cox P, Williams M, Meir P. 2010. Multiple mechanisms of Amazonian forest biomass losses in three dynamic global vegetation models under climate change. *New Phytologist* **187**(3): 647-665.

Gamon JA, Huemmrich KF, Wong CYS, Ensminger I, Garrity SR, Hollinger DY, Noormets A, Peñuelas J. 2016. A Remotely Sensed Pigment Index Reveals Photosynthetic Phenology in Evergreen Conifers. *Proceedings of the National Academy of Sciences* **113**(46): 13087-13092.

Garrish V, Cernusak LA, Winter K, Turner BL. 2010. Nitrogen to phosphorus ratio of plant biomass versus soil solution in a tropical pioneer tree, Ficus insipida. *Journal of Experimental Botany* **61**(13): 3735-3748.

Gibson RK, Bradstock RA, Penman T, Keith DA, Driscoll DA. 2015. Climatic, vegetation and edaphic influences on the probability of fire across mediterranean woodlands of south-eastern Australia. *Journal of Biogeography* **42**(9): 1750-1760.

Givnish TJ, Wong SC, Stuart-Williams H, Holloway-Phillips M, Farquhar GD. 2014. Determinants of maximum tree height in Eucalyptus species along a rainfall gradient in Victoria, Australia. *Ecology* **95**(11): 2991-3007.

Gleason SM, Blackman CJ, Cook AM, Laws CA, Westoby M. 2014. Whole-plant capacitance, embolism resistance and slow transpiration rates all contribute to longer desiccation times in woody angiosperms from arid and wet habitats. *Tree physiology* **34**(3): 275-284.

Graham EA, Mulkey SS, Kitajima K, Phillips NG, Wright SJ. 2003. Cloud cover limits net CO_2 uptake and growth of a rainforest tree during tropical rainy seasons. *Proceedings of the National Academy of Sciences* **100**(2): 572-576.

Gratani L. 2014. Plant Phenotypic Plasticity in Response to Environmental Factors. *Advances in Botany* **2014**: 1-17.

Greenwood S, Ruiz-Benito P, Martínez-Vilalta J, Lloret F, Kitzberger T, Allen CD, Fensham R, Laughlin DC, Kattge J, Bönisch G. 2017. Tree mortality across biomes is promoted by drought intensity, lower wood density and higher specific leaf area. *Ecology Letters* **20**(4): 539-553.

Guehl J-M, Bonal D, Ferhi A, Barigah TS, Farquhar G, Granier A 2004. Community-level diversity of carbon-water relations in rainforest trees. In: Gourlet-Fleury SG, Jean-Marc Laroussinie, Olivier ed. *Ecology and management of a neotropical rainforest: lessons drawn from Paracou, a long-term experimental research site in French Guiana*. Paris: Elsevier, 75-94.

Harb A, Krishnan A, Ambavaram MM, Pereira A. 2010. Molecular and physiological analysis of drought stress in Arabidopsis reveals early responses leading to acclimation in plant growth. *Plant physiology* **154**(3): 1254-1271.

Harrington RA, Fownes JH, Meinzer FC, Scowcroft PG. 1995. Forest growth along a rainfall gradient in Hawaii: Acacia koa stand structure, productivity, foliar nutrients, and water- and nutrient-use efficiencies. *Oecologia* **102**(3): 277-284.

Hartig F 2022. DHARMa: Residual Diagnostics for Hierarchical (Multi-Level / Mixed) Regression Models.

Harwood T 2019. 9s climatology for continental Australia 1976-2005: BIOCLIM variable suite. *CSIRO Data Collection*: Commonwealth Scientific and Industrial Research Organisation (CSIRO).

Hasper TB, Dusenge ME, Breuer F, Uwizeye FK, Wallin G, Uddling J. 2017. Stomatal CO_2 Responsiveness and Photosynthetic Capacity of Tropical Woody Species in Relation to Taxonomy and Functional Traits. *Oecologia* **184**(1): 43-57.

Haverroth EJ, Oliveira LA, Andrade MT, Taggart M, McAdam SAM, Zsögön A, Thompson AJ, Martins SCV, Cardoso AA. 2023. Abscisic acid acts essentially on stomata, not on the xylem, to improve drought resistance in tomato. *Plant, Cell & Environment* **46**(11): 3229-3241.

Hellmuth EO. 1971. Eco-physiological studies on plants in arid and semi-arid regions in Western Australia: III. Comparative studies on photosynthesis, respiration and water relations of ten arid zone and two semi-arid zone plants under winter and late summer climatic conditions. *The Journal of Ecology*: 225-259.

Henn JJ, Buzzard V, Enquist BJ, Halbritter AH, Klanderud K, Maitner BS, Michaletz ST, Pötsch C, Seltzer L, Telford RJ. 2018. Intraspecific trait variation and phenotypic plasticity mediate alpine plant species response to climate change. *Frontiers in Plant Science* **9**: 1548.

Herendeen PS, Friis EM, Pedersen KR, Crane PR. 2017. Palaeobotanical redux: revisiting the age of the angiosperms. *Nature Plants* **3**(3): 1-8.

Hikosaka K, Ishikawa K, Borjigidai A, Muller O, Onoda Y. 2006. Temperature acclimation of photosynthesis: mechanisms involved in the changes in temperature dependence of photosynthetic rate. *Journal of Experimental Botany* **57**(2): 291-302.

Hill RS, Brodribb TJ. 1999. Southern Conifers in Time and Space. *Australian Journal of Botany* **47**(5): 639-696.

Hoefnagel MH, Atkin OK, Wiskich JT. 1998. Interdependence between chloroplasts and mitochondria in the light and the dark. *Biochimica et Biophysica Acta (BBA)-Bioenergetics* **1366**(3): 235-255.

Hofmann GE, Todgham AE. 2010. Living in the Now: Physiological Mechanisms to Tolerate a Rapidly Changing Environment. *Annual Review of Physiology* **72**: 127-145.

Hsiao TC, Acevedo E, Fereres E, Henderson D. 1976. Water stress, growth and osmotic adjustment. *Philosophical Transactions of the Royal Society of London. B, Biological Sciences* **273**(927): 479-500.

Hu Y, Sperotto RA, Koubouris G, Stojnić S, Bellaloui N. 2023. Tree Ecophysiology in the Context of Climate Change. *Journal of Forestry Research* **34**(1): 1-5.

Huang G, Hayes PE, Ryan MH, Pang J, Lambers H. 2017. Peppermint trees shift their phosphorus-acquisition strategy along a strong gradient of plant-available phosphorus by increasing their transpiration at very low phosphorus availability. *Oecologia* **185**(3): 387-400.

Huang G, Rymer PD, Duan H, Smith R, Tissue DT. 2015. Elevated Temperature Is More Effective Than Elevated CO_2 in Exposing Genotypic Variation in *Telopea Speciosissima* Growth Plasticity: Implications for Woody Plant Populations Under Climate Change. *Global Change Biology* **21**(10): 3800-3813.

Hughes L, Cawsey E, Westoby M. 1996. Climatic range sizes of Eucalyptus species in relation to future climate change. *Global Ecology and Biogeography Letters* **5**(1): 23-29.

James A, Lawn R, Cooper M. 2008. Genotypic variation for drought stress response traits in soybean. II. Inter-relations between epidermal conductance, osmotic potential, relative water content, and plant survival. *Australian Journal of Agricultural Research* **59**(7): 670-678.

Johnson DJ, Condit R, Hubbell SP, Comita LS. 2017. Abiotic niche partitioning and negative density dependence drive tree seedling survival in a tropical forest. *Proceedings of the Royal Society B: Biological Sciences* **284**(1869): 20172210.

Kadam NN, Xiao G, Melgar RJ, Bahuguna RN, Quinones C, Tamilselvan A, Prasad PVV, Jagadish KS. 2014. Agronomic and physiological responses to high temperature, drought, and elevated CO_2 interactions in cereals. *Advances in agronomy* **127**: 111-156.

Kala J, De Kauwe MG, Pitman AJ, Medlyn BE, Wang Y-P, Lorenz R, Perkins-Kirkpatrick SE. 2016. Impact of the representation of stomatal conductance on model projections of heatwave intensity. *Scientific Reports* **6**(1): 23418.

Karnosky DF. 2003. Impacts of Elevated Atmospheric CO_2 on Forest Trees and Forest Ecosystems: Knowledge Gaps. *Environment International* **29**(2-3): 161-169.

Kattge J, Knorr W. 2007. Temperature acclimation in a biochemical model of photosynthesis: a reanalysis of data from 36 species. *Plant, Cell & Environment* **30**(9): 1176-1190.

Klein T, Ramon U. 2019. Stomatal Sensitivity to CO_2 Diverges Between Angiosperm and Gymnosperm Tree Species. *Functional Ecology* **33**(8): 1411-1424.

Köhler IH, Macdonald AJ, Schnyder H. 2016. Last-century increases in intrinsic water-use efficiency of grassland communities have occurred over a wide range of vegetation composition, nutrient inputs, and soil pH. *Plant physiology* **170**(2): 881-890.

Kooyman RM, Laffan SW, Westoby M. 2017. The incidence of low phosphorus soils in Australia. *Plant and Soil* **412**(1-2): 143-150.

Kreft H, Jetz W. 2007. Global patterns and determinants of vascular plant diversity. *Proceedings of the National Academy of Sciences* **104**(14): 5925-5930.

Kruse J, Rennenberg H, Adams MA. 2011. Steps towards a mechanistic understanding of respiratory temperature responses. *New Phytologist* **189**(3): 659-677.

Kurten EL, Bunyavejchewin S, Davies SJ. 2018. Phenology of a dipterocarp forest with seasonal drought: Insights into the origin of general flowering. *Journal of Ecology* **106**(1): 126-136.

Laenen B, Shaw B, Schneider H, Goffinet B, Paradis E, Désamoré A, Heinrichs J, Villarreal J, Gradstein S, McDaniel S. 2014. Extant diversity of bryophytes emerged from successive post-Mesozoic diversification bursts. *Nature Communications* **5**(1): 5134.

Lambers H, Finnegan PM, Laliberté E, Pearse SJ, Ryan MH, Shane MW, Veneklaas EJ. 2011. Phosphorus Nutrition of Proteaceae in Severely Phosphorus-Impoverished Soils: Are There Lessons To Be Learned for Future Crops? *Plant physiology* **156**(3): 1058-1066.

Lambers H, Raven JA, Shaver GR, Smith SE. 2008. Plant nutrient-acquisition strategies change with soil age. *Trends in Ecology & Evolution* **23**(2): 95-103.

Leakey A, Press M, Scholes J. 2003. High-temperature inhibition of photosynthesis is greater under sunflecks than uniform irradiance in a tropical rain forest tree seedling. *Plant, Cell & Environment* **26**(10): 1681-1690.

Lehtonen S, Silvestro D, Karger DN, Scotese C, Tuomisto H, Kessler M, Peña C, Wahlberg N, Antonelli A. 2017. Environmentally driven extinction and opportunistic origination explain fern diversification patterns. *Scientific Reports* **7**(1): 4831.

Leimu R, Fischer M. 2008. A Meta-Analysis of Local Adaptation in Plants. *PLOS ONE* **3**(12): e4010.

Lenth R 2023. emmeans: Estimated Marginal Means, aka Least-Squares Means.

Li X, Blackman CJ, Choat B, Duursma RA, Rymer PD, Medlyn BE, Tissue DT. 2018. Tree hydraulic traits are coordinated and strongly linked to climate-of-origin across a rainfall gradient. *Plant, Cell & Environment* **41**(3): 646-660.

Li X, Blackman CJ, Peters JM, Choat B, Rymer PD, Medlyn BE, Tissue DT. 2019. More than iso/anisohydry: Hydroscapes integrate plant water use and drought tolerance traits in 10 eucalypt species from contrasting climates. *Functional Ecology* **33**(6): 1035-1049.

Li X, Kristiansen K, Rosenqvist E, Liu F. 2019. Elevated CO_2 Modulates the Effects of Drought and Heat Stress on Plant Water Relations and Grain Yield in Wheat. *Journal of Agronomy and Crop Science* **205**(4): 362-371.

Li X, Piao S, Wang K, Wang X, Wang T, Ciais P, Chen A, Lian X, Peng S, Peñuelas J. 2020. Temporal trade-off between gymnosperm resistance and resilience increases forest sensitivity to extreme drought. *Nature Ecology & Evolution* **4**(8): 1075-1083.

Liang X, Wang D, Ye Q, Zhang J, Liu M, Liu H, Yu K, Wang Y, Hou E, Zhong B. 2023. Stomatal responses of terrestrial plants to global change. *Nature Communications* **14**(1): 2188.

Limousin J-M, Yépez EA, McDowell NG, Pockman WT. 2015. Convergence in Resource Use Efficiency Across Trees With Differing Hydraulic Strategies in Response to Ecosystem Precipitation Manipulation. *Functional Ecology* **29**(9): 1125-1136.

Linares JC, Camarero JJ. 2012. From pattern to process: linking intrinsic water-use efficiency to drought-induced forest decline. *Global Change Biology* **18**(3): 1000-1015.

Liu Y, Parolari AJ, Kumar M, Huang C-W, Katul GG, Porporato A. 2017. Increasing atmospheric humidity and CO_2 concentration alleviate forest mortality risk. *Proceedings of the National Academy of Sciences* **114**(37): 9918-9923.

Lombardozzi D, Bonan GB, Smith NG, Dukes JS, Fisher RA. 2015. Temperature Acclimation of Photosynthesis and Respiration: A Key Uncertainty in the Carbon Cycle-climate Feedback. *Geophysical Research Letters* **42**(20): 8624-8631.

Loveys BR, Atkinson L, Sherlock D, Roberts RL, Fitter AH, Atkin OK. 2003. Thermal Acclimation of Leaf and Root Respiration: An Investigation Comparing Inherently Fast- and Slow-growing Plant Species. *Global Change Biology* **9**(6): 895-910.

Lüdecke D, Ben-Shachar MS, Patil I, Waggoner P, Makowski D. 2021a. performance: An R package for assessment, comparison and testing of statistical models. *Journal of Open Source Software* **6**(60): 3139-3147.

Lüdecke D, Patil I, Ben-Shachar MS, Wiernik BM, Waggoner P, Makowski D. 2021b. see: An R package for visualizing statistical models. *Journal of Open Source Software* **6**(64): 3393.

Máčel M, Lawson C, Mortimer SR, Šmilauerová M, Bischoff A, Crémieux L, Doležal J, Edwards AR, Lanta V, Bezemer TM, et al. 2007. Climate vs. Soil Factors in Local Adaptation of Two Common Plant Species. *Ecology* **88**(2): 424-433.

Magallón S, Sánchez-Reyes LL, Gómez-Acevedo SL. 2019. Thirty clues to the exceptional diversification of flowering plants. *Annals of Botany* **123**(3): 491-503.

Magnusson A, Skaug H, Nielsen A, Berg C, Kristensen K, Maechler M, van Bentham K, Bolker B, Brooks M, Brooks MM. 2017. Package 'glmmtmb'. *R Package Version 0.2. 0* **25**(2): 378-400.

Maherali H, Pockman WT, Jackson RB. 2004. Adaptive Variation in the Vulnerability of Woody Plants to Xylem Cavitation. *Ecology* **85**(8): 2184-2199.

Maire V, Wright IJ, Prentice IC, Batjes NH, Bhaskar R, van Bodegom PM, Cornwell WK, Ellsworth D, Niinemets Ü, Ordonez A. 2015. Global effects of soil and climate on leaf photosynthetic traits and rates. *Global Ecology and Biogeography* **24**(6): 706-717.

Marchin RM, Backes D, Ossola A, Leishman MR, Tjoelker MG, Ellsworth DS. 2022. Extreme heat increases stomatal conductance and drought-induced mortality risk in vulnerable plant species. *Global Change Biology* **28**(3): 1133-1146.

Marchin RM, Ossola A, Leishman MR, Ellsworth DS. 2020. A simple method for simulating drought effects on plants. *Frontiers in Plant Science* **10**: 14.

Márquez DA, Stuart-Williams H, Farquhar GD, Busch FA. 2022. Cuticular conductance of adaxial and abaxial leaf surfaces and its relation to minimum leaf surface conductance. *New Phytologist* **233**(1): 156-168.

Martin-StPaul N, Delzon S, Cochard H. 2017. Plant resistance to drought depends on timely stomatal closure. *Ecology Letters* **20**(11): 1437-1447.

Mathews S, Bonser SP. 2005. Life histories, ecological tolerance limits, and the evolution of geographic range size in Eucalyptus (Myrtaceae). *Australian Journal of Botany* **53**(6): 501-508.

Matthews MA, Boyer JS. 1984. Acclimation of Photosynthesis to Low Leaf Water Potentials. *Plant physiology* **74**(1): 161-166.

McDowell NG. 2011. Mechanisms linking drought, hydraulics, carbon metabolism, and vegetation mortality. *Plant physiology* **155**(3): 1051-1059.

McDowell NG, Pockman WT, Allen CD, Breshears DD, Cobb NS, Kolb TE, Plaut J, Sperry JS, West AG, Williams DG, et al. 2008. Mechanisms of Plant Survival and Mortality During Drought: Why Do Some Plants Survive While Others Succumb to Drought? *New Phytologist* **178**(4): 719-739.

McDowell NG, Sapes G, Pivovaroff A, Adams HD, Allen CD, Anderegg WRL, Arend M, Breshears DD, Brodribb T, Choat B, et al. 2022. Mechanisms of woody-plant mortality under rising drought, CO_2 and vapour pressure deficit. *Nature Reviews Earth & Environment* **3**(5): 294-308.

McElwain JC, Willis K, Lupia R 2005. Cretaceous CO_2 decline and the radiation and diversification of angiosperms. *A history of atmospheric CO_2 and its effects on plants, animals, and ecosystems*: Springer, 133-165.

McElwain JC, Yiotis C, Lawson T. 2016. Using modern plant trait relationships between observed and theoretical maximum stomatal conductance and vein density to examine patterns of plant macroevolution. *New Phytologist* **209**(1): 94-103.

Medlyn B, Dreyer E, Ellsworth D, Forstreuter M, Harley P, Kirschbaum M, Le Roux X, Montpied P, Strassemeyer J, Walcroft A. 2002. Temperature response of parameters of a

biochemically based model of photosynthesis. II. A review of experimental data. *Plant, Cell & Environment* **25**(9): 1167-1179.

Medlyn BE, Barton CVM, Broadmeadow MSJ, Ceulemans R, De Angelis P, Forstreuter M, Freeman M, Jackson SB, Kellomaki S, Laitat E, et al. 2001. Stomatal conductance of forest species after long-term exposure to elevated CO_2 concentration: a synthesis. *New Phytologist* **149**(2): 247-264.

Meena YK, Kaur N. 2019. Towards an Understanding of Physiological and Biochemical Mechanisms of Drought Tolerance in Plant. *Annual Research & Review in Biology*: 1-13.

Meir P, Metcalfe DB, Costa A, Fisher RA. 2008. The fate of assimilated carbon during drought: impacts on respiration in Amazon rainforests. *Philosophical Transactions of the Royal Society B: Biological Sciences* **363**(1498): 1849-1855.

Metcalfe DB, Meir P, Aragão LE, Lobo-do-Vale R, Galbraith D, Fisher R, Chaves MM, Maroco J, da Costa ACL, de Almeida SS. 2010. Shifts in plant respiration and carbon use efficiency at a large-scale drought experiment in the eastern Amazon. *New Phytologist* **187**(3): 608-621.

Meteorology CaBo. 2015. Climate Change in Australia Information for Australia's Natural Resource Management Regions: Technical Report. Australia.

Meteorology CaBo. 2022. State of the Climate 2022. State of the Climate. Australia.

Miller J, Williams RJ, Farquhar GD. 2001. Carbon isotope discrimination by a sequence of Eucalyptus species along a subcontinental rainfall gradient in Australia. *Functional Ecology* **15**(2): 222-232.

Murchie EH, Hubbart S, Chen Y, Peng S, Horton P. 2002. Acclimation of Rice Photosynthesis to Irradiance Under Field Conditions. *Plant physiology* **130**(4): 1999-2010.

Nepstad DC, Tohver IM, Ray D, Moutinho P, Cardinot G. 2007. Mortality of Large Trees and Lianas following Experimental Drought in an Amazon Forest. *Ecology* **88**(9): 2259-2269.

Nicotra AB, Atkin OK, Bonser SP, Davidson AM, Finnegan EJ, Mathesius U, Poot P, Purugganan MD, Richards CL, Valladares F, et al. 2010. Plant Phenotypic Plasticity in a Changing Climate. *Trends in Plant Science* **15**(12): 684-692.

Niinemets Ü. 2001. Global-scale climatic controls of leaf dry mass per area, density, and thickness in trees and shrubs. *Ecology* **82**(2): 453-469.

Nolf M, Creek D, Duursma R, Holtum J, Mayr S, Choat B. 2015. Stem and leaf hydraulic properties are finely coordinated in three tropical rain forest tree species. *Plant, Cell & Environment* **38**(12): 2652-2661.

Norby RJ, DeLucia EH, Gielen B, Calfapietra C, Giardina CP, King JS, Ledford J, McCarthy HR, Moore DJP, Ceulemans R, et al. 2005. Forest Response to Elevated CO_2 is Conserved Across a Broad Range of Productivity. *Proceedings of the National Academy of Sciences* **102**(50): 18052-18056.

Norby RJ, O'Neill EG, Luxmoore RJ. 1986. Effects of Atmospheric CO_2 Enrichment on the Growth and Mineral Nutrition of *Quercus Alba* Seedlings in Nutrient-Poor Soil. *Plant physiology* **82**(1): 83-89.

Novick KA, Ficklin DL, Grossiord C, Konings AG, Martínez-Vilalta J, Sadok W, Trugman AT, Williams AP, Wright AJ, Abatzoglou JT, et al. 2024. The impacts of rising vapour pressure deficit in natural and managed ecosystems. *Plant, Cell & Environment* **47**(9): 3561-3589.

Oliveras I, Malhi Y. 2016. Many shades of green: the dynamic tropical forest–savannah transition zones. *Philosophical Transactions of the Royal Society B: Biological Sciences* **371**(1703): 20150308.

Onstein RE. 2019. Darwin's Second 'Abominable Mystery': Trait Flexibility as the Innovation Leading to Angiosperm Diversity. *New Phytologist* **228**(6): 1741-1747.

Orians GH, Milewski AV. 2007. Ecology of Australia: the effects of nutrient-poor soils and intense fires. *Biological Reviews* **82**(3): 393-423.

Palma AC, Winter K, Aranda J, Dalling JW, Cheesman AW, Turner BL, Cernusak LA. 2020. Why Are Tropical Conifers Disadvantaged in Fertile Soils? Comparison of Podocarpus Guatemalensis With an Angiosperm Pioneer, Ficus Insipida. *Tree physiology* **40**(6): 810-821.

Pedhazur EJ, Kerlinger FN. 1982. *Multiple regression in behavioral research: Explanation and prediction*.

Perkins-Kirkpatrick S, Lewis S. 2020. Increasing trends in regional heatwaves. *Nature Communications* **11**(1): 3357.

Pfautsch S, Renard J, Tjoelker MG, Salih A. 2015. Phloem as Capacitor: Radial Transfer of Water into Xylem of Tree Stems Occurs via Symplastic Transport in Ray Parenchyma. *Plant physiology* **167**(3): 963-971.

Pfennigwerth AA, Bailey JK, Schweitzer JA. 2017. Trait variation along elevation gradients in a dominant woody shrub is population-specific and driven by plasticity. *Aob Plants* **9**(4): plx027.

Pommerening A, Muszta A. 2016. Relative plant growth revisited: Towards a mathematical standardisation of separate approaches. *Ecological Modelling* **320**: 383-392.

Poorter H, Niinemets Ü, Poorter L, Wright IJ, Villar R. 2009. Causes and consequences of variation in leaf mass per area (LMA): a meta-analysis. *New Phytologist* **182**(3): 565-588.

Prasad PVV, Pisipati SR, Momčilović I, Ristić Z. 2011. Independent and Combined Effects of High Temperature and Drought Stress During Grain Filling on Plant Yield and Chloroplast EF-Tu Expression in Spring Wheat. *Journal of Agronomy and Crop Science* **197**(6): 430-441.

Qaderi MM, Kurepin LV, Reid DM. 2006. Growth and physiological responses of canola (Brassica napus) to three components of global climate change: temperature, carbon dioxide and drought. *Physiologia Plantarum* **128**(4): 710-721.

Qian H, Zhang J, Jin Y, Deng T. 2023. Effects of Evolutionary History on Assembly of Flowering Plants in Regions Across Africa. *Ecography* **2023**(9): e06775.

Qurani CG, Yoshimura K. 2021. Effect of Low Light Condition on the Growth and Carbon Use of Legume Seedlings. *Asian Journal of Forestry* **5**(2): 51-59.

R Core Team 2023. R: A Language and Environment for Statistical Computing. Vienna, Austria: R Foundation for Statistical Computing.

Rebetzke GJ, Condon AG, Farquhar G, Appels R, Richards R. 2008. Quantitative trait loci for carbon isotope discrimination are repeatable across environments and wheat mapping populations. *Theoretical and Applied Genetics* **118**(1): 123-137.

Rees M, Condit R, Crawley M, Pacala S, Tilman D. 2001. Long-term studies of vegetation dynamics. *Science* **293**(5530): 650-655.

Reich PB. 2014. The World-wide 'Fast–slow' Plant Economics Spectrum: A Traits Manifesto. *Journal of Ecology* **102**(2): 275-301.

Reich PB, Hungate BA, Luo Y. 2006. Carbon-nitrogen interactions in terrestrial ecosystems in response to rising atmospheric carbon dioxide. *Annu. Rev. Ecol. Evol. Syst.* **37**(1): 611-636.

Reich PB, Oleksyn J, Wright IJ. 2009. Leaf phosphorus influences the photosynthesis–nitrogen relation: a cross-biome analysis of 314 species. *Oecologia* **160**(2): 207-212.

Reich PB, Sendall KM, Stefański A, Wei X, Rich RL, Montgomery R. 2016. Boreal and Temperate Trees Show Strong Acclimation of Respiration to Warming. *Nature* **531**(7596): 633-636.

Richards R, Rebetzke G, Condon A, Van Herwaarden A. 2002. Breeding opportunities for increasing the efficiency of water use and crop yield in temperate cereals. *Crop science* **42**(1): 111-121.

Rowland L, Zaragoza-Castells J, Bloomfield KJ, Turnbull MH, Bonal D, Burban B, Salinas N, Cosio E, Metcalfe DJ, Ford A. 2017. Scaling leaf respiration with nitrogen and phosphorus in tropical forests across two continents. *New Phytologist* **214**(3): 1064-1077.

Rúa MA, Antoninka A, Antunes PM, Chaudhary VB, Gehring CA, Lamit LJ, Piculell BJ, Bever JD, Zabinski CA, Meadow JF, et al. 2016. Home-Field Advantage? Evidence of Local

Adaptation Among Plants, Soil, and Arbuscular Mycorrhizal Fungi Through Meta-Analysis. *BMC Evolutionary Biology* **16**(1): 122.

Sage RF. 1994. Acclimation of Photosynthesis to Increasing Atmospheric CO_2: The Gas Exchange Perspective. *Photosynthesis Research* **39**(3): 351-368.

Sanad MN, Campbell KG, Gill KS. 2016. Developmental Program Impacts Phenological Plasticity of Spring Wheat Under Drought. *Botanical Studies* **57**(1): 35.

Sankaran M. 2019. Droughts and the ecological future of tropical savanna vegetation. *Journal of Ecology* **107**(4): 1531-1549.

Sarker BC, Hara M, Uemura M. 2005. Proline synthesis, physiological responses and biomass yield of eggplants during and after repetitive soil moisture stress. *Scientia Horticulturae* **103**(4): 387-402.

Schneider CA, Rasband WS, Eliceiri KW. 2012. NIH Image to ImageJ: 25 years of image analysis. *Nature Methods* **9**(7): 671-675.

Schneider H, Schuettpelz E, Pryer KM, Cranfill R, Magallón S, Lupia R. 2004. Ferns diversified in the shadow of angiosperms. *Nature* **428**(6982): 553-557.

Scholz FG, Bucci SJ, Goldstein G, Meinzer FC, Franco AC, Miralles-Wilhelm F. 2007. Removal of nutrient limitations by long-term fertilization decreases nocturnal water loss in savanna trees. *Tree physiology* **27**(4): 551-559.

Schulze E-D, Turner NC, Nicolle D, Schumacher J. 2006. Leaf and wood carbon isotope ratios, specific leaf areas and wood growth of Eucalyptus species across a rainfall gradient in Australia. *Tree physiology* **26**(4): 479-492.

Schulze E-D, Williams R, Farquhar G, Schulze W, Langridge J, Miller J, Walker BH. 1998. Carbon and nitrogen isotope discrimination and nitrogen nutrition of trees along a rainfall gradient in northern Australia. *Functional Plant Biology* **25**(4): 413-425.

Schuster A-C, Burghardt M, Alfarhan A, Bueno A, Hedrich R, Leide J, Thomas J, Riederer M. 2016. Effectiveness of cuticular transpiration barriers in a desert plant at controlling water loss at high temperatures. *Aob Plants* **8**: plw027.

Schuster A-C, Burghardt M, Riederer M. 2017. The ecophysiology of leaf cuticular transpiration: are cuticular water permeabilities adapted to ecological conditions? *Journal of Experimental Botany* **68**(19): 5271-5279.

Schwinning S, Weiner J. 1998. Mechanisms Determining the Degree of Size Asymmetry in Competition Among Plants. *Oecologia* **113**(4): 447-455.

Shindo S, Itô M, Ueda K, Kato M, Hasebe M. 1999. Characterization of MADS Genes in the Gymnosperm <i>Gnetum Parvifolium</I> and Its Implication on the Evolution of Reproductive Organs in Seed Plants. *Evolution & Development* **1**(3): 180-190.

Silva FCE, Shvaleva A, Maroco J, Almeida M, Chaves M, Pereira J. 2004. Responses to water stress in two Eucalyptus globulus clones differing in drought tolerance. *Tree physiology* **24**(10): 1165-1172.

Skelton RP, West AG, Dawson TE. 2015. Predicting plant vulnerability to drought in biodiverse regions using functional traits. *Proceedings of the National Academy of Sciences* **112**(18): 5744-5749.

Slot M, Kitajima K. 2015. Whole-plant respiration and its temperature sensitivity during progressive carbon starvation. *Functional Plant Biology* **42**(6): 579-588.

Slot M, Zaragoza-Castells J, Atkin OK. 2008. Transient shade and drought have divergent impacts on the temperature sensitivity of dark respiration in leaves of Geum urbanum. *Functional Plant Biology* **35**(11): 1135-1146.

Snyder KA, James JJ, Richards JH, Donovan LA. 2008. Does Hydraulic Lift or Nighttime Transpiration Facilitate Nitrogen Acquisition? *Plant and Soil*: 159-166.

Sobieszczuk-Nowicka E, Kubala S, Zmienko A, Małecka A, Legocka J. 2016. From accumulation to degradation: reprogramming polyamine metabolism facilitates dark-induced senescence in barley leaf cells. *Frontiers in Plant Science* **6**: 168363.

Sperry JS, Hacke UG, Pittermann J. 2006. Size and function in conifer tracheids and angiosperm vessels. *American journal of botany* **93**(10): 1490-1500.

Stewart GR, Turnbull MH, Schmidt S, Erskine PD. 1995. ^{13}C natural abundance in plant communities along a rainfall gradient: a biological integrator of water availability. *Functional Plant Biology* **22**(1): 51-55.

Stock WD 2014. Plant ecophysiological diversity. In: Allsopp N, Colville JF, Verboom GA eds. *Fynbos: Ecology, evolution, and conservation of a megadiverse region*: Oxford University Press, 248.

Stotz GC, Salgado-Luarte C, Escobedo VM, Valladares F, Gianoli E. 2021. Global Trends in Phenotypic Plasticity of Plants. *Ecology Letters*: 2267-2281.

Sturchio MA, Chieppa J, Chapman SK, Canas G, Aspinwall MJ. 2021. Temperature Acclimation of Leaf Respiration Differs Between Marsh and Mangrove Vegetation in a Coastal Wetland Ecotone. *Global Change Biology*: 612-629.

Sulpice R, Ishihara H, Schlereth A, Cawthray GR, Encke B, Giavalisco P, Ivakov A, Arrivault S, Jost R, Krohn N. 2014. Low levels of ribosomal RNA partly account for the very high photosynthetic phosphorus-use efficiency of P roteaceae species. *Plant, Cell & Environment* **37**(6): 1276-1298.

Takahashi K, Otsubo S. 2017. How Betula ermanii maintains a positive carbon balance at the individual leaf level at high elevations. *American Journal of Plant Sciences* **8**(3): 482-494.

Ter Steege H, Pitman NC, Killeen TJ, Laurance WF, Peres CA, Guevara JE, Salomão RP, Castilho CV, Amaral IL, de Almeida Matos FD. 2015. Estimating the global conservation status of more than 15,000 Amazonian tree species. *Science advances* **1**(10): e1500936.

Thompson WA, Eldridge DJ, Bonser SP. 2006. Structure of biological soil crust communities in Callitris glaucophylla woodlands of New South Wales, Australia. *Journal of Vegetation Science* **17**(3): 271-280.

Tissue DT, Thomas RS, Strain BR. 1993. Long-term Effects of Elevated CO_2 and Nutrients on Photosynthesis and Rubisco in Loblolly Pine Seedlings. *Plant Cell & Environment*: 859-865.

Tjoelker MG, Oleksyn J, Reich PB. 1999. Acclimation of respiration to temperature and CO_2 in seedlings of boreal tree species in relation to plant size and relative growth rate. *Global Change Biology* **5**(6): 679-691.

Tjoelker MG, Oleksyn J, Reich PB. 2001. Modelling respiration of vegetation: evidence for a general temperature-dependent Q10. *Global Change Biology* **7**(2): 223-230.

Towers IR, Vesk PA, Wenk Elizabeth H, Gallagher RV, Windecker Saras M, Wright IJ, Falster Daniel S. 2024. Revisiting the role of mean annual precipitation in shaping functional trait distributions at a continental scale. *New Phytologist* **241**(5): 1900-1909.

Trueba S, Pan R, Scoffoni C, John GP, Davis SD, Sack L. 2019. Thresholds for leaf damage due to dehydration: declines of hydraulic function, stomatal conductance and cellular integrity precede those for photochemistry. *New Phytologist* **223**(1): 134-149.

Trueba S, Pouteau R, Lens F, Feild TS, Isnard S, Olson ME, Delzon S. 2017. Vulnerability to xylem embolism as a major correlate of the environmental distribution of rain forest species on a tropical island. *Plant, Cell & Environment* **40**(2): 277-289.

Tuomisto H, Zuquim G, Cárdenas G. 2014. Species richness and diversity along edaphic and climatic gradients in Amazonia. *Ecography* **37**(11): 1034-1046.

Urban J, Ingwers M, McGuire MA, Teskey RO. 2017a. Stomatal conductance increases with rising temperature. *Plant Signaling & Behavior* **12**(8): e1356534.

Urban J, Ingwers MW, McGuire MA, Teskey RO. 2017b. Increase in leaf temperature opens stomata and decouples net photosynthesis from stomatal conductance in Pinus taeda and Populus deltoides x nigra. *Journal of Experimental Botany* **68**(7): 1757-1767.

van der Sleen P, Groenendijk P, Vlam M, Anten NPR, Boom A, Bongers F, Pons TL, Terburg G, Zuidema PA. 2015. No growth stimulation of tropical trees by 150 years of CO_2 fertilization but water-use efciency increased. *Nature Geoscience* **8**: 24-28.

Van Mantgem PJ, Stephenson NL, Byrne JC, Daniels LD, Franklin JF, Fulé PZ, Harmon ME, Larson AJ, Smith JM, Taylor AH. 2009. Widespread increase of tree mortality rates in the western United States. *Science* **323**(5913): 521-524.

Viscarra Rossel RA, Bui EN. 2016. A new detailed map of total phosphorus stocks in Australian soil. *Science of the Total Environment* **542**: 1040-1049.

Viscarra Rossel RA, Chen C, Grundy M, Searle R, Clifford D 2018a. Soil and Landscape Grid Australia-Wide 3D Soil Property Maps (3") - Release 1. *CSIRO Data Collection*: Commonwealth Scientific and Industrial Research Organisation (CSIRO).

Viscarra Rossel RA, Chen C, Grundy M, Searle R, Clifford D, Odgers N, Holmes K, Griffin T, Liddicoat C, Kidd D 2018b. Soil and Landscape Grid National Soil Attribute Maps—Total Phosphorus (3" resolution)—Release 1. v5. *CSIRO Data Collection*.

Viscarra Rossel RA, Chen C, Grundy M, Searle R, Clifford D, Odgers N, Holmes K, Griffin T, Liddicoat C, Kidd D 2018c. Soil and Landscape Grid National Soil Attribute Maps - Total Nitrogen (3" resolution) - Release 1. v5. *CSIRO Data Collection.*: Commonwealth Scientific and Industrial Research Organisation (CSIRO).

Vitasse Y, Bresson C, Kremer A, Michalet R, Delzon S. 2010. Quantifying Phenological Plasticity to Temperature in Two Temperate Tree Species. *Functional Ecology*: 1211-1218.

Wager HG. 1941. On the respiration and carbon assimilation rates of some arctic plants as related to temperature. *The New Phytologist* **40**(1): 1-19.

Wang D, Heckathorn SA, Wang X, Philpott SM. 2012. A meta-analysis of plant physiological and growth responses to temperature and elevated CO 2. *Oecologia* **169**: 1-13.

Wang R, Huang W, Chen L, Ma L, Guo C, Liu X. 2011. Anatomical and Physiological Plasticity in Leymus Chinensis (Poaceae) Along Large-Scale Longitudinal Gradient in Northeast China. *PLOS ONE*: e26209.

Westerband AC, Wright IJ, Maire V, Paillassa J, Prentice IC, Atkin OK, Bloomfield KJ, Cernusak LA, Dong N, Gleason SM, et al. 2023. Coordination of photosynthetic traits across soil and climate gradients. *Global Change Biology* **29**(3): 856-873.

White DA, Turner NC, Galbraith JH. 2000. Leaf water relations and stomatal behavior of four allopatric Eucalyptus species planted in Mediterranean southwestern Australia. *Tree physiology* **20**(17): 1157-1165.

Wickham H. 2016. *ggplot2: Elegant Graphics for Data Analysis*: Springer-Verlag New York.

Will RE, Wilson SM, Zou CB, Hennessey TC. 2013. Increased vapor pressure deficit due to higher temperature leads to greater transpiration and faster mortality during drought for tree seedlings common to the forest–grassland ecotone. *New Phytologist* **200**(2): 366-374.

Wong S-C, Cowan IR, Farquhar GD. 1979. Stomatal conductance correlates with photosynthetic capacity. *Nature* **282**: 424-426.

Wong SC, Canny MJ, Holloway-Phillips M, Stuart-Williams H, Cernusak LA, Márquez DA, Farquhar GD. 2022. Humidity gradients in the air spaces of leaves. *Nature Plants* **8**(8): 971-978.

Wright IJ, Reich PB, Westoby M. 2003. Least-cost input mixtures of water and nitrogen for photosynthesis. *The American Naturalist* **161**(1): 98-111.

Wright IJ, Westoby M. 2002. Leaves at low versus high rainfall: coordination of structure, lifespan and physiology. *New Phytologist* **155**(3): 403-416.

Xiao L, Labandeira C, Dilcher D, Ren D. 2021. Florivory of Early Cretaceous flowers by functionally diverse insects: implications for early angiosperm pollination. *Proceedings of the Royal Society B* **288**(1953): 20210320.

Xue D, Zhang X, Lu X, Chen G, Chen Z. 2017. Molecular and Evolutionary Mechanisms of Cuticular Wax for Plant Drought Tolerance. *Frontiers in Plant Science*(8): 258957.

Yin C, Berninger F, Li CY. 2006. Photosynthetic Responses of Populus Przewalski Subjected to Drought Stress. *Photosynthetica*(44): 62-68.

Yu J, Chen L, Xu M, Huang B. 2012. Effects of Elevated CO_2 on Physiological Responses of Tall Fescue to Elevated Temperature, Drought Stress, and the Combined Stresses. *Crop science* **52**(4): 1848-1858.

Zandalinas SI, Mittler R, Balfagón D, Arbona V, Gómez-Cadenas A. 2018. Plant adaptations to the combination of drought and high temperatures. *Physiologia Plantarum* **162**(1): 2-12.

Zanne AE, Tank DC, Cornwell WK, Eastman JM, Smith SA, FitzJohn RG, McGlinn DJ, O'Meara BC, Moles AT, Reich PB, et al. 2013. Three Keys to the Radiation of Angiosperms Into Freezing Environments. *Nature*: 89-92.

Zhang JW, Cregg BM. 1996. Variation in stable carbon isotope discrimination among and within exotic conifer species grown in eastern Nebraska, USA. *Forest Ecology and Management* **83**(3): 181-187.

Zhao J, Hartmann H, Trumbore SE, Ziegler W, Zhang Y. 2013. High Temperature Causes Negative Whole-plant Carbon Balance Under Mild Drought. *New Phytologist*: 330-339.

Zhao K, Qu Y, Wang D, Liu Z, Rong Y. 2023. Artificial Grassland Had Higher Water Use Efficiency in Year with Less Precipitation in the Agro-Pastoral Ecotone. *Plants* **12**(6): 1239.

Zomer RJ, Xu J, Trabucco A. 2022. Version 3 of the Global Aridity Index and Potential Evapotranspiration Database. *Scientific Data* **9**(1): 409.